Supporting Information
for

Bright chromenylium polymethine dyes enable fast, four-color in vivo imaging with shortwave infrared detection

Emily D. Cosco[#,^] Bernardo A. Arús[^], Anthony L. Spearman[#], Timothy L. Atallah[#], Irene Lim,[#] Olivia S. Leland,[#] Justin R. Caram,[#] Thomas S. Bischof[^], Oliver T. Bruns[^,&,*] and Ellen M. Sletten[#,*]

[#]*Department of Chemistry and Biochemistry, University of California, Los Angeles, Los Angeles, California 90095, United States*
^Helmholtz Pioneer Campus, Helmholtz Zentrum München, D-85764, Neuherberg, Germany
&School of Medicine, Technical University Munich, D-80333 München, Germany

*Oliver T. Bruns: oliver.bruns@helmholtz-muenchen.de
*Ellen M. Sletten: sletten@chem.ucla.edu

Table of Contents

I. General experimental procedures

Instrumentation

Thin layer chromatography was performed using Silica Gel 60 F_{254} (EMD Millipore) plates. Flash chromatography was executed with technical grade silica gel with 60 Å pores and 40–63 μm mesh particle size (Sorbtech Technologies). Solvent was removed under reduced pressure with a Büchi Rotavapor with a Welch self-cleaning dry vacuum pump and further dried with a Welch DuoSeal pump. Aqueous solvent was removed by lyophilization with a LABCONCO FreeZone Benchtop Freeze Dryer. Bath sonication was performed using a Branson 3800 ultrasonic cleaner or an Elma S15Elmasonic. Nuclear magnetic resonance (^{1}H NMR, ^{13}C NMR) spectra were taken on Bruker Avance 300, AV-500 or AV-600 instruments and processed with MestReNova software. All ^{1}H NMR and ^{13}C NMR peaks are reported in ppm in reference to their respective solvent signals. High resolution mass spectra (electrospray ionization (ESI)) were obtained on a Thermo Scientific Q Exactive™ Plus Hybrid Quadrupole-Orbitrap™ M with Dionex UltiMate 3000 RSLCnano System. IR spectra were obtained on a Perkin-Elmer UATR Two FT-IR spectrometer and are reported in terms of frequency of absorption (cm^{-1}). Nanomaterial size was analyzed with a Malvern Zetaziser Nano dynamic light scattering in plastic 1 cm cuvettes. Zeta potentials were measured with a Malvern Zetasizer Nano dynamic light scattering with a DTS1070 capillary cell for samples. Absorbance spectra were collected on a JASCO V-770 UV-Visible/NIR spectrophotometer with a 2000 nm/min scan rate after blanking with the appropriate solvent or on a PerkinElmer LAMBDA 1050+ UV/VIS/NIR Spectrophotometer with a reference sample. Photoluminescence spectra were obtained on a Horiba Instruments PTI QuantaMaster Series fluorometer with InGaAs detector Horiba Edison DSS IGA 020L. Absolute quantum yields were taken in a Horiba KSPHERE-Petite. Quartz cuvettes (1 cm) were used for absorbance and photoluminescence measurements. Absorption coefficients in DCM were calculated with serial dilutions with Hamilton syringes in volumetric glassware. Error was taken as the standard deviation of the triplicate experiments. Relative quantum yields were determined in DCM relative to IR-26 in DCM (see Note S1 for details on photoluminescence quantum yield measurements).

Abbreviations

DCM = dichloromethane; DMSO = dimethylsulfoxide; ET = exposure time; EtOH = ethanol; EtOAc = ethyl acetate; fps = frames per second; i.v. = intravenous; i.p. intraperitoneal; LP = longpass; NIR = near-infrared; NMR = nuclear magnetic resonance; PBS = phosphate buffered saline; PEG = polyethylene glycol; ROI = region of interest; SP = shortpass; SWIR = shortwave infrared; THF = tetrahydrofuran; VIS = visible.

Animal procedures

Animal experiments were conducted in conformity with the institutional guidelines. Non-invasive whole mouse imaging was performed on athymic nude female mice (6-15 weeks old, weight between 20-25 g), purchased from Envigo or Charles River Laboratories. Mice were anesthetized with inhaled isoflurane/oxygen. Tail vein injections were performed with a catheter assembled from a 30-gauge needle connected through plastic tubing to a syringe prefilled with isotonic saline solution. The bevel of the needle was then inserted into the tail vein and secured using tissue adhesive. The plastic tubing was then connected to a syringe (30-gauge needle) prefilled with the probe of interest. All probes were filtered through a 0.22 μm syringe filter prior to i.v. injection.

SWIR imaging apparatus

For whole mouse imaging, a custom-built setup was used. Lumics laser units: LU1064DLD350-S70AN03 (35 W) “1065 nm”; LU0980D350-D30AN (35W) “968 nm”, and LU0890D400-U10AF (40W) “892 nm”, LU0785DLU250-S70AN03 (25 W) "785 nm” were used for excitation. Laser modules are specced to ± 10 nm. Laser outputs were coupled in a 4x1 fan-out fiber-optic bundle (Thorlabs BF46LS01) of 600 μm core diameter for each optical path. The output from the fiber was fixed in an excitation cube (Thorlabs KCB1EC/M), reflected off of a mirror (Thorlabs BBE1-E03), and passed through a positive achromat (Thorlabs AC254-050-B), SP filter (specified for each experiment) and an engineered diffuser (Thorlabs ED1-S20-MD or ED1-S50-MD) to provide uniform illumination over the working area. In a typical experiment, the excitation flux at the object was adjusted to be close to 100 $mWcm^{-2}$ (power density used is defined separately in each experiment, with an error of ± 3%). The working area was covered by a heating mat coated with blackout fabric (Thorlabs BK5). Emitted light was directed onto an Allied Vision Goldeye G-032 Cool TEC2 camera with a sensor temperature set point of -30 °C or a Goldeye G-033 TECless camera. Emitted light was directed through a custom filter set (defined for each experiment) and a C-mount camera lens (Navitar, SWIR-35). The assembly was partially enclosed to avoid excess light while enabling manipulation of the field of view during operation. Camera and lasers were externally controlled and synchronized by delivering trigger pulses of 5V TTL (5V Transistor-Transistor Logic) to the laser drivers and camera using a programmable trigger controller with pulses generated with an Atmel Atmega328 micro-controller unit and programmed using Arduino Nano Rev 3 MCU (A000005) in the Arduino integrated development environment (IDE). Acquired imaging data is then transferred to the PC via either a Gigabit Ethernet (GigE), or CameraLink (CL) interface. For image acquisition with the G-032 camera, the toolbox of MATLAB programming environment was used in combination with a MATLAB script (software used can be found at https://gitlab.com/brunslab/ccda) to preview and collect the required image data in 14-bit depth. For image acquisition with the G-033 camera, FireBird Camera Link Frame Grabber (1xCLD-2PE8 or 1xCLD-2PE4, Active Silicon) along with ActiveCapture (Active Silicon) was used to collect image data in 8-bit or 12-bit depth.

Image processing procedures:

Images were processed using the Fiji distribution[1] of ImageJ[2] and Python3. All images were background corrected to correct for non-linearities in the detector and/or excitation. Raw images underwent no further processing. Multiplexed images that underwent unmixing were subjected to either manual or an automated linear unmixing method (see Note S6), specified in the experimental procedures for each figure. All still images are displayed as single frames and converted to 8-bit PNG files for display, unless stated otherwise. Videos were frame averaged to reduce file size, if necessary, before compression with FFmpeg to a .mov file.

II. Supporting Charts

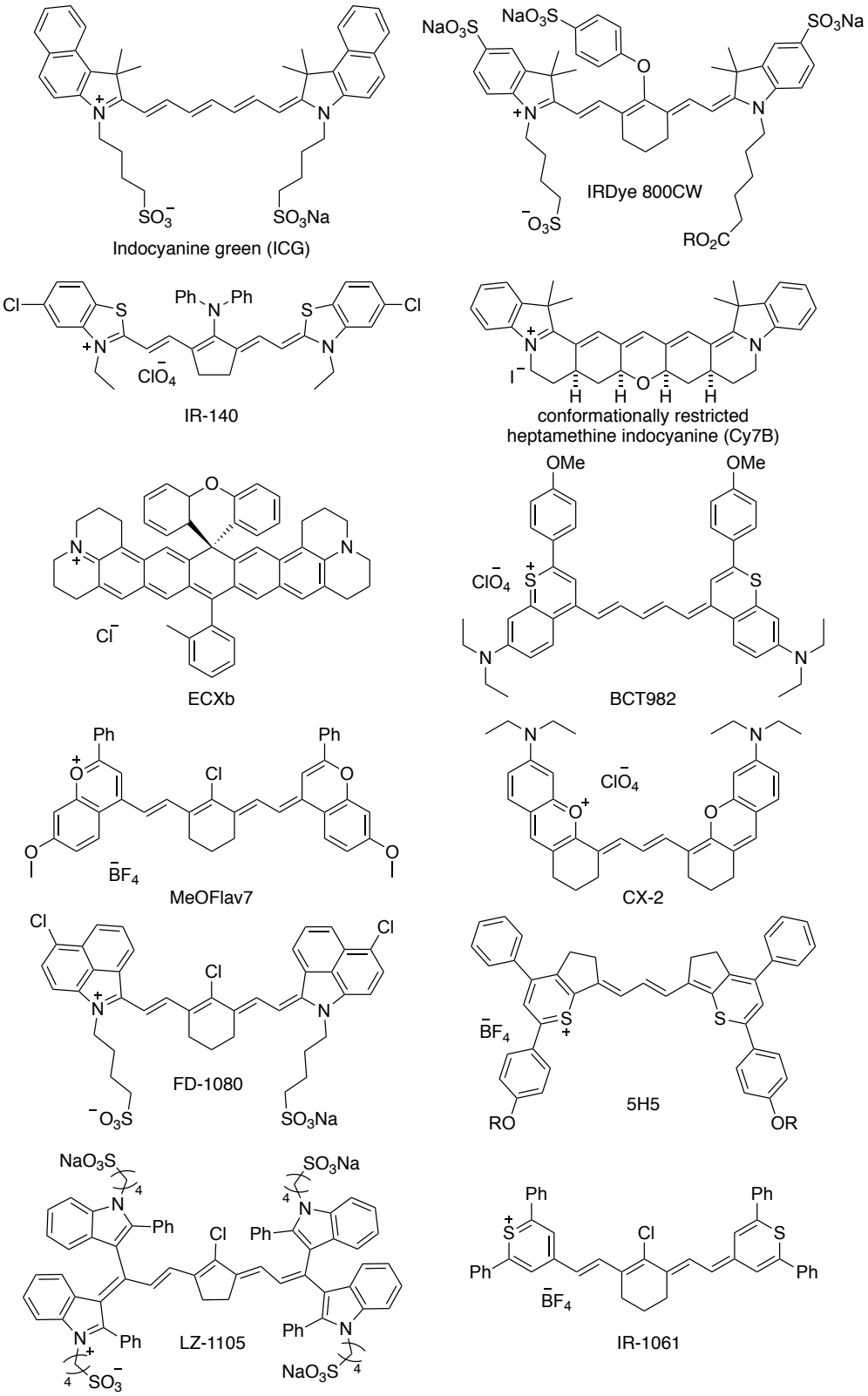

Chart S1. Full structures of dyes outlined in Figure 1c (which are not included in Chart S2).

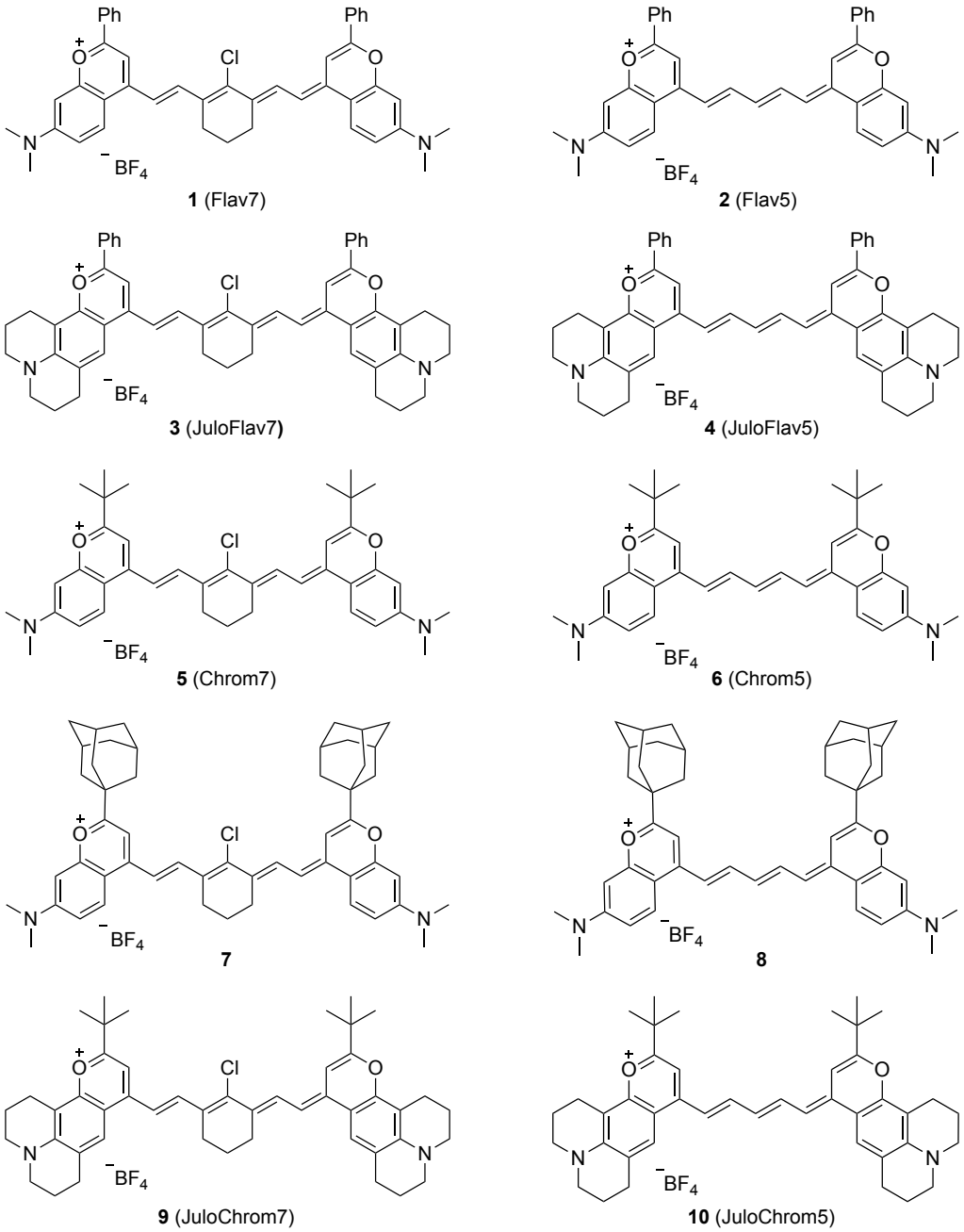

Chart S2. Full structures of all flavylium and chromenylium polymethine dyes compared in the manuscript.

III. Supporting Schemes

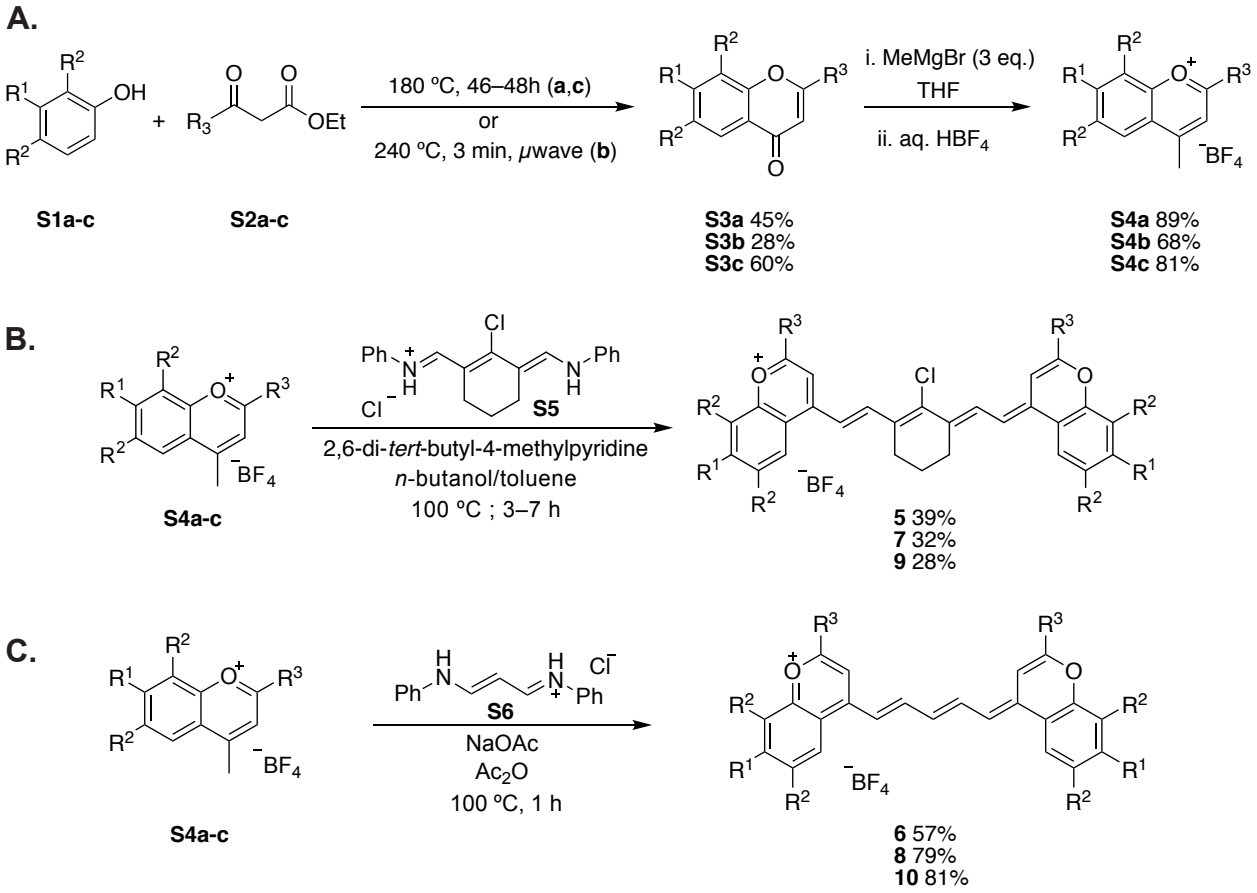

Scheme S1. Synthesis of chromenylium heterocycles, heptamethine dyes and pentamethine dyes. A) Synthesis of chromenylium heterocycles. B) Synthesis of chromenylium heptamethine dyes **5**, **7**, **9**. C) Synthesis of chromenylium pentamethine dyes **6**, **8**, **10**. D) Legend.

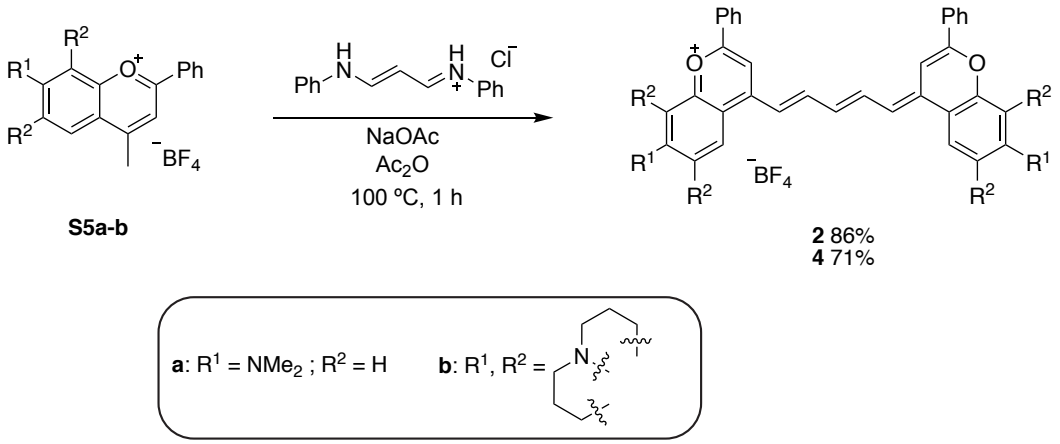

Scheme S2. Synthesis of flavylium pentamethine dyes **2** and **4**, and legend.

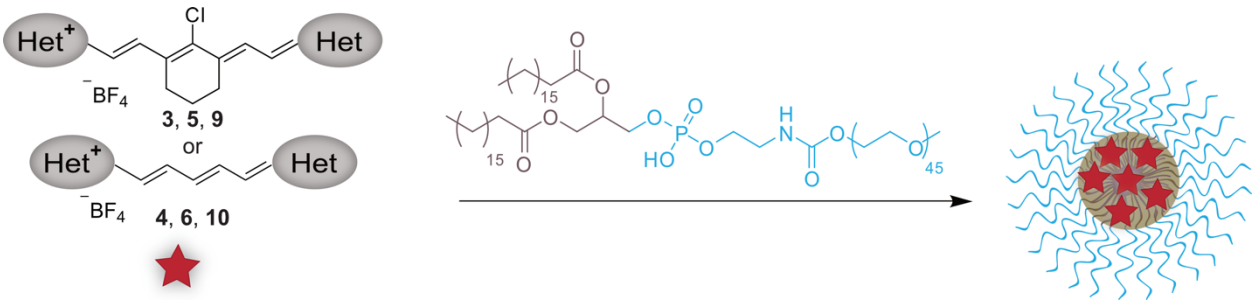

Scheme S3. Assembly of PEG-phospholipid micelles of chromenylium and flavylium polymethine dyes **3** (JuloFlav7), **4** (JuloFlav5), **5** (Chrom7), **6** (Chrom5), **9** (JuloChrom7), and **10** (JuloChrom5).

IV. Supporting Tables

Table S1. Photophysics of hepta- and pentamethine dyes in DCM with error

	dye	$\lambda_{max,abs}$ (nm)	ε_{max} ($M^{-1}cm^{-1}$)	$\lambda_{max,em}$ (nm)	Φ_F (%)	brightness(ε_{max}) ($M^{-1}cm^{-1}$)	SWIR brightness ($M^{-1}cm^{-1}$)
heptamethine	**1** (Flav7)	1027	241,000 ± 1,000	1053	0.61 ± 0.02	1,470 ± 50	1,430 ± 50
	3 (JuloFlav7)	1061	238,000 ± 7,000	1088	0.46 ± 0.01	1,090 ± 50	1,090 ± 40
	5 (Chrom7)	975	252,000 ± 5,000	996	1.70 ± 0.02	4,300 ± 100	2,420 ± 60
	7	977	267,000 ± 8,000	997	1.61 ± 0.02	4,300 ± 100	2,480 ± 80
	9 (JuloChrom7)	1008	228,000 ± 6,000	1033	1.58 ± 0.08	3,600 ± 200	3,300 ± 200
pentamethine	**2** (Flav5)	862	327,000 ± 7,000	883	6.1 ± 0.1	19,900 ± 500	910 ± 20
	4 (JuloFlav5)	897	254,000 ± 5,000	925	5.3 ± 0.2	13,500 ± 600	1,200 ± 50
	6 (Chrom5)	819	380,000 ± 10,000	836	28 ± 2	106,000 ± 8000	1,140 ± 90
	8	818	320,000 ± 10,000	837	28.3 ± 0.5	91,000 ± 3000	940 ± 30
	10 (JuloChrom5)	852	389,000 ± 3,000	872	18.3 ± 0.4	71,000 ± 2000	1,240 ± 30

Table S2. Photophysics of existing bright NIR dyes

Relevant spectral region (Figure 1c)	dye	Solvent	$\lambda_{max,abs}$ (nm)	ε_{max} ($M^{-1}cm^{-1}$)	Φ_F (%)	brightness ($M^{-1}cm^{-1}$)	citation
i	ICG	EtOH	787	194,000	13.2	25,600	a
	IRDye 800CW	PBS	775	242,000	9	21,800	b
	IR-140	EtOH	804	174,000	16.7	29,000	a
	Cy7B	DCM	775	303,000	40	121,200	c
ii	ECXb	DCM	879	132,000	13.3	17,500	d
iii	BTC892	DCM	944	260,000	0.68	1,800	e
	MeOFlav7	DCM	984	190,000	0.52	990	f
	CX-2	Chloroform	981	191,000	0.45	860	g

a. Rurack, K.; Spieles, M. *Anal. Chem.* **2011**, 83, 1232–1242.
b. Obnisbi, S.; Lomnes, S. J.; Laurence, R. G.; Gogbasbian, A.; Mariant, G.; Frangioni, J. V. *Mol. Imaging* **2005**, *4*, 172–181.
c. Matikonda, S. S.; Hammersley, G.; Kumari, N.; Grabenhorst, L.; Glembockyte, V.; Tinnefeld, P.; Ivanic, J.; Levitus, M.; Schnermann, M. J. *J. Org. Chem.* **2020**, 85, 5907–5915.
d. Lei, Z.; Li, X.; Luo, X.; He, H.; Zheng, J.; Qian, X.; Yang, Y. *Angew. Chemie Int. Ed.* **2017**, *56*, 2979–2983.
e. Wang, S.; Fan, Y.; Li, D.; Sun, C.; Lei, Z.; Lu, L.; Wang, T.; Zhang, F. *Nat. Commun.* **2019**, *10*, 1058.
f. Cosco et al. 2020.
g. Lei, Z.; Sun, C.; Pei, P.; Wang, S.; Li, D.; Zhang, X.; Zhang, F. *Angew. Chemie Int. Ed.* **2019**, *58*, 8166–8171.

Table S3. Emissive properties and rates of hepta- and pentamethine dyes in DCM with error

	dye	Φ_F (%)	τ (ps)	k_r (ns^{-1})	k_{nr} (ns^{-1})
heptamethine	**1** (Flav7)	0.61 ± 0.02	68 ± 1	0.090 ± 0.003	14.6 ± 0.5
	3 (JuloFlav7)	0.46 ± 0.01	56 ± 1	0.083 ± 0.003	17.9 ± 0.7
	5 (Chrom7)	1.70 ± 0.04	148 ± 1	0.117 ± 0.003	6.7 ± 0.09
	7	1.61 ± 0.04	151 ± 1	0.106 ± 0.003	6.5 ± 0.2
	9 (JuloChrom7)	1.58 ± 0.08	118 ± 1	0.134 ± 0.007	8.3 ± 0.4
pentamethine	**2** (Flav5)	6.1 ± 0.1	311 ± 1	0.197 ± 0.003	3.02 ± 0.05
	4 (JuloFlav5)	5.3 ± 0.2	296 ± 1	0.180 ± 0.008	3.2 ± 0.1
	6 (Chrom5)	28 ± 2	1022 ± 1	0.27 ± 0.02	0.70 ± 0.04
	8	28.3 ± 0.5	1054 ± 1	0.268 ± 0.004	0.68 ± 0.01
	10 (JuloChrom5)	18.3 ± 0.4	753 ± 1	0.243 ± 0.005	1.09 ± 0.02

V. Supporting Figures

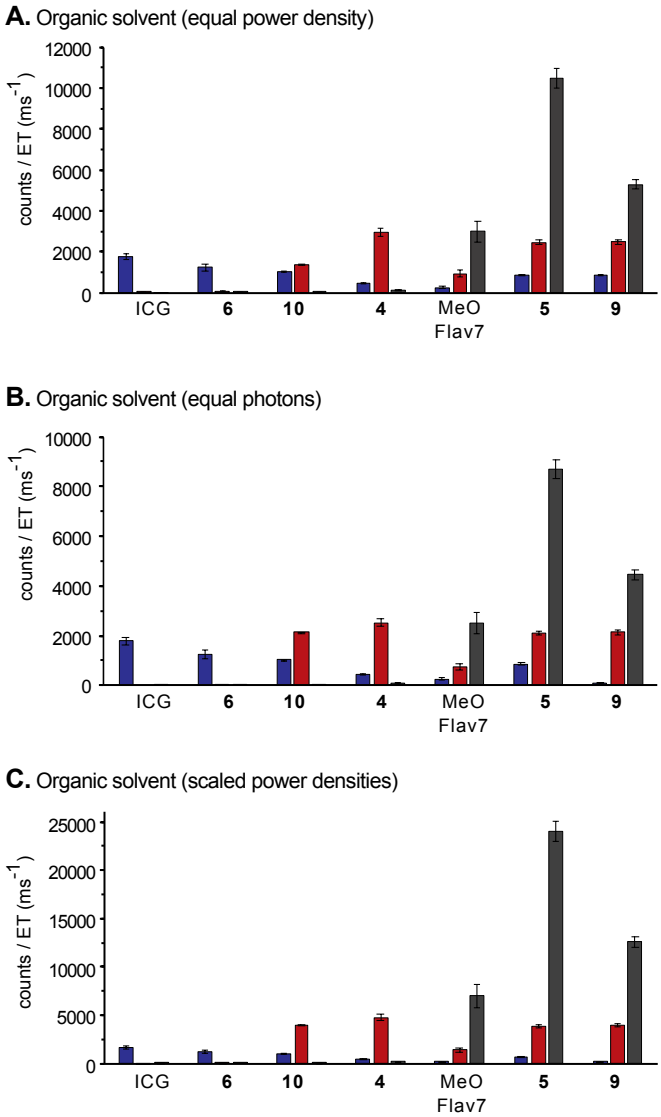

Figure S1. Brightness comparisons in organic solvent obtained in a SWIR imaging setup with different excitation and collection 1100–1700 nm. Quantification of mean intensity over ROI/exposure time (ms) from SWIR images of Eppendorf tubes containing 0.25 µM of each dye in organic solvent (flavylium and chromenylium dyes in DCM; ICG in EtOH) after excitation with 785 nm, 892 nm, or 968 nm lasers of equal power densities (A; 785 nm = 100 mWcm^{-2}, 892 nm = 101 mWcm^{-2}, 968 nm = 100 mWcm^{-2}), equal photon number (B; 785 nm = 100 mWcm^{-2}, 892 = 88 mWcm^{-2}, 968 nm = 81 mWcm^{-2}), or power densities scaled to INCIRP guidelines (C; 785 nm = 100 mWcm^{-2}, 892 nm = 163 mWcm^{-2}; 968 nm = 232 mWcm^{-2}) and LP1000 nm detection (variable exposure time (ET) and frame rate). Error represents variation in concentration assessed by UV-VIS spectrometry measurements.

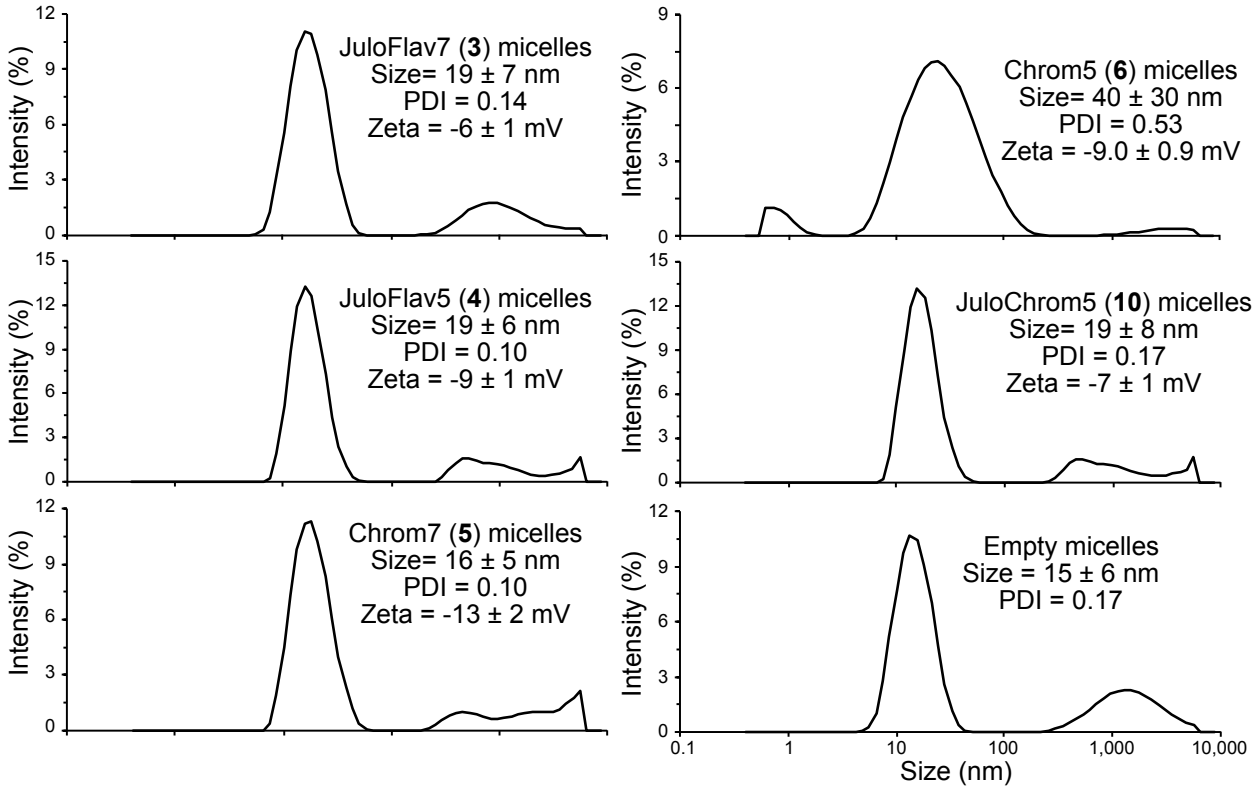

Figure S2. Dynamic light scattering (DLS) characterization, size distribution by intensity and zeta measurements, of PEG-phospholipid micelles composed of 18:0 PEG2000 lipids containing either no dye, or one of dyes used for imaging: **3**–**6**, **10**. Data are the average of three replicate measurements. Size values and PDI values are taken and calculated from the majority peak. Note: minor micelle aggregation is occurring between 0.5–10,000 μm. As intensity is proportional to diameter to the sixth power, aggregate species is a small amount of the total sample.

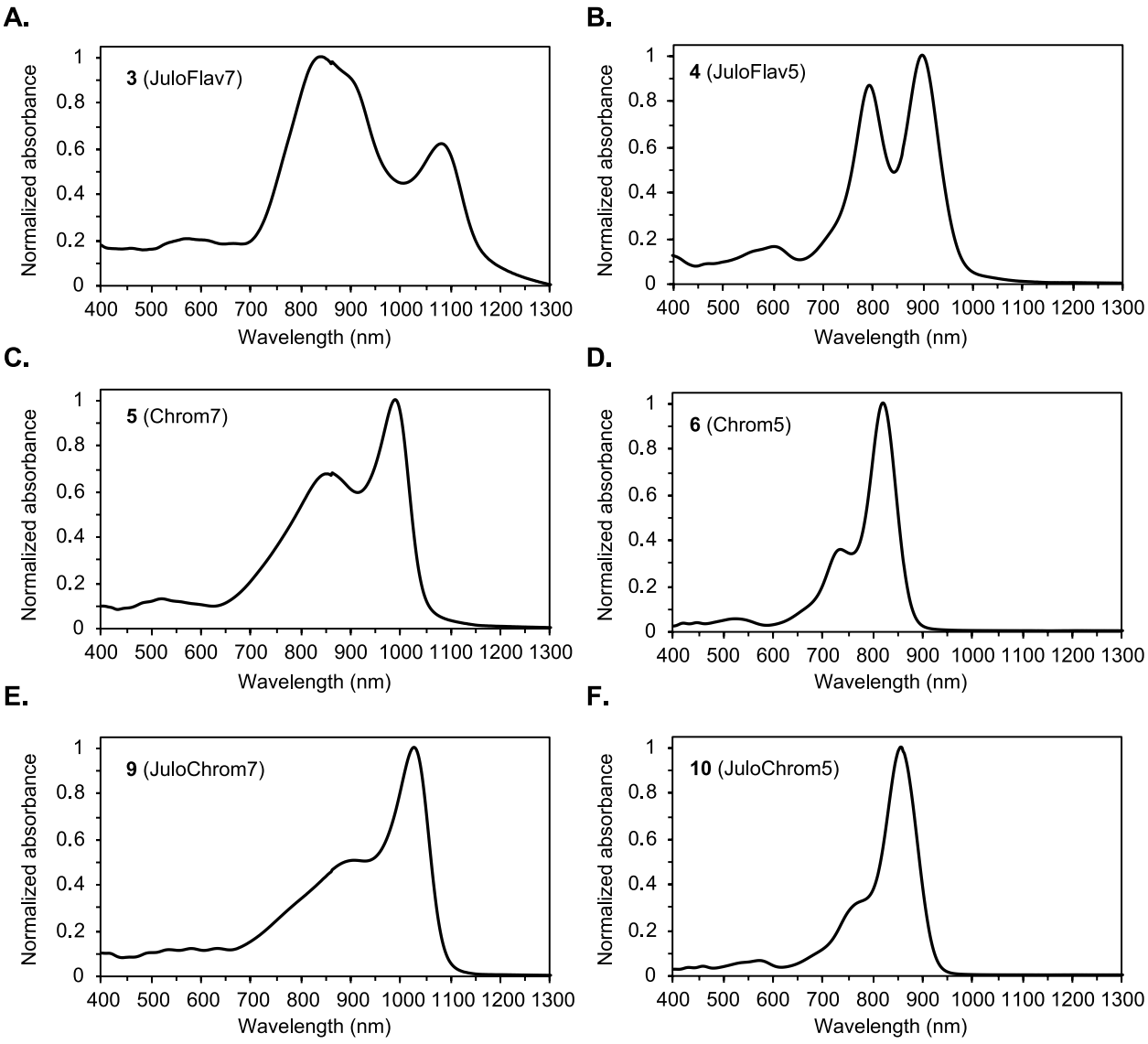

Figure S3. Normalized absorbance traces of PEG-phospholipid micelles of chromenylium and flavylium polymethine dyes in PBS buffer at 3–5 μM (path length = 2.0 mm).

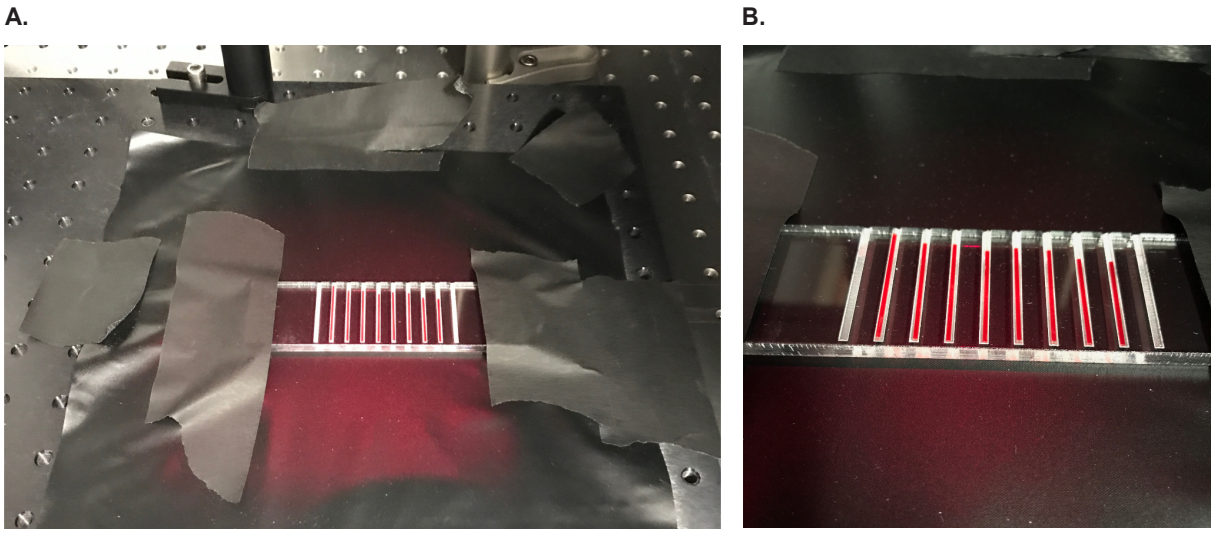

Figure S4. Visible light photographs of the capillary imaging configuration. A) Image of dye-filled capillaries in a transparent plastic holder placed in the imaging configuration. Lasers and camera are situated directly above the field of view. B) Close-up of the capillary holder and dye-filled capillaries. The red color is due to reflections from a 650 nm pilot light on the lasers.

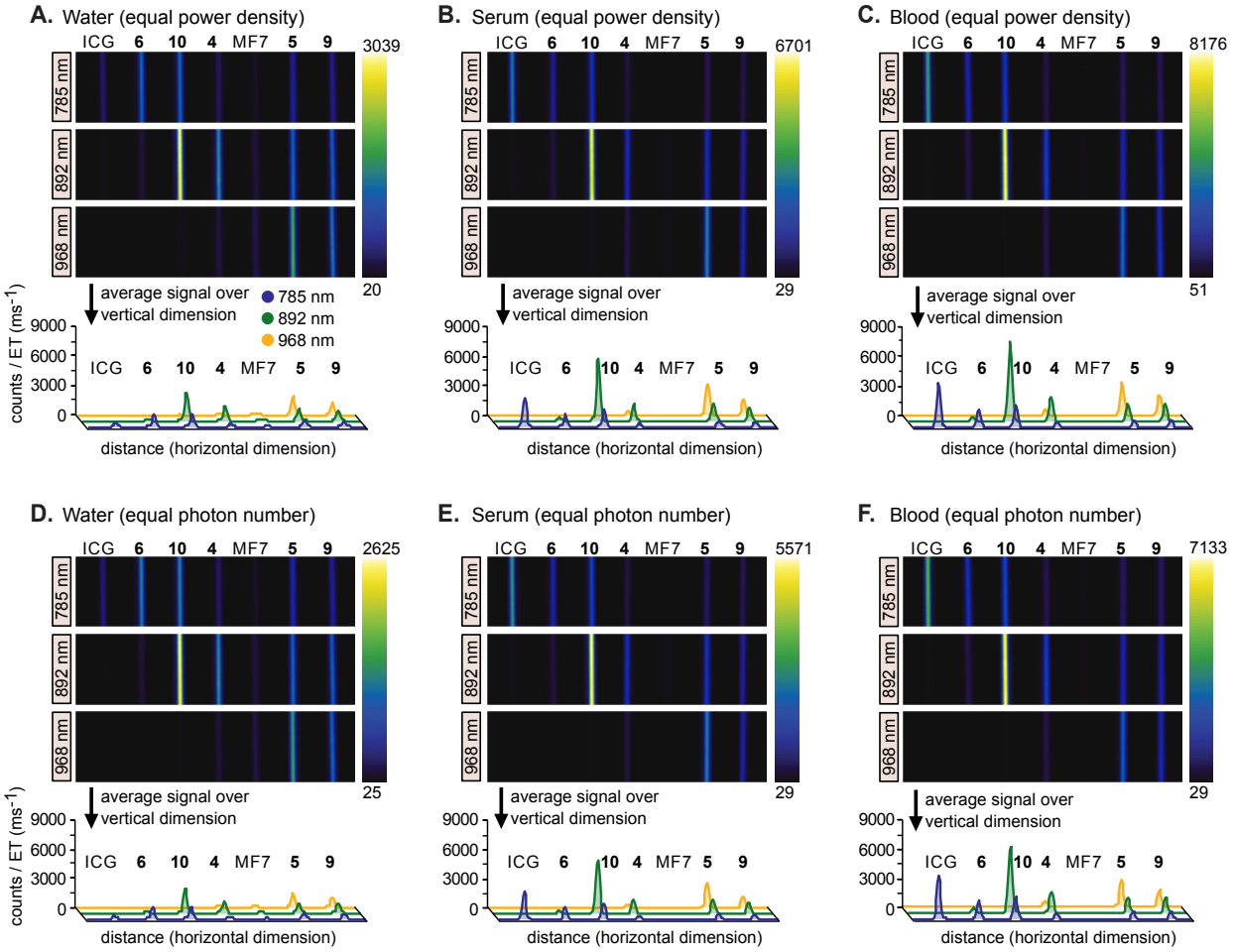

Figure S5. Brightness comparisons in imaging configuration using equal power densities across laser wavelengths (A–C) and equal photon numbers across laser wavelengths (D–F). Images upon 785 (A–F = 33 mWcm^{-2}), 892 (A–C = 33 mWcm^{-2}; D–F = 29 mWcm^{-2}), and 968 (A–C = 33 mWcm^{-2}; D–F = 27 mWcm^{-2}), nm ex. and LP1000 nm detection (variable exposure time (ET) and frame rate) of capillaries containing equal moles of dyes **4**–**6**, **9**, and **10** (lipid formulations) and benchmark dyes ICG (free) and MeOFlav7 (abbreviated MF7) (lipid formulation) when dissolved in water (A, D), fetal bovine serum (FBS) (B, E), or sheep blood (C, F). Displayed images were averaged over 200 frames and normalized by the ET used in each image. The intensities per ms ET were averaged over the vertical dimension displayed in the image. The averaged intensities are plotted over the horizontal dimension and displayed in the graphs below each image.

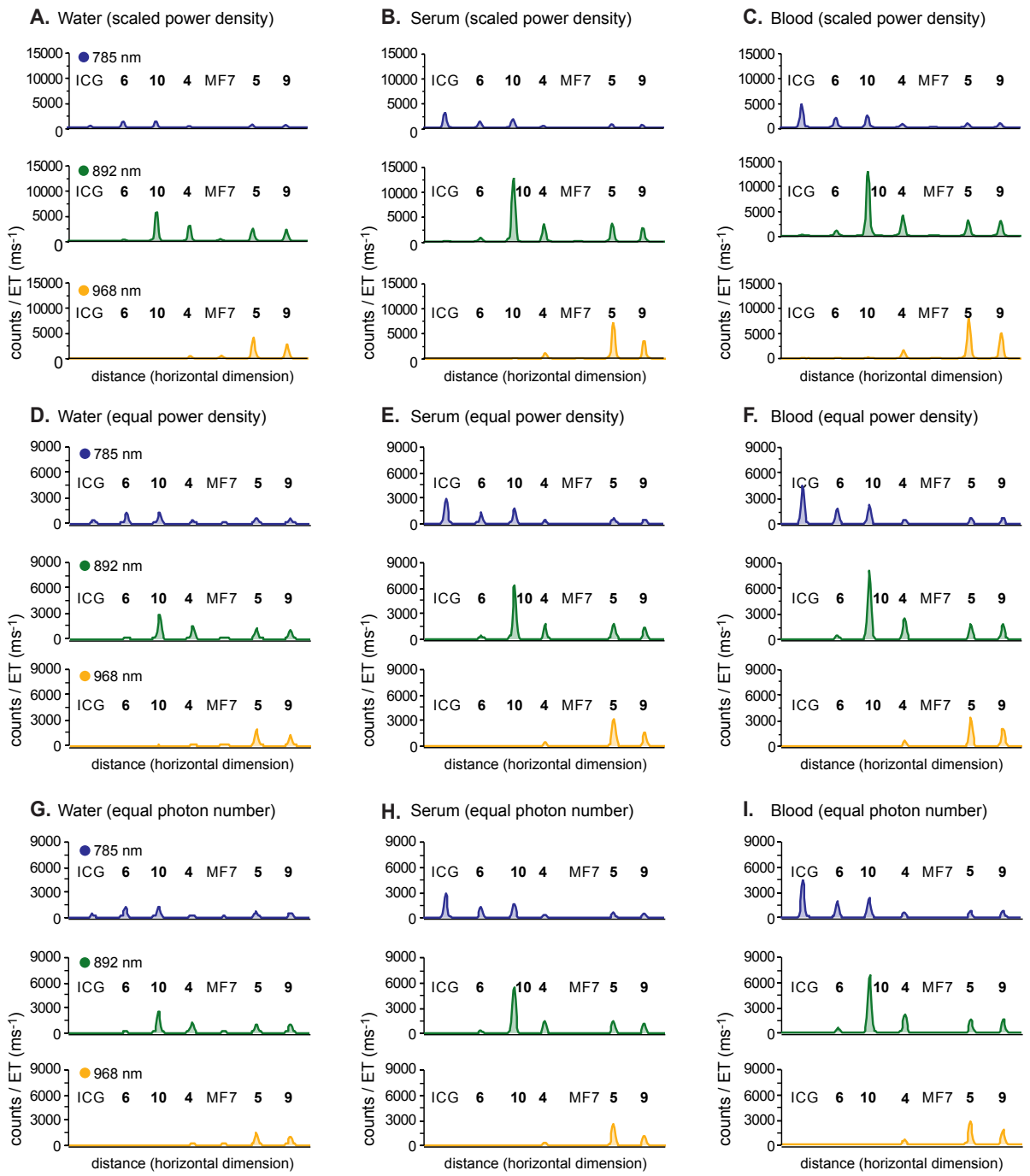

Figure S6. Graphs from brightness comparison in **Figure 5a-c** and **Figure S5** displayed individually for visual clarity. A–C) Scaled power densities. D–F) Equal power densities. G–I) Equal photon numbers. Power densities: 785 (A–I = 33 mWcm^{-2}), 892 (A–C = 54 mWcm^{-2} D–F = 33 mWcm^{-2}; G–I = 29 mWcm^{-2}), 968 (A–C = 77 mWcm^{-2} D–F = 33 mWcm^{-2}; G–I = 27 mWcm^{-2}). LP1000 nm detection (variable exposure time (ET) and frame rate). Capillaries contained equal moles of dyes **4**–**6**, **9**, and **10** (lipid formulations) and benchmark dyes ICG (free) and MeOFlav7 (abbreviated MF7) (lipid formulation) when dissolved in water (A, D, G), fetal bovine serum (FBS) (B, E, H), or sheep blood (C, F, I). Graphs represent the intensity of each image averaged over the vertical dimension, and plotted over the horizontal dimension.

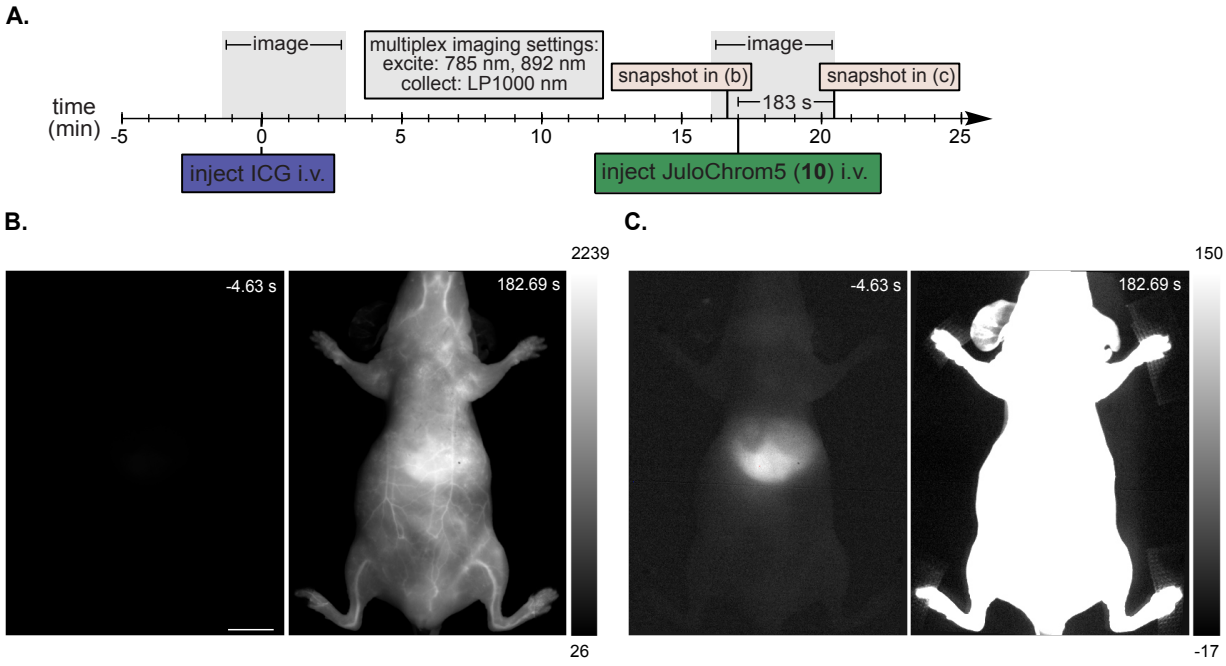

Figure S7. Images from comparative brightness experiment taken after ICG injection and before injection (left) and after injection (right) of JuloChrom5 (**10**), showing residual signal from ICG in the 892 nm channel. A) Experimental timeline for the imaging experiment in B–C. B) Normal contrast images. C) Contrast-enhanced images. Ex. 785 nm (64 $mWcm^{-2}$), 892 nm (104 $mWcm^{-2}$); collect: LP1000 nm, 2.0 ms ET, 150 fps. Single frames are displayed. Scale bar = 1 cm.

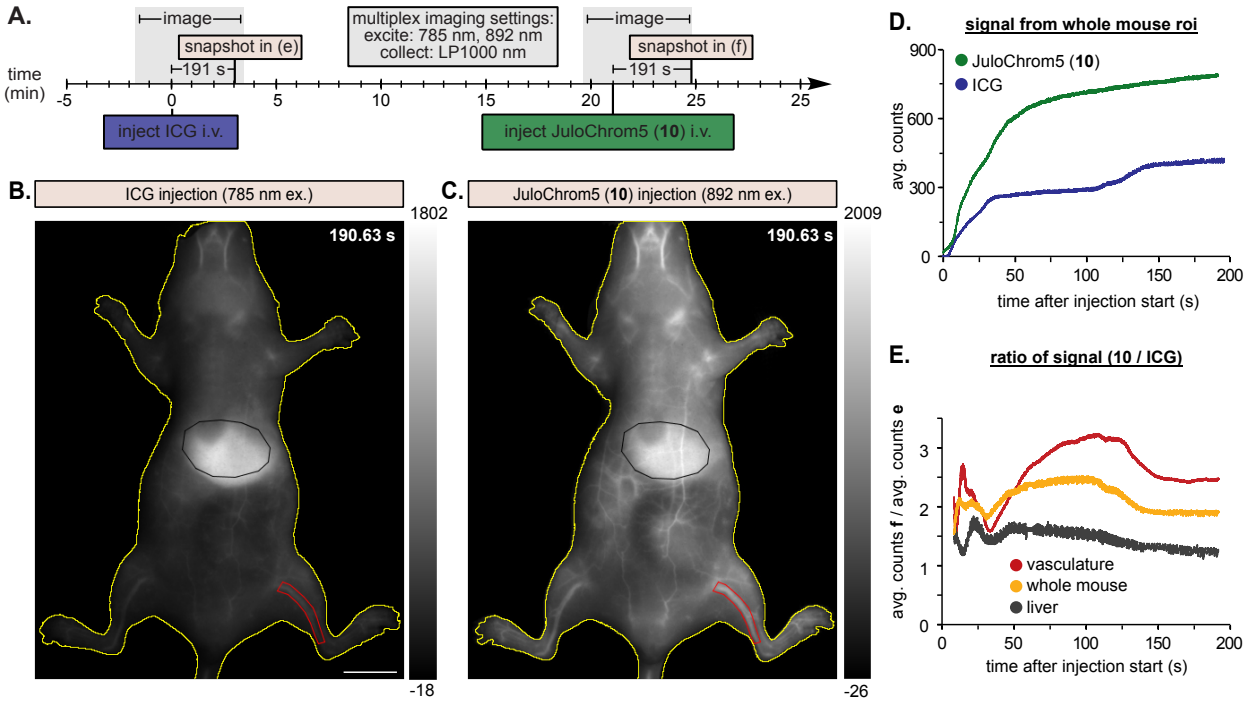

Figure S8. Replicate *in vivo* comparative brightness experiment. A) Experimental timeline for the imaging experiment in B–C. B–C) Images after injection of ICG (50 nmol) upon 785 nm (64 $mWcm^{-2}$) ex. (b) and after injection of JuloChrom5 (**10**) (50 nmol) upon 892 nm (104 $mWcm^{-2}$) ex. (f). Collect: LP1000 nm, 1.6 ms ET, 150 fps (for 2-channel collection). Single frames at the time point which displayed the highest intensity over the whole mouse ROI obtained during acquisition are displayed. D) Intensity quantification from images in B–C, taken by averaging intensity over the whole mouse at each frame after i.v. injection, where t = 0 is the initial frame in which signal is visualized. D) Ratio of intensities (JuloChrom5 (**10**)/ICG) from ROIs quantified in B–C. Scale bar = 1cm.

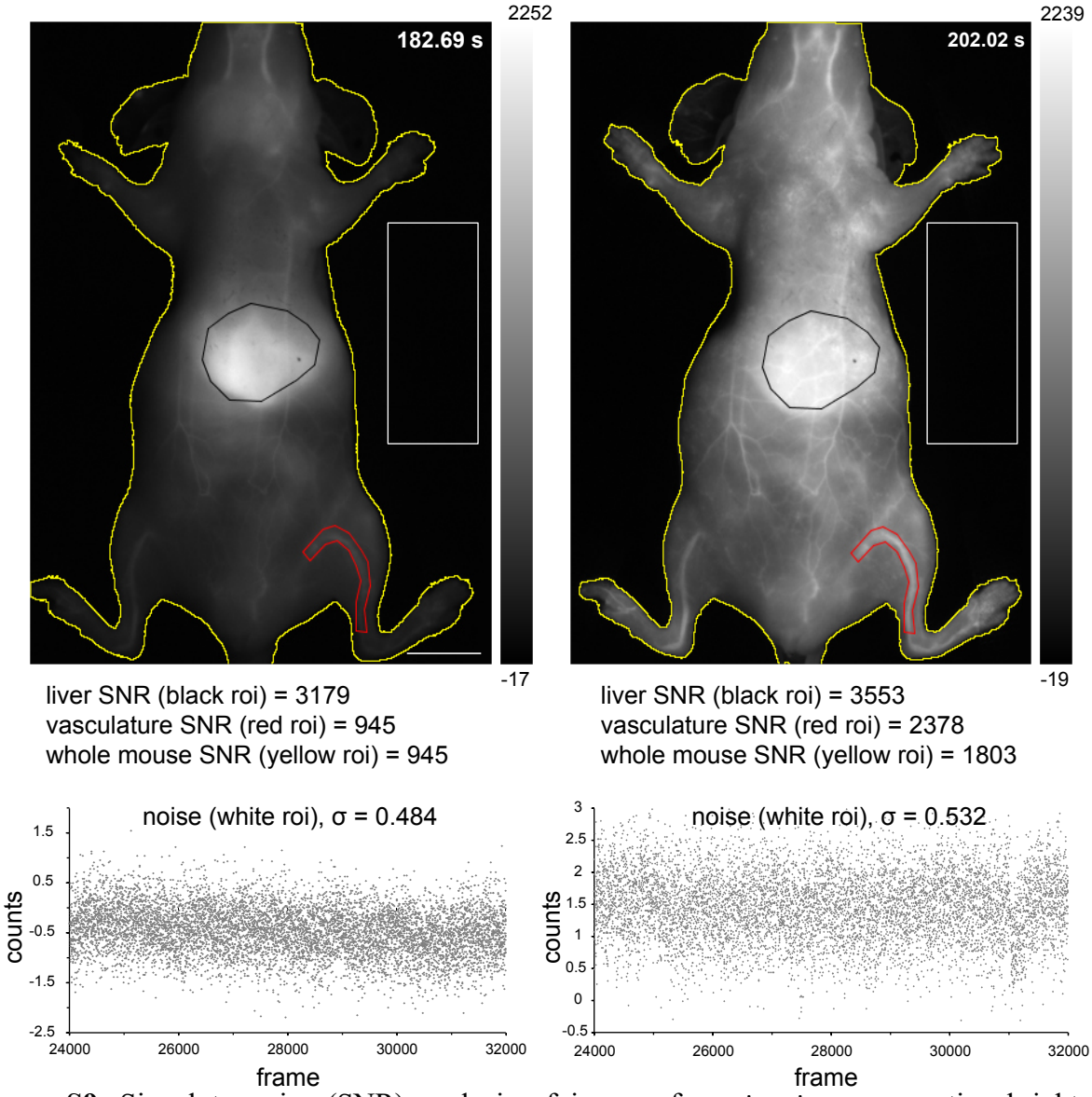

Figure S9. Signal to noise (SNR) analysis of images from *in vivo* comparative brightness experiment (Figure 5e-f). SNR was calculated as $SNR = \frac{\mu}{\sigma}$ where μ is the mean of signal in a ROI over 100 frames (starting at the listed time point) and σ is the standard deviation of signal in the white ROI over 8000 frames (including analyzed time point). ICG injection (50 nmol) is in (A), 785 nm channel, while and JuloFlav5 injection (50 nmol) is in (B), 892 nm channel. Ex. 785 nm (64 $mWcm^{-2}$), 892 nm (104 $mWcm^{-2}$); collect: LP1000 nm, 2.0 ms ET, 150 fps. Single frames are displayed. Scale bar = 1 cm.

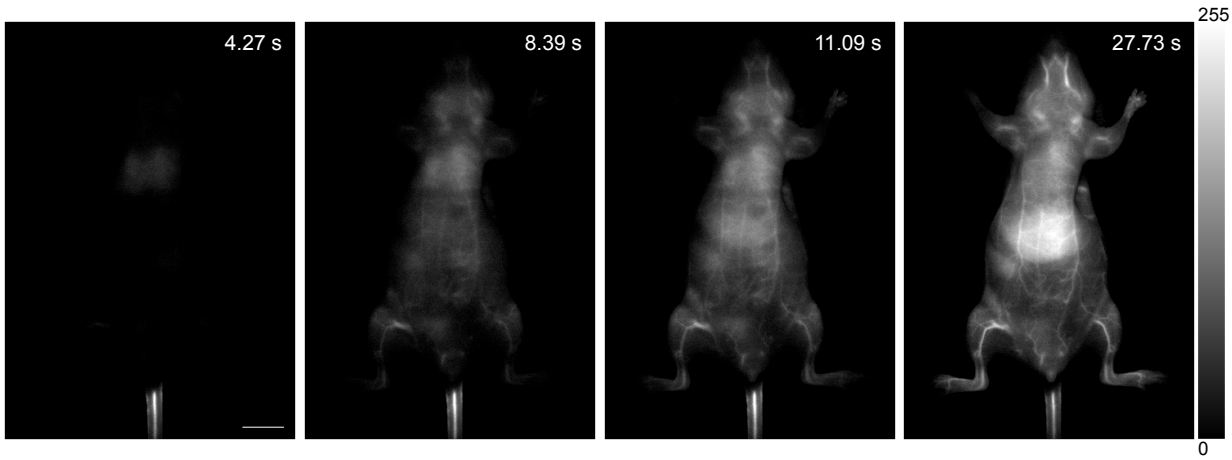

Figure S10. Single color imaging at 300 fps. Images after injection of Chrom7 (**5**) (141 nmol) upon 968 nm (100 $mWcm^{-2}$) laser ex. Collect: LP1100 nm, 3 ms ET, 300 fps. Single frames are displayed. Images are representative of two replicate experiments. Scale bar = 1cm.

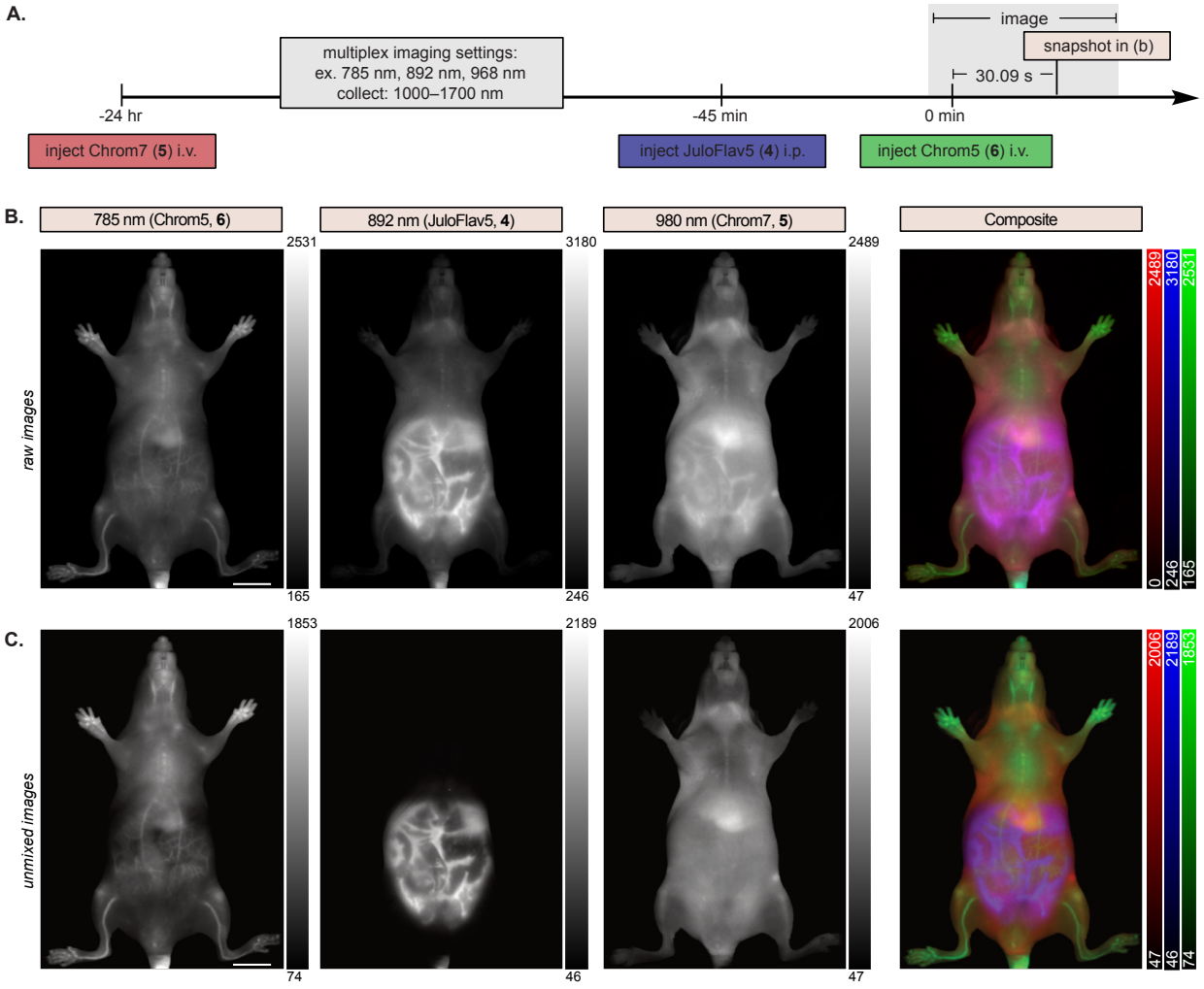

Figure S11. High-speed three-color imaging. A) Experimental timeline for experiment in B–C (not to scale). B) Single channel and composite raw images from three-color excitation multiplexed SWIR imaging at 100 fps. C) Corresponding unmixed single channel and composite images. Stills are from 30 s after injection. Injection amounts are as follows: Chrom5 (**6**) = 130 nmol; JuloFlav5 (**4**) = 80 nmol; Chrom7 (**5**) = 110 nmol. Ex. 785 nm (80 $mWcm^{-2}$). 892 nm (87 $mWcm^{-2}$), 968 nm (94 $mWcm^{-2}$), collect LP1000 nm, 3.3 ms, 100 fps, single frames are displayed. Scale bar = 1 cm.

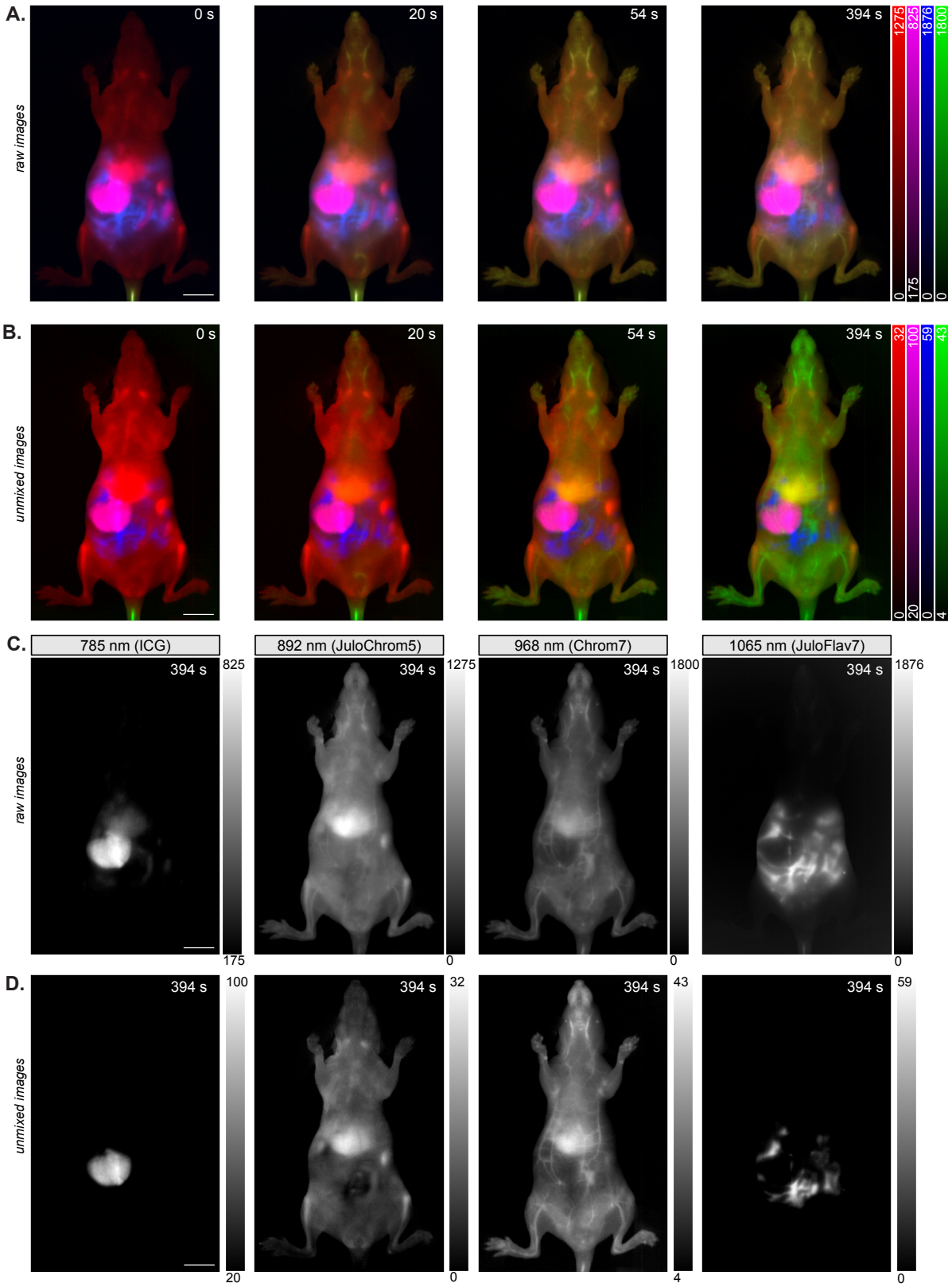

Figure S12. Comparison of raw vs. unmixed data for video-rate 4-color imaging. A) Raw composite images. B) Unmixed composite images. C) Raw single channel images at 394 s after

injection. D) Unmixed single channel images at 394 s after inejction. Injection amounts are: ICG = 200 nmol; JuloChrom5 (**10**) = 50 nmol; Chrom7 (**5**) = 45 nmol; JuloFlav7 (**3**) = 45 nmol. Ex. 785 nm (45 mWcm^{-2}). 892 nm (75 mWcm^{-2}), 968 nm (103 mWcm^{-2}), 1065 nm (156 mWcm^{-2}); collect LP1100 nm, 7.8 ms, 30 fps, single frames are displayed. Scale bar = 1 cm.

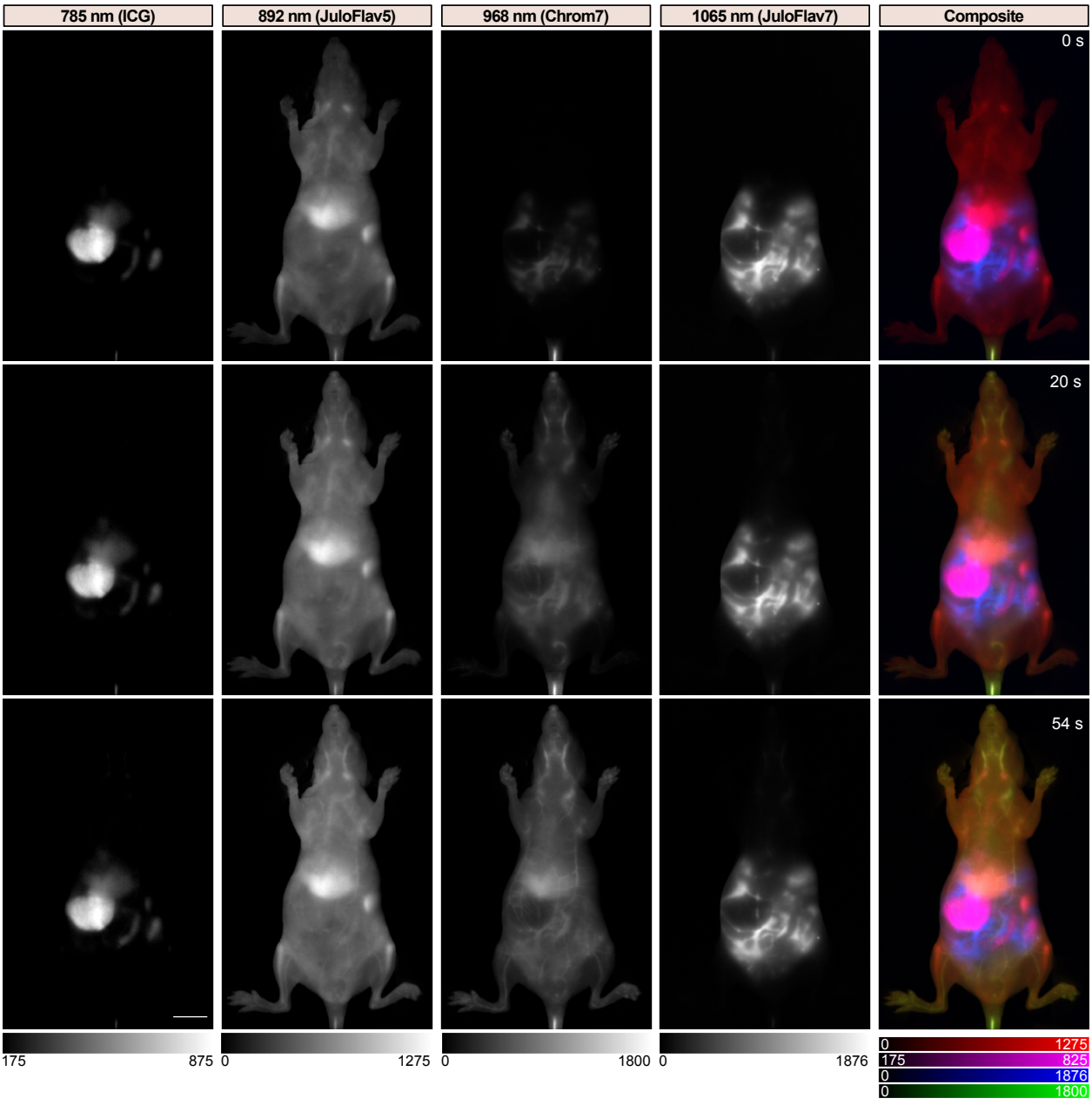

Figure S13. Video-rate 4-color imaging, with individual channels displayed, raw data. Injection amounts are: ICG = 200 nmol; JuloChrom5 (**10**) = 50 nmol; Chrom7 (**5**) = 45 nmol; JuloFlav7 (**3**) = 45 nmol. Ex. 785 nm (45 mWcm^{-2}). 892 nm (75 mWcm^{-2}), 968 nm (103 mWcm^{-2}), 1065 nm (156 mWcm^{-2}); collect LP1100 nm, 7.8 ms, 30 fps, single frames are displayed. Scale bar = 1 cm.

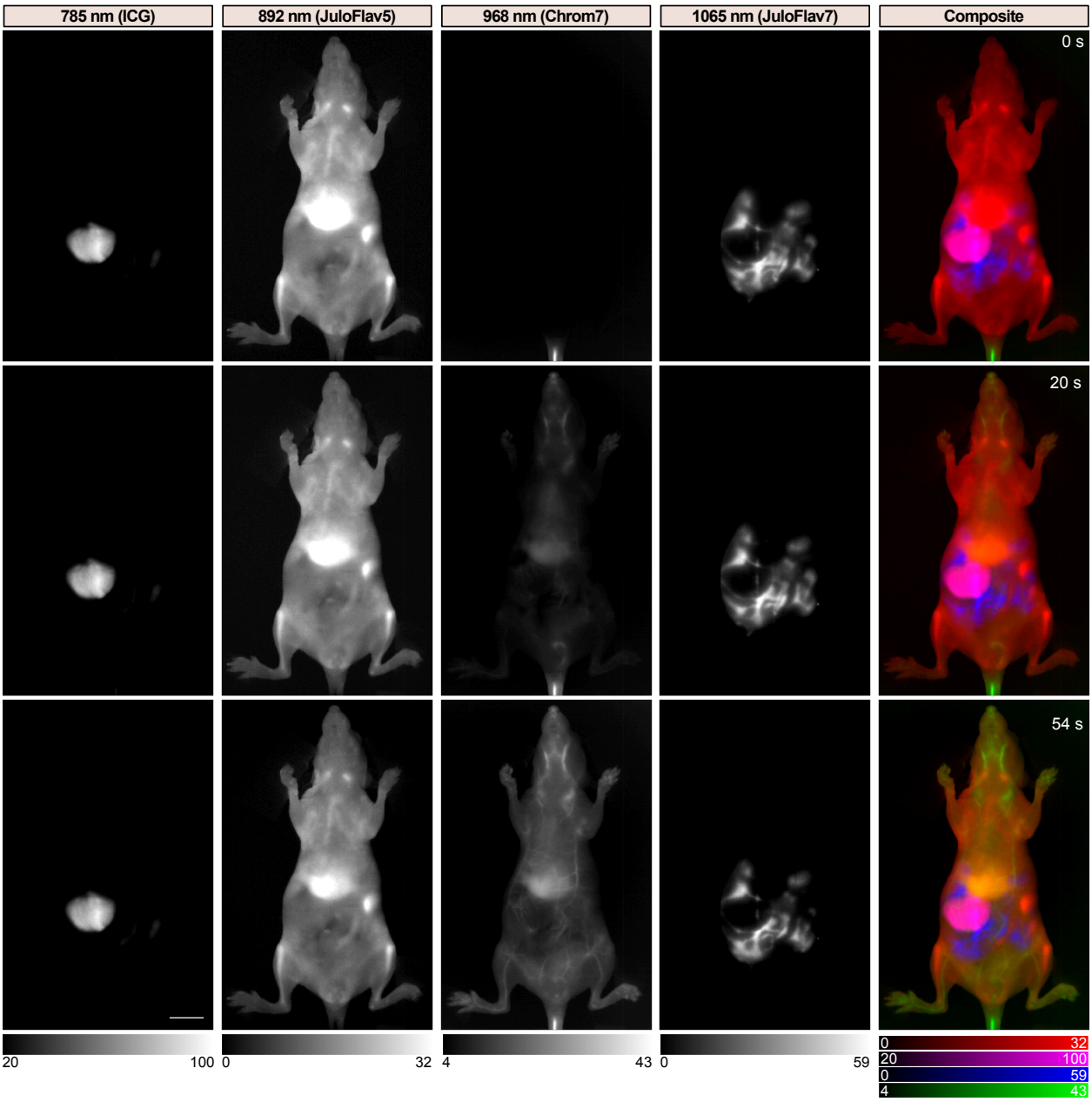

Figure S14. Video-rate 4-color imaging, with individual channels displayed, unmixed data. Injection amounts are: ICG = 200 nmol; JuloChrom5 (**10**) = 50 nmol; Chrom7 (**5**) = 45 nmol; JuloFlav7 (**3**) = 45 nmol. Ex. 785 nm (45 $mWcm^{-2}$). 892 nm (75 $mWcm^{-2}$), 968 nm (103 $mWcm^{-2}$), 1065 nm (156 $mWcm^{-2}$); collect LP1100 nm, 7.8 ms, 30 fps, single frames are displayed. Scale bar = 1 cm.

VI. Supplementary videos

Video S1. *Single color imaging at 300 fps*
One per every 4 frames was kept in an image sequence. Image sequence was reduced in file size by constant rate factor of 12, using ffmpeg (vcodec h264) and is displayed in 3-fold slow motion.
Experimental details correspond to that of ***Figure S10****.*

Video S2. *High speed 3-color imaging*
One per every 4 frames was kept in an image sequence from the unmixed data. Image sequence was reduced in file size by constant rate factor of 5, using ffmpeg (vcodec h264) and is displayed in real-time.
Experimental details correspond to that of ***Figure S11****.*

Video S3. *Video rate 4-color imaging*
No frames were omitted from the unmixed data. Image sequence was reduced in file size by constant rate factor of 14. using ffmpeg (vcodec h264) and is displayed in real-time.
Experimental details correspond to that of ***Figure 6****.*

VII. Figure experimental procedures

Figure 2, c–d. Absorption spectra were obtained of dilute dye solutions in DCM (approx. OD = 1) in a 10 mm cuvette. Spectra were baseline corrected to the signal at 1300 nm for the heptamethine dyes and to 1000 nm for **6** and **8**, 1100 nm for **10**, and 1200 nm for **4**. Spectra for **6** and **8** were corrected for non-linearity between gratings. Displayed spectra are normalized to 1.0. Emission spectra were obtained in dilute solutions of dyes in DCM (OD < 0.1) in a 10 mm cuvette, with excitation at 885 nm for the heptamethine dyes and at 755 nm for the pentamethine dyes.

Figure 2, e–g. Quantum yields were acquired as described in **Note S1**. Photophysics were acquired as described in the general experimental procedures. Brightness and "SWIR brightness" were calculated from the listed equations.

Figure 3, a–c. Excited state lifetimes were acquired and calculated as described in **Note S2**.

Figure 3, d–e. The contribution of change in k_r and k_{nr} to the $\Delta\Phi_F$ for chromenylium vs. flavylium dyes was obtained as described in **Note S3**.

Figure 4. Single crystals of dye **4** were obtained by slow evaporation from DMSO. Single crystals of dye **5** were obtained by layered diffusion of DCM with *n*-hexane. Crystallization parameters are provided in the "Crystallographic information."

Figure 5, a–c. Micelles were prepared as described in experimental procedures for **Figure S2**. MeOFlav7 micelles were prepared following literature procedure.[3] ICG was prepared in water. 2 μM solutions were prepared using dilutions from water into water, FBS, and sheep blood. Solutions were transferred to capillary tubes (Perschman DEM18 Mini Caps ISO7000), and placed in a transparent plastic holder for imaging. Imaging was performed with Goldeye G-032 in an

upright configuration with Navitar (SWIR-35) SWIR C-mount lens and LP filters (1x FELH1000 (Thorlabs), 3x LP1000 (#84-766 Edmund Optics). Camera settings were as follows: gain = 1, temperature = -30 ºC, ET = 35 ms. The excitation used 785 nm, 892 nm, and 968 nm lasers in an excitation unit with SP filters 2x FESH1000 (Thorlabs) and engineered diffuser ED1-S50 (Thorlabs). Power densities for each irradiation wavelength were as follows: 785 nm = 33 $mWcm^{-2}$; 892 nm = 54 $mWcm^{-2}$; 968 nm = 77 $mWcm^{-2}$. Excitation was modulated using external triggering, with variable "on" time to modulate effective exposure time while keeping camera exposure time at 35 ms. Images were divided by the laser "on" time used in acquisition to normalize signal across all images. A rectangular ROI was drawn over the relevant area and used to crop images to the displayed size. The intensity over this ROI (averaged in the Y dimension) is plotted below each figure. LUT table CET-L16[4] was applied to all images for manuscript display in 8-bit format.

Figure 5, d–h. Imaging was performed with Goldeye G-033 in an upright configuration with Navitar (SWIR-35) SWIR C-mount lens and LP filters 1x FELH1000 (Thorlabs), 3x LP1000 (#84-766 Edmund Optics). Camera settings were as follows: gain = 1, ET = 2 ms, frame rate = 300 fps. The Arduino-programmed laser/camera "on" time = 2000 microseconds; "off" time = 1300 microseconds. The excitation used 785 nm and 892 nm lasers in an excitation unit with SP filters 2x FESH1000 (Thorlabs) and engineered diffuser ED1-S50 (Thorlabs). Power densities for each irradiation wavelength were as follows: 785 nm = 64 $mWcm^{-2}$; 892 nm =104 $mWcm^{-2}$. The mouse was dosed with 50 nmol of each dye, delivered i.v. at the timepoints listed in the timeline in (d). Micelles of **10** were prepared as described in experimental procedures for **Figure S2**. The mouse was imaged at the timepoints after injection listed in (d). Images were analyzed by taking the intensities over the ROIs and graphing signal over the injection time (g) and relative signal of **10**/ICG (h).

Figure 6. Imaging was performed with Goldeye G-033 in an upright configuration with Navitar (SWIR-35) SWIR C-mount lens and LP filters 1x FELH1100 (Thorlabs), 2x LP1100 (#84-768 Edmund Optics). Camera settings were as follows: gain = 1, ET = 7.8 ms, frame rate = 120 fps. The Arduino-programmed laser/camera "on" time = 7800 microseconds; "off" time = 500 microseconds. The excitation used 785 nm, 892 nm, 968 nm, and 1065 nm lasers in an excitation unit with SP filters 2x SP1100 (#64-339 Edmund Optics) and engineered diffuser ED1-S50 (Thorlabs). Power densities for each irradiation wavelength were as follows: 785 nm = 45 $mWcm^{-2}$; 892 nm =75 $mWcm^{-2}$; 968 nm = 103 $mWcm^{-2}$; 1065 nm = 156 $mWcm^{-2}$. The mouse was dosed with: ICG = 200 nmol; JuloChrom5 (**10**) = 50 nmol; Chrom7 (**5**) = 45 nmol; JuloFlav7 (**3**) = 45 nmol with delivery i.v. (JuloChrom5 (**10**), ICG, Chrom7 (**5**)) or i.p. (JuloFlav7 (**3**)) at the time points listed in the timeline in (a). Micelles of **10**, **5**, and **3** were prepared as described in experimental procedures for **Figure S2**. The mouse was imaged at the time points after injection listed in the timeline in (a). Heart rate and breathing rate traces were obtained from plotting the intensity over time from the ROIs in (c). Images were linearly unmixed using an automated unmixing method using Python3 described in **Note S6**. Data are representative of two biological replicates.

VIII. Supporting figure experimental procedures

Figure S1. *Brightness comparisons in a SWIR imaging configuration in organic solvent.*
Solutions in DCM of each flavylium/chromenylium dye and in EtOH of ICG at 0.25 μM were prepared and transferred to 1.5 mL Eppendorf tubes. Imaging was performed with Goldeye G-032 in an upright configuration with Navitar (SWIR-35) SWIR C-mount lens and LP filters (1x FELH1000 (Thorlabs), 3x LP1000 (#84-766 Edmund Optics). Camera settings were as follows: gain = 1, temperature = -30 ºC, ET = 0.3–2.5 ms. The excitation used 785 nm, 892 nm, and 968 nm lasers in an excitation unit with SP filters 2x FESH1000 (Thorlabs) and engineered diffuser ED1-S50 (Thorlabs). Power densities for each irradiation wavelength were as follows: equal power densities (A): 785 nm = 100 $mWcm^{-2}$, 892 nm = 101 $mWcm^{-2}$, 968 nm = 100 $mWcm^{-2}$; equal photon number (B): 785 nm = 100 $mWcm^{-2}$, 892 = 88 $mWcm^{-2}$, 968 nm = 81 $mWcm^{-2}$; power densities scaled to INCIRP guidelines (C) 785 nm = 100 $mWcm^{-2}$, 892 nm = 163 $mWcm^{-2}$; 968 nm = 232 $mWcm^{-2}$. Images were averaged over 200 frames before analysis. Rectangular ROIs were drawn over the Eppendorf locations and used to obtain intensity values for each sample. Intensities were divided by the exposure time used for each acquisition to obtain counts/ms.

Figure S2. *Absorbance traces of PEG-phospholipid micelles of polymethine dyes.*
Micelles were fabricated according to the following procedure: 0.4 mg of each dye (dyes **3**, **4**, **5**, **6**, **8**, **10**) was dissolved in 4 mL DMSO and added to 8 mL of a 6 mg/mL solution of 18:0 PEG2000 PE (1,2-distearoyl-*sn*-glycero-3-phosphoethanolamine-*N*-[methoxy(polyethylene glycol)-2000] ammonium salt (Avanti Polar Lipids) in a 50 mL falcon tube. The solution was sonicated in a probe sonicator for 3 min on ice. The solution was then transferred to a 10 kDa MW cutoff filter (Amicon Ultra-15) and centrifuged at 4000 rpm. Sequential washes with 1x PBS were performed, until the remaining DMSO consisted of <1%. The micelles were then concentrated by centrifugation (4000 rpm) to ~12.5 mL. Concentrations were calculated according to **Note S4**. Absorbance traces were obtained without dilution in a 2 mm cuvette. Spectra were baseline corrected to the signal at 1300 nm. Displayed spectra are normalized to 1.0.

Figure S3. *Dynamic light scattering (DLS) characterization of PEG-phospholipid micelles.*
Size data by DLS were acquired after a 1:100 (20 μL to 2 mL, 14 μM with respect to the lipid) dilution in MilliQ water, after filtering through a 0.22 μm cellulose acetate syringe filter. SOP parameters were as follows: sample refractive index 1.4, 3 measurements, no delay between measurements, 25 °C with 120 second equilibration time. Zeta measurements were acquired with the standard operating procedure parameters: five measurements, 10–50 runs, no delay between measurements, 25 °C with a 60 second equilibration time. The material was indicated as mPEG-DSPE with RI at 1.400 and absorption at 0.001. The dispersant was indicated as water with RI at 1.330. A Smolvchowski model was applied as a general option. Data is representative of five replicate measurements. Errors are the standard deviations of the five replicates.

Figure S4. *Visible light photographs of the capillary imaging configuration.*
Experimental procedures are reported in the procedures for **Figure 5a–c** and **Figure S5**.

Figure S5. *Brightness comparisons in imaging configuration using equal power densities and equal photon numbers.*

Experimental procedures are reported in the procedures for **Figure 5a–c**, but with different irradiation power densities. Power densities for the experiment with equal power densities (A–C) were: 785 nm = 33 $mWcm^{-2}$; 892 nm = 33 $mWcm^{-2}$; 968 nm = 33 $mWcm^{-2}$. Power densities for equal photon numbers (D-F) were: 785 nm = 33 $mWcm^{-2}$; 892 nm = 29 $mWcm^{-2}$; 968 nm = 27 $mWcm^{-2}$.

Figure S6. *Graphs from brightness comparison in **Figure 5a-c** and **Figure S5** displayed individually for visual clarity.*
Experimental procedures are reported in the procedures for **Figure 5a–c** and **Figure S5**.

Figure S7. *Images from comparative brightness experiment taken after ICG injection and before and after injection of JuloChrom5 (**10**), showing residual signal from ICG in the 892 nm channel.*
Experimental procedures are reported in the procedures for **Figure 5d–h**.

Figure S8. *Replicate in vivo comparative brightness experiment.*
Experimental procedures are reported in the procedures for **Figure 5d–h**.

Figure S9. *Signal to noise (SNR) analysis of images from in vivo comparative brightness experiment*.
Experimental procedures are reported in the procedures for **Figure 5d-h**.

Figure S10. *Single color imaging at 300 fps.*
Imaging was performed with Goledye G-033 in an upright configuration with Navitar (SWIR-35) SWIR C-mount lens and LP filters 1x FELH1150 (Thorlabs), and 1x LP1100 (#84-768 Edmund Optics). Camera settings were as follows: gain = 1, ET = 3 ms, frame rate = 300 fps. The excitation used 968 nm laser in an excitation unit with SP filter 1x SP1100 (#64-339 Edmund Optics) and engineered diffuser ED1-S50 (Thorlabs). Power density of irradiation was 100 $mWcm^{-2}$. The mouse was dosed with 141 nmol Chrom7 (**5**) i.v.

Figure S11. *High-speed three-color imaging.*
Imaging was performed with Goldeye G-033 in an upright configuration with Navitar (SWIR-35) SWIR C-mount lens and LP filters 1x FELH1000 (Thorlabs), 2x LP1000 (#84-768 Edmund Optics). Camera settings were as follows: gain = 1, ET = 3.3 ms, frame rate = 300 fps. The Arduino-programmed laser/camera "on" time = 2800 microseconds; "off" time = 500 microseconds. The excitation used 785 nm, 892 nm, 968 nm lasers in an excitation unit with SP filters 2x FESH1000 (Thorlabs) and engineered diffuser ED1-S50 (Thorlabs). Power densities for each irradiation wavelength were as follows: 785 nm = 80 $mWcm^{-2}$; 892 nm =87 $mWcm^{-2}$; 968 nm = 94 $mWcm^{-2}$. The mouse was dosed with: Chrom5 (**6**) = 130 nmol; JuloFlav5 (**4**) = 80 nmol; Chrom7 (**5**) = 110 nmol with delivery i.v. (Chrom5 (**6**), Chrom7 (**5**)) or i.p. (JuloFlav5 (**4**)) at the timepoints indicated in the timeline in (A). Micelles of **6, 5**, and **4** were prepared as described in experimental procedures for **Figure S2**. The mouse was imaged at the time points after injection listed in the timeline in (A). Images were manually unmixed using the following equations:

$$980_f = 980_r - (0.28 * 892_r) \quad \text{Eq. 1}$$

$$892_f = 892_r - (0.4 * 785_r - (0.6 * 968_f)) \quad \text{Eq. 2}$$

$$785_f = 785_r - (0.2 * 980_r - (0.11 * 785_r)) \quad \text{Eq. 3}$$

Where the subscripts (f) and (r) represent “final” and “raw” images, respectively.

Figure S12–14. *Video-rate 4-color imaging.*
Experimental procedures are reported in the procedures for **Figure 6**.

IX. Supplementary notes

Note S1. Photoluminescence quantum yield measurements

The photoluminescence quantum yield (Φ_F) of a molecule or material is defined as follows,

$$\Phi_F = \frac{P_E}{P_A} \quad \text{(Eq. 4)}$$

where P_E and P_A are the number of photons absorbed and emitted, respectively. To determine the quantum yield, we either use a relative method with a known standard in the same region of the electromagnetic spectrum, or an absolute method, in which the number of photons absorbed and emitted are measured independently. Here, we used (1) a relative method with IR-26 as the known standard for all new heptamethine derivatives (**5**, **7**, **9**) and (2) an absolute method for all pentamethine derivatives (**2**, **4**, **6**, **8**, **10**). Quantum yields for dyes 1 and 3 were taken from measurements acquired previously.[3]

(1) For the relative method, to compare an unknown to a reference with a known quantum yield, the following relationship was used:

$$\Phi_{F,x} = \Phi_{F,r}(m_x/m_f)(\eta_x{}^2/\eta_r{}^2) \quad \text{(Eq. 5)}$$

where m represents the slope of the line (y = mx + b) obtained from graphing integrated fluorescence intensity versus optical density across a series of samples, η is the refractive index of the solvent, and the subscripts x and r represent values of the unknown and reference, respectively. The ($\Phi_{F,r}$) of IR-26 was taken to be a constant, 0.05%, as we have previously measured,[5] and which agrees with several recent measurements.[6,7]

Here, we measured relative fluorescence quantum yields of each dye in DCM. To obtain a plot of integrated fluorescence intensity versus absorbance for the reference and unknown, five solutions and a solvent blank were prepared and their absorbance and emission spectra (with an excitation wavelength of 885 nm) were acquired. IR-26 and the unknown dyes were diluted in DCM to concentrations with optical densities less than 0.1 to minimize effects of reabsorption. The baseline corrected (to 1500 nm) fluorescence traces were integrated, and the raw integrals were corrected by subtracting the integral over an identical range from fluorescence traces of the blank solvent. The integrated fluorescence intensities were then plotted against the baseline corrected absorbance values at the relevant wavelength (885 nm), and the slope and error in slope were obtained ($R^2 >$ 0.99 for all traces) (**Figure S15**).

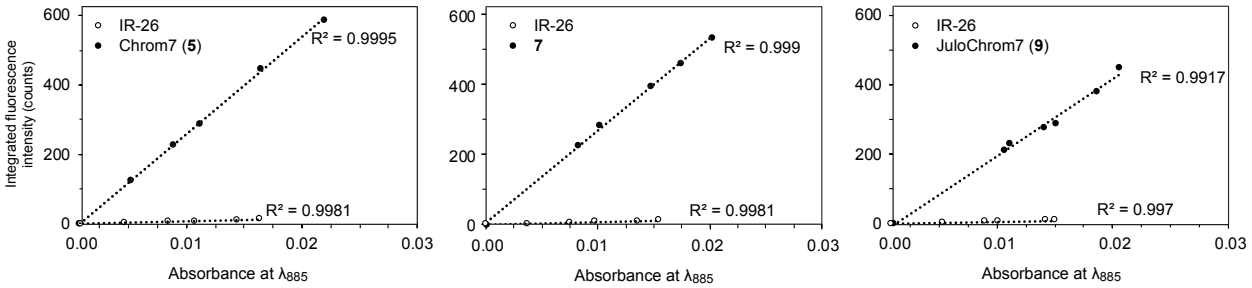

Figure S15. Integrated fluorescence intensity vs. absorbance at 885 nm plots for IR-26 vs. each unknown dye sample in DCM.

The refractive indices were omitted from the calculation as all samples were measured in the same solvent (DCM). The fluorescence quantum yields were then calculated using **Eq. 5** and are reported in **Figure 2g** and **Table S1**. Error measurements were propagated from the error in slope of the reference and the unknown.

The methods employed here were validated with comparison of IR-26 to IR-1061, giving a Φ_F value of 0.32 ± 0.01 %, which agrees with our prior absolute quantum yield measurement.[5]

Acquisition settings for relative fluorescence quantum yield measurements: For quantum yield measurements, fluorescence traces were acquired with ex. 885 nm with a 900 nm SP filter (Thorlabs FES 900) and collection from 920– or 930–1500 nm. The slits were 5.76 mm (15 nm) for excitation and 11.52 mm (30 nm) for emission. The step size used was 1.0 nm, integration time 0.1 s, and traces were acquired after an automatic detector background subtraction, and with the default excitation correction. Absorbances traces were acquired with a 2000 nm/min acquisition speed, and a 1 nm step size, after blanking with dichloromethane. All samples were observed an OD of ≤0.1 to minimize sample reabsorption effects.

(1) For absolute quantum yield measurements, an integrating sphere was used (Horiba KSPHERE-Petite). Detector-corrected emission traces (collecting over the spectral region containing emission of the sample, λ_{em}) and "excitation traces" (emission spectra collecting over the spectral region containing the excitation wavelength, λ_{ex}) of the sample dissolved in DCM (sample, x) and DCM in the absence of sample (solvent, r) were collected. From these traces, absolute quantum yields were calculated from the following equation:

$$\Phi_F = \frac{P_E}{P_A} = \frac{\int_{\lambda_{em}} (I_x(\lambda_{em}) - I_r(\lambda_{em}))\, d\lambda_{em}}{\int_{\lambda_{ex}} (I_r(\lambda_{ex}) - I_x(\lambda_{ex}))\, d\lambda_{ex}} \quad \text{(Eq. 6)}$$

Where, I = intensity. All reported quantum yields are the average of three independent measurements and the error is taken as the standard deviation.

Acquisition settings for absolute fluorescence quantum yield measurements: Samples in a 10 mm x 10 mm quartz cuvette were illuminated with the excitation lamp on the fluorometer and detected at 90º. Direct scatter into the detector is obfuscated by a Teflon baffle. Step sizes of 1 nm, and integration times of 0.1 s were used. A correction file was used to account for the non-linearity of the detector. All samples were observed an OD of ≤0.1 to minimize sample reabsorption effects. Parameters which were variable for each sample are outlined in **Table S4.**

Table S4. Acquisition settings for fluorescence quantum yield measurements.

Dye	Ex. λ (nm)	λ_{ex}(nm)	λ_{em} (nm)	Ex. slits (nm)	Em. slits (nm)
2 (Flav5)	808	778–830	850–1300	14	21
4 (JuloFlav5)	770	740–800	810–1230	11.5	11.5
6 (Chrom5)	750	720–780	780–1200	12	12
8	750	720–780	780–1200	12	12
10 (JuloChrom5)	770	740–800	800–1220	12	12

Photoluminescence quantum yields are displayed in **Figure 2g**, and with errors in **Table S1**.

Note S2. Time Resolved Photoluminescence (TRPL) Measurements

We recorded PL lifetimes using a home-built, all-reflective epifluorescence setup. Dye sample solutions (OD ~1.0) were excited at the front of a 1 cm cuvette using the pulsed laser output from an optical parametric amplifier [Spirit-OPA, MKS-Spectra Physics] pumped by ytterbium-fiber amplified pulsed laser (1040 nm, 29µJ, ~300 fs, at 10 kHz with pulse-picker) [Spirit HE 30, MKS-Spectra Physics]:

For the heptamethine dyes, the OPA excitation was tuned to 970 nm (70 µJcm^{-2}, ~200 fs) and the emission was then collected and filtered with a 90:10 beamsplitter [BSX10R, Thorlabs], two 1000 nm longpass filters [10CGA-1000, Newport], one 1050 nm longpass filter [FELH1050, Thorlabs], and a hot mirror [10HMR-0, Newport] and finally reflectively coupled into a single-mode fiber [F-SMF-28-C-10FC, Newport] and detected using a superconducting nanowire single photon detector (SNSPD, IRF = 47 ± 1 ps) [Quantum Opus One].

For the pentamethine dyes, the OPA excitation was tuned to 780 nm (900-100 µJcm^{-2}, ~200 fs) and the emission was then collected and filtered with the 90:10 beamsplitter, one 800 nm longpass filters [10CGA-800, Newport], two 830 nm longpass filter [10CGA-800, Newport], and the hot mirror and finally reflectively coupled into the single-mode fiber and detected using a superconducting nanowire single photon detector (SNSPD) (IRF = 59 ± 1 ps) [Quantum Opus One].

Time correlated single photon counting (TCSPC) traces were histogrammed using a HydraHarp 400 and corresponding software [Picoquant]. All measurements were carried out at room temperature. Curve fitting was performed with Igor Pro.

The instrument response function (IRF) was determined from the weighted average of two gaussian curves (**Figure S16**).

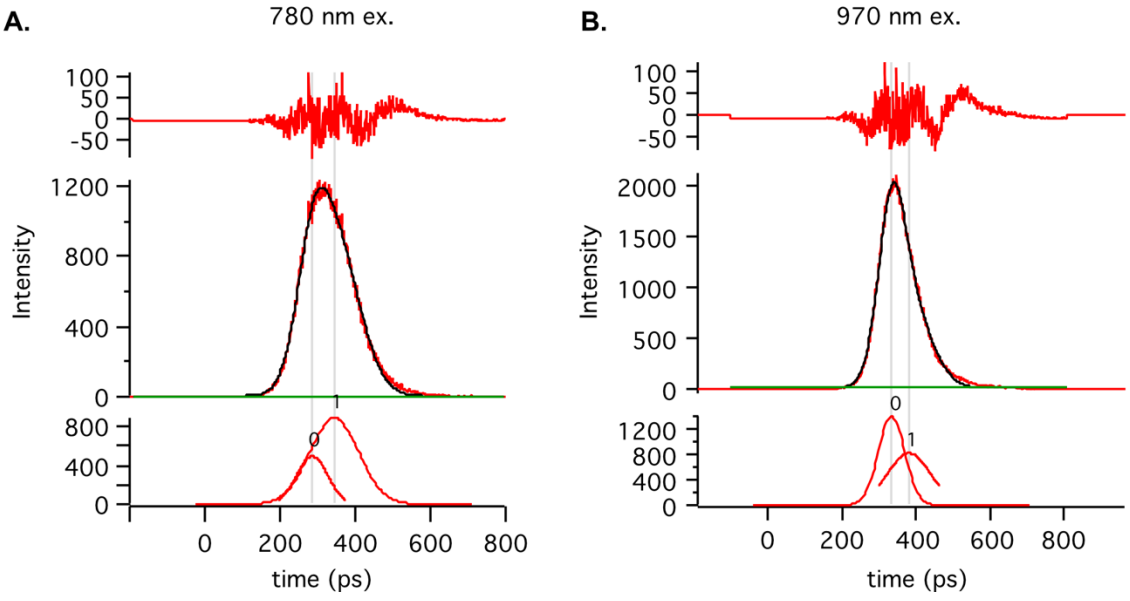

Figure S16. Instrument response functions and multipeak fits for a) 780 nm ex. used for all pentamethine dyes and b) 970 nm ex. used for all heptamethine dyes.

TRPL decay curves were fit to a single exponential using the convolution integral of the IRF and the impulse response function (**Figure S17**):

$$I(t) = \left(\frac{a}{2}\right)\left(e^{-k\left((t-t_o)-\frac{\sigma^2 k}{2}\right)}\right)\left(1+\text{erf}\left[\frac{(t-t_o)-\sigma^2 k}{\sqrt{2}\sigma}\right]\right)+c \qquad \text{(Eq. 7)}$$

where I = intensity, a = amplitude, k = total excited state decay rate, t = time, t_o = initial time, σ = IRF width, and c = constant.

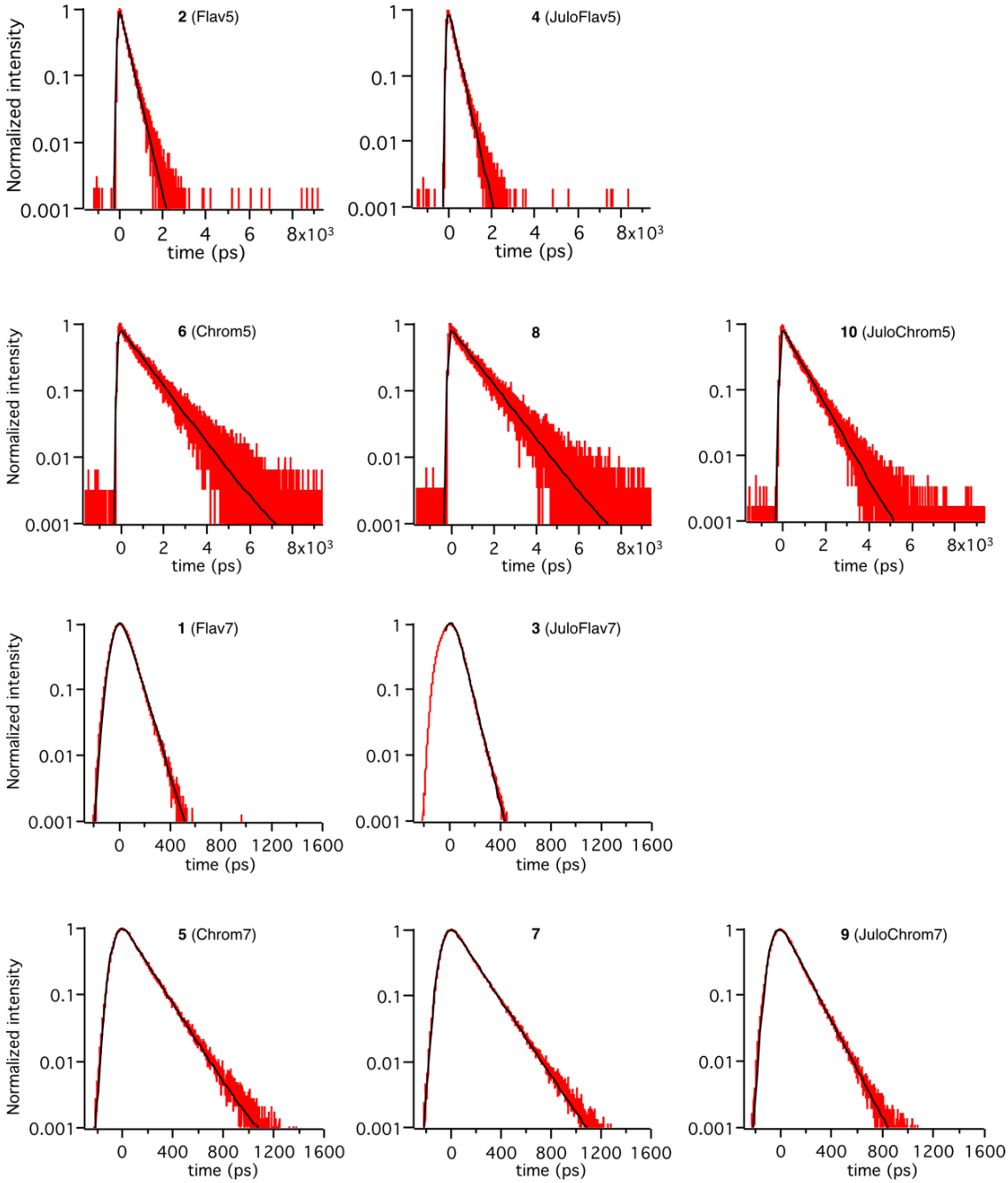

Figure S17. Decay curves (red) and single exponential fits (black).

The excited state lifetime is defined as the inverse of total excited state decay rate:

$$\tau = \frac{1}{k} \quad \text{(Eq. 8)}$$

Errors in τ were taken as ± 1 ps, the value of the detector resolution. Errors in fitting parameters were sufficiently small such that they are negligible when considering the detector resolution.

The radiative (k_r) and non-radiative (k_{nr}) rates were calculated according to the following equations:

$$k_r = \frac{\Phi_F}{\tau} \quad \text{(Eq. 9)}$$

$$k_{nr} = \frac{1-\Phi_F}{\tau} \quad \text{(Eq. 10)}$$

Errors in k_r and k_{nr} were taken as the propagated error from the errors in τ and Φ_F.

Lifetimes and radiative and non-radiative rates, are displayed in **Figure 3a**, and with errors in **Table S3.**

Note S3. **Contribution of change in k_r and k_{nr} to the $\Delta\Phi_F$ for chromenylium vs. flavylium dyes**

The relative contribution of k_r and k_{nr} to the $\Delta\Phi_F$ between the chromenylium and flavylium dye structures was determined according to the following analysis.

From the definition of Φ_F in terms of k_r and k_{nr}:

$$\Phi_F(k_r, k_{nr}) = \frac{k_r}{k_r + k_{nr}} \quad \text{(Eq. 11)}$$

The change in fluorescence quantum yield, $\Delta\Phi_F$, can be determined by:

$$\Delta\Phi_F(k_r, k_{nr}, \Delta k_r, \Delta k_{nr}) = \Phi_F(k_r + \Delta k_r, k_{nr} + \Delta k_{nr}) - \Phi_F(k_r, k_{nr}) \quad \text{(Eq. 12)}$$

Where each rate constant (k_r, k_{nr}) represents that of the flavylium dye and each change in rate constant, ($\Delta k_r, \Delta k_{nr}$) represents the difference in rate constant between the chromenylium and flavylium dyes (chromenylium – flavylium). Eq. 9 can be divided into components:

$$\Delta\Phi_F(k_r, k_{nr}, \Delta k_r, \Delta k_{nr}) =$$

$$\Delta\Phi_F(k_r, k_{nr}, \Delta k_r, 0) + \Delta\Phi_F(k_r, k_{nr}, 0, \Delta k_{nr}) + \mathcal{O}_{\Delta k_r \Delta k_{nr}} \quad \text{(Eq. 13)}$$

Since the mixed partial derivatives of $\Phi_F(k_r, k_{nr})$ with respect to k_r and k_{nr} are non-zero, i.e. $\frac{\partial}{\partial k_r}\frac{\partial}{\partial k_{nr}}\Phi_F(k_r, k_{nr}) \neq 0$, then $\mathcal{O}_{\Delta k_r \Delta k_{nr}} \neq 0$. Simultaneous changes in k_r and k_{nr} result in a component that can change $\Phi_F(k_r, k_{nr})$ depending on both k_r and k_{nr} together. Hence accounting for the total change in $\Phi_F(k_r, k_{nr})$ in terms of the separate changes of k_r and k_{nr} is not possible. Therefore, we determine the remaining term requiring the non-linear mixing of changes in both k_r and k_{nr} together, $\mathcal{O}_{\Delta k_r \Delta k_{nr}}$, from the unaccounted fraction in the change. The relative contribution from each component in the equation to the overall $\Delta\Phi_F$ can be calculated as a ratio of $\Delta\Phi_F$ attributed to each component over the total $\Delta\Phi_F$ resulting from all components:

$$R_{\Delta k_r} = \frac{\Delta\Phi_F(k_r, k_{nr}, \Delta k_r, 0)}{\Delta\Phi_F(k_r, k_{nr}, \Delta k_r, \Delta k_{nr})} \quad \text{(Eq. 14)}$$

Eq. 14 gives the ratio component of the $\Delta\Phi_F$ attributed solely to the change in k_r.

$$R_{\Delta k_{nr}} = \frac{\Delta\Phi_F(k_r, k_{nr}, 0, \Delta k_{nr})}{\Delta\Phi_F(k_r, k_{nr}, \Delta k_r, \Delta k_{nr})} \quad \text{(Eq. 15)}$$

Eq. 15 gives the ratio component of the $\Delta\Phi_F$ attributed solely to the change in k_{nr}.

$$R_{\mathcal{O}_{\Delta k_r \Delta k_{nr}}} = 1 - \left(R_{\Delta k_r} + R_{\Delta k_{nr}}\right) = \frac{\mathcal{O}_{\Delta k_r \Delta k_{nr}}}{\Delta\Phi_F(k_r, k_{nr}, \Delta k_r, \Delta k_{nr})} \quad \text{(Eq. 16)}$$

Eq. 16 gives the ratio component of the $\Delta\Phi_F$ due to both the non-radiative and radiative component simultaneously changed leading to even further non-linear change of the quantum yield as the non-radiative and radiative rates act together.

The values of $R_{\Delta k_r}$, $R_{\Delta k_{nr}}$, and $R_{\mathcal{O}_{\Delta k_r \Delta k_{nr}}}$ were determined for each chromenylium dye compared to the closest structurally analogous flavylium dye, to best represent the impact of structural changes at the C2 position of the heterocycle. These pairs are outlined in the Figure 3d. The resulting contributions to overall $\Delta\Phi_F$ are plotted in Figure 3e.

The analysis used here to compare of k_r and k_{nr} contributions to $\Delta\Phi_F$ is limited to cases where a change in Φ_F is observed between chromophores, and to cases where the non-linear component is non-negative and is not the dominating contributor to change in Φ_F.

Note S4. *Photobleaching experiments*

Solutions of dye in DMSO were prepared and diluted to an optical density of ~1, as measured by a JASCO V-770 UV-Vis/NIR spectrophotometer. Solutions were drawn up into capillary tubes (Drummond, 0.4 mm I.D., 75 mm) and placed in a capillary holder for alignment. Images were acquired of three capillary tube samples using 1,100 nm LP filtering (1x 1,100 nm and 2x 1,150 nm LP filters were used: (Edmund Optics, #84766) and (Edmund Optics, #89665)). Solutions were irradiated with a "784 nm" laser (LUMICS, LU0785D250-U70AN), or "974 nm" laser (LUMICS, LU0975DLU350-S30AN03) (all set to 100 $\pm$ 0.5 mWcm^{-2}) and images were collected between 20 and 100 fps with variable exposure times depending on the brightness of the sample (Flav7 = 8 ms, 100 fps; Chrom7 = 15 ms, 67 fps; Flav5 = 5 ms, 100 fps, Chrom5 = 50 ms, 20 fps). As intensity changes were small on the ms scale, frames corresponding to seconds in integers were analyzed. Additional frames were omitted from the analysis for simplicity. Images were background subtracted using a frame collected using no laser irradiation, and a linear roi was drawn along the length of each tube. The normalized average intensity (colors) and standard deviation (grey) of the three trials are plotted below as raw data (**Figure S18**).

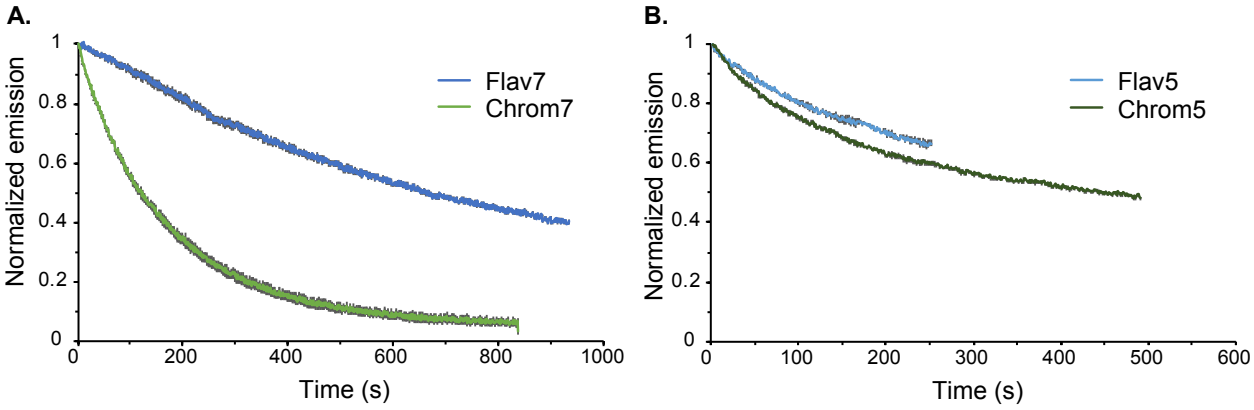

Figure S18. Raw photobleaching data obtained for heptamethine dyes (A) using 974 nm irradiation and pentamethine dyes (B) using 786 nm irradiation.

All photobleaching data were fit to a mono-exponential decay and the rate constants were obtained from the first order reaction equation:

$$\ln[A] = -kt + \ln[A_o] \qquad \text{(Eq. 17)}$$

where A and A_o represent the emission collected at time t and the initial emission collected, respectively. All R^2 values were > 0.95. The raw photobleaching rates (k_{raw}) are reported below (Table S5).

The raw photobleaching rates were corrected by the photon flux density absorbed by the sample (N_{abs}) (cm^{-2} s^{-1}). N_{abs} is dependent on the photon flux density of irradiated photons, (N_p) and the optical density of the sample at the wavelength of irradiation (Abs), according to the following equations:

$$N_p = Fluence \div \frac{hc}{\lambda} \qquad \text{(Eq. 18)}$$

$$N_{Abs} = N_p \times (1 - 10^{-Abs}) \quad \text{(Eq. 19)}$$

$$k_{rel} = k_{raw}/N_{Abs} \quad \text{(Eq. 20)}$$

Where *Fluence* is measured in W cm^{-2}, h is Planck's constant (J s), and c is the speed of light (m s^{-1}), and λ is wavelength (m).

Each rate was normalized to the rate seen with Flav5 such that:

$$\text{Relative stability} = k_{rel\,(Flav)}/k_{rel\,(dye)} \quad \text{(Eq. 21)}$$

Values for *Fluence*, *Abs*, N_{abs}, k_{rel}, and relative stability are displayed in Table S5.

Equation 19 is derived from the definition of transmittance:

$$Abs = -log_{10}\left(\frac{I}{I_o}\right) \quad \text{(Eq. 22)}$$

$$I = I_o 10^{-Abs} \quad \text{(Eq. 23)}$$

$$N_{Trans} = N_p 10^{-Abs} \quad \text{(Eq. 24)}$$

$$N_{Abs} = N_p - N_{Trans} \quad \text{(Eq. 25)}$$

$$N_{Abs} = N_p \times (1 - 10^{-Abs}) \quad \text{(Eq. 19)}$$

Where I = transmitted intensity, I_o = incident intensity, N_{trans} = photon flux density of transmitted photons.

Table S5.

Sample	λ_{ex} (nm)	*Fluence* (Wcm^{-2})	k_{raw} (s^{-1})	*Abs*	N_{abs} (cm^{-2}s^{-1})	k_{rel} (s^{-1})	relative stability (to Flav dye)
Flav7 (**1**)	974	0.100	0.00100	0.57	3.58 x10^{17}	2.80 x 10^{-21}	1.00
Chrom7 (***5***)	974	0.100	0.00328	0.91	4.30 x10^{17}	7.62 x 10^{-21}	0.37
Flav5 (**2**)	786	0.100	0.00155	0.26	1.77 x10^{17}	8.73 x 10^{-21}	1.00
Chrom5 (***6***)	786	0.100	0.00132	0.45	2.55 x10^{17}	5.19 x 10^{-21}	1.68

To compare photobleaching rates to each other by the k_{rel} value, we predicted that the photobleaching rate k_{rel} will be constant across different N_{abs} values. We tested this by performing photobleaching experiments on Flav7 at three different power densities (100 mWcm^{-2}, 50 mWcm^{-2} and 30 mWcm^{-2}), and obtained results within 5% error from each other.

We also anticipated that the photobleaching rate k_{rel} would be constant across different wavelengths of excitation. To test the second prediction, Chrom7 was photobleached with two different laser wavelengths (784 nm and 974 nm), and we observed a 34% lower rate for the 784

nm case compared to the 974 nm case. Additionally, Flav5 was photobleached using a 784 nm laser and an 890 nm laser, which resulted in a 20% lower photobleaching rate for 784 nm vs 890 nm. Thus, substantial differences are obtained when comparing between laser wavelengths, and we have chosen to present relative stability data only when the excitation source is constant. If other comparisons are made, the 20–35% error we observed between rates should be considered.

Note S5. **Determination of dye concentration within micelles**

As micelle fabrication includes several washing and transfer steps, and various amounts of dye could be lost from the nanomaterial during these steps, we applied a method to allow accurate quantification of the amount of dye in a micelle solution.

After micelle fabrication (see experimental procedures for Figure S2), an aliquot was removed from the micelle stock and lyophilized overnight. The resulting dry powder was dissolved in DCM for analysis by UV-VIS spectroscopy. The concentration of the dye in organic solvent was determined using Beer's law, $c = \frac{\varepsilon \times l}{A}$ and correlated to the appropriate volume of the original aliquot to determine dye concentration in the aqueous micellular solution.

Note S6. **Method description – Linear Unmixing**

The excitation spectra of the dyes used in these experiments have some overlap between imaging channels. We use a linear unmixing method to generate images representing the quantity of each dye present in an image, enhancing contrast and simplifying interpretation. We assume that each dye has a consistent excitation spectrum, which is linear with concentration. We also assume that the signals are additive, such that the signal measured at each pixel for a given laser can be expressed as:

$$I(\lambda_1) = \eta(\lambda_1) + c_{dye1}A_{dye1}(\lambda_1) + c_{dye2}A_{dye2}(\lambda_1)\ldots \quad \text{(Eq. 26)}$$

where η is the background signal (camera noise, stray light, etc), c is the concentration of the dye, and A is the signal generated by that dye. Overall this leads to a system of equations:

$$\underline{I} = \underline{\underline{A}}\,\underline{c} + \underline{\eta} \quad \text{(Eq. 27)}$$

where the number of underlines represents the number of dimensions for the quantity (vector vs. matrix). Thus, our task is to determine A and η, such that we can convert from a signal measured in intensity space to a signal in concentration space.

We measure noise by obtaining images of a blank field of view, which are then subtracted from subsequent measurements. To calibrate the relative amount of signal emitted by each dye in each imaging channel, we begin by placing vials containing solutions of each dye in the field of view and acquire images, using the same conditions as in the *in vivo* experiments. We select regions of interest (ROI) representing each vial, and determine the mean signal generated by each dye, in each imaging channel. Inversion of Eq. 27 yields a value for A, which is then used to generate unmixed images representing the contribution of each dye to the overall signal. The unmixing process was implemented in Python 3.7.3 with numpy 1.16.2 on Windows 10 64-bit.

X. Synthetic procedures and characterization

General procedures

Chemical reagents were purchased from Accela, Acros Organics, Alfa Aesar, Carl Roth, Fisher Scientific, Sigma-Aldrich, or TCI and used without purification unless noted otherwise. Anhydrous and deoxygenated solvents (toluene, THF) were dispensed from a Grubb's-type Phoenix Solvent Drying System constructed by JC Meyer. Anhydrous solvent (*n*-butanol) was prepared by drying over 4 Å molecular sieves for at least 3 days. Oxygen was removed by three consecutive freeze–pump–thaw cycles in air-free glassware directly before use.

Synthetic procedures:

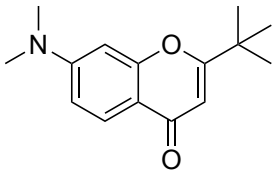

2-(*tert*-butyl)-7-(dimethylamino)-4*H*-chromen-4-one (**S3a**): 3-(dimethylamino)phenol (299 mg, 2.18 mmol, 1.00 equiv.) and ethyl pivaloylacetate (700 µL, 3.93 mmol, 1.00 equiv.) were combined in an oven-dried 1 dram vial and heated at 180 ºC for 40 h. The solution was cooled to room temperature, evaporated onto silica, and purified via column chromatography with a 10:1 to 4:1 hexanes/EtOAc gradient. The procedure gave a light pink solid (238 mg, 0.970 mmol, 45%). R_f = 0.4 in 1:2 hexanes/EtOAc. ^{1}H NMR (300 MHz, Chloroform-*d*) δ 7.96 (d, *J* = 9.0 Hz, 1H), 6.70 (dd, *J* = 9.0, 2.4 Hz, 1H), 6.45 (d, *J* = 2.4 Hz, 1H), 6.10 (s, 1H), 3.05 (s, 6H), 1.30 (s, 9H). ^{13}C NMR (126 MHz, Chloroform-*d*) δ 178.4, 174.7, 158.6, 154.1, 126.4, 113.1, 110.5, 106.1, 97.0, 40.2, 36.3, 28.0. HRMS (ESI$^+$) calcd for $C_{15}H_{20}NO_2^+$ $[M+H]^+$: 246.1489; found: 246.1482. Absorbance (CH_2Cl_2): 264, 296, 337 nm.

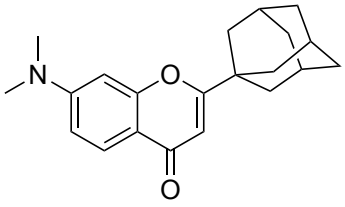

2-((3*r*,5*r*,7*r*)-adamantan-1-yl)-7-(dimethylamino)-4*H*-chromen-4-one (**S3b**): 3-(dimethylamino)phenol (150 mg, 1.09 mmol, 1.00 equiv.) and ethyl 3-(1-adamantyl)-3-oxopropionate (316 µL, 1.31 mmol, 1.20 equiv.) were added to a glass 10 mL microwave vial and heated to 240 ºC for 3 min. The crude product was cooled and evaporated onto silica for purification via column chromatography with a 10:1 to 3:1 hexanes/EtOAc gradient. Impure fractions were further purified with a 250:1 to 14:1 toluene/acetone gradient to obtain a grey solid (99.6 mg, 0.308 mmol, 28%). R_f = 0.4 in 1:2 hexanes/EtOAc. ^{1}H NMR (500 MHz, Chloroform-*d*) δ 7.96 (d, *J* = 9.0 Hz, 1H), 6.71 (dd, *J* = 9.1, 2.5 Hz, 1H), 6.46 (d, *J* = 2.4 Hz, 1H), 6.03 (s, 1H), 3.06 (s, 6H), 2.17 – 2.03 (m, 3H), 1.93 (d, *J* = 3.0 Hz, 6H), 1.84 – 1.65 (m, 6H). ^{13}C NMR (126 MHz, Chloroform-*d*) δ 178.6, 174.6, 158.7, 154.1, 126.5, 113.4, 110.5, 106.0, 97.1, 40.3, 39.6, 38.0, 36.6, 28.1. HRMS (ESI$^+$) calcd for $C_{21}H_{26}NO_2^+$ $[M+H]^+$: 324.1958; found: 324.1949. Absorbance (CH_2Cl_2): 264, 297, 339 nm.

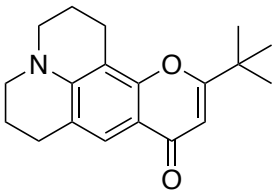

11-(*tert*-butyl)-2,3,6,7-tetrahydro-1*H*,5*H*,9*H*-pyrano[2,3-*f*]pyrido[3,2,1-*ij*]quinolin-9-one (**S3c**): 8-hydroxyjulolidine (315 mg, 1.66 mmol, 1.00 equiv) and ethyl pivaloylacetate (500 µL, 2.81 mmol, 1.69 equiv.) were added to a 20 mL vial, and heated at 180 ºC for 48 h. The solution was cooled to room temperature, evaporated onto silica, and purified via column chromatography with an 8:1 to 3:1 hexanes/EtOAc gradient to yield an off-white solid (295 mg, 0.992 mmol, 60%). R_f = 0.4 in 1:2 hexanes/EtOAc. ^{1}H NMR (600 MHz, Chloroform-*d*) δ 7.53 (s, 1H), 6.05 (s, 1H), 5.25 (s, 1H), 3.27 – 3.15 (m, 4H), 2.83 (t, *J* = 6.5 Hz, 2H), 2.74 (t, *J* = 6.2 Hz, 2H), 1.96 (p, *J* = 6.3 Hz, 2H), 1.90 (p, *J* = 6.2 Hz, 2H), 1.27 (s, 9H). ^{13}C NMR (126 MHz, Chloroform-*d*) δ 178.4, 173.9, 153.9, 146.9, 122.1, 119.9, 112.2, 105.58, 105.55, 49.9, 49.4, 36.4, 28.1, 27.6, 21.5, 20.7, 20.5. HRMS (ESI$^+$) calcd for $C_{19}H_{24}NO_2^+$ $[M+H]^+$: 298.1802; found: 298.1793. Absorbance (CH_2Cl_2): 272, 300, 355 nm.

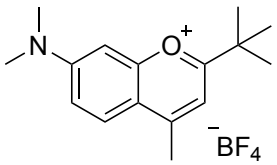

2-(*tert*-butyl)-7-(dimethylamino)-4-methylchromenylium tetrafluoroborate (**S4a**): Chromone **S3a** (500 mg, 2.04 mmol, 1.00 equiv.) was dissolved in THF (20 mL) in a flame-dried 100 mL 3-neck flask in an N_2 atmosphere. The solution was cooled to 0 ºC, and methylmagnesium bromide (1.0 M in THF, 5.1 mL, 2.5 equiv.) was added dropwise. The reaction mixture was warmed to room temperature and stirred for 21 h. The reaction was quenched with fluoroboric acid (50% aqueous, 300 µL), and with the addition of 5% fluoroboric acid, extracted into DCM. The extract was dried with Na_2SO_4, filtered, and evaporated. The crude product was purified by precipitation upon addition of EtOAc, filtration, and rinsing with additional EtOAc to yield a bright orange solid (604 mg, 1.82 mmol, 89%). ^{1}H NMR (500 MHz, Acetone-d_6) δ 8.27 (d, *J* = 9.6 Hz, 1H), 7.59 (dd, *J* = 9.6, 2.5 Hz, 1H), 7.50 (s, 1H), 7.25 (d, *J* = 2.6 Hz, 1H), 3.45 (s, 6H), 2.93 (s, 3H), 1.52 (s, 9H). ^{13}C NMR (126 MHz, Acetone-d_6) δ 181.0, 166.1, 160.5, 159.1, 129.7, 119.2, 118.3, 112.5, 96.7, 41.2, 38.7, 28.3, 20.0. HRMS (ESI$^+$) calcd for $C_{16}H_{22}NO^+$ $[M]^+$: 244.1696; found: 244.1693. Absorbance (CH_2Cl_2): 285, 331, 468 nm. Emission (CH_2Cl_2, ex. 450 nm): 534 nm.

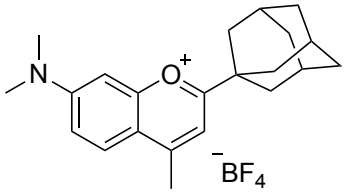

2-((3*r*,5*r*,7*r*)-adamantan-1-yl)-7-(dimethylamino)-4-methylchromenylium tetrafluoroborate (**S4b**): Chromone **S3b** (79 mg, 0.24 mmol, 1.0 equiv.) was added to a flame dried 25 mL 2-neck flask in a N_2 atmosphere and dissolved in THF (3.2 mL). The solution was cooled to 0 ºC and methylmagnesium bromide (1.0 M in THF, 0.75 mL, 3.1 equiv.) was added dropwise. The reaction was warmed to room temperature and stirred for 14 h before quenching with fluoroboric acid (50%, aqueous, 150 µL). After further addition of 5% fluoroboric acid, the product was extracted into DCM, dried with Na_2SO_4, filtered, and evaporated. The crude product was purified by precipitation upon addition of toluene, collected by vacuum filtration, and rinsed briefly with cold EtOAc to yield a bright orange solid (68 mg, 0.17 mmol, 68%). ^{1}H NMR (500 MHz, Acetone-d_6) δ 8.26 (d, *J* = 9.7 Hz, 1H), 7.58 (dd, *J* = 9.6, 2.5 Hz, 1H), 7.42 (s, 1H), 7.25 (d, *J* = 2.6 Hz, 1H), 3.45 (s, 6H), 2.94 (s, 3H), 2.17 (d, *J* = 1.4 Hz, 9H), 1.95 – 1.79 (m, 6H). ^{13}C NMR (126 MHz,

Acetone-d_6) δ 180.5, 166.1, 160.5, 159.0, 129.6, 119.1, 118.3, 112.5, 96.7, 41.2, 40.6, 40.3, 36.7, 28.8, 20.0. HRMS (ESI$^+$) calcd for $C_{22}H_{28}NO^+$ [M]$^+$: 322.2165; found: 322.2164. Absorbance (CH_2Cl_2): 286, 331, 469 nm. Emission (CH_2Cl_2, ex. 450 nm): 534 nm.

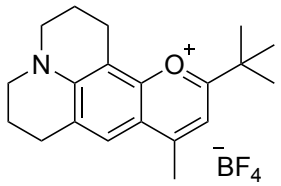

11-(*tert*-butyl)-9-methyl-2,3,6,7-tetrahydro-1*H*,5*H*-pyrano[2,3-*f*]pyrido[3,2,1-*ij*]quinolin-12-ium tetrafluoroborate (**S4c**): Chromone **S3c** (256 mg, 0.861 mmol, 1.00 equiv.) was added to a flame dried 50 mL 2-neck flask in a N_2 atmosphere and dissolved in THF (8.8 mL). Methylmagnesium bromide (1.0 M in THF, 2.6 mL, 3.0 equiv.) was added dropwise and the solution was stirred at room temperature for 12 h. The reaction was quenched with fluoroboric acid (50% aqueous, 200 µL). The product was extracted into DCM with the addition of 5% fluoroboric acid, dried with Na_2SO_4, filtered, and evaporated. The product was purified by precipitation upon addition of cold EtOAc, filtration and rinsing with cold EtOAc to obtain a magenta solid (268 mg, 0.669 mmol, 81%). ^{1}H NMR (500 MHz, Acetonitrile-d_3) δ 7.65 (s, 1H), 7.02 (s, 1H), 3.53 (q, J = 5.4 Hz, 4H), 2.95 (t, J = 6.4 Hz, 2H), 2.93 – 2.87 (m, 2H), 2.67 (s, 3H), 2.05 – 1.96 (m, 4H), 1.44 (s, 9H). ^{13}C NMR (126 MHz, Acetonitrile-d_3) δ 178.3, 161.6, 155.2, 153.7, 129.7, 124.7, {peak at 118.6–118.1 beneath CD_3CN solvent peak}, 111.1, 105.6, 51.8, 51.3, 38.5, 28.4, 28.4, 21.0, 20.2, 19.9, 19.7. HRMS (ESI$^+$) calcd for $C_{20}H_{26}NO^+$ [M]$^+$: 296.2009; found: 296.2002. Absorbance (CH_2Cl_2): 300, 351, 488 nm. Emission (CH_2Cl_2, ex. 450 nm): 557 nm.

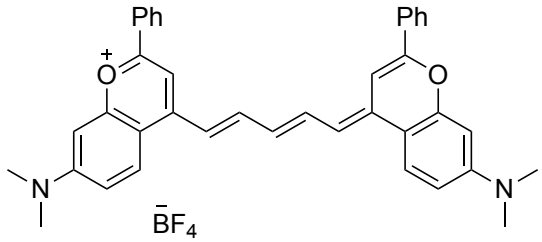

7-(dimethylamino)-4-((1*E*,3*E*)-5-((*E*)-7-(dimethylamino)-2-phenyl-4*H*-chromen-4-ylidene)penta-1,3-dien-1-yl)-2-phenylchromenylium tetrafluoroborate (**2, Flav5)**: Flavylium **S5a** (see Ref. **Error! Bookmark not defined.** for synthesis) (164 mg, 0.467 mmol, 1.00 equiv.), malonaldehyde bis(phenylimine) monohydrochloride (59.0 mg, 0.228 mmol, 0.490 equiv.) and sodium acetate (128 mg, 1.25 mmol, 2.68 equiv.) were added to a 25 mL Schlenk tube under a N_2 atmosphere. Acetic anhydride (4.0 mL) was added and the solution was freeze-pump-thawed x3 before heating to 100 ºC for 65 min. The reaction was cooled, ~16 mL of toluene was added, and the product was collected by vacuum filtration. The product was rinsed with toluene and water before drying *in vacuo*. A bronze solid resulted (127 mg, 0.194 mmol, 86%). ^{1}H NMR (500 MHz, DMSO-d_6) δ 8.20 (t, J = 12.9 Hz, 2H), 8.13 – 8.03 (m, 4H), 7.99 (d, J = 9.4 Hz, 2H), 7.66 (s, 2H), 7.62 – 7.53 (m, 6H), 7.08 (d, J = 13.3 Hz, 2H), 6.91 (dd, J = 9.3, 2.6 Hz, 2H), 6.83 (t, J = 12.4 Hz, 1H), 6.77 (d, J = 2.6 Hz, 2H), 3.13 (s, 12H). ^{13}C NMR (126 MHz, DMSO-d_6) δ 156.1, 155.3, 154.1, 148.9, 145.5, 131.5, 131.1, 129.1, 126.0, 125.8, 115.3, 113.1, 110.8, 101.5, 97.3 {peak at 38.9–40.1 beneath DMSO- d_6 solvent peak.}. HRMS (ESI$^+$) calcd for $C_{39}H_{35}N_2O_2^+$ [M]$^+$: 563.2693; found: 563.2675. IR (film): 2926, 2867, 1629, 1456, 1052, 995, 902, 883 cm^{-1}. Absorbance (CH_2Cl_2): 548, 778, 862 nm. Emission (CH_2Cl_2, ex. 755 nm): 883 nm.

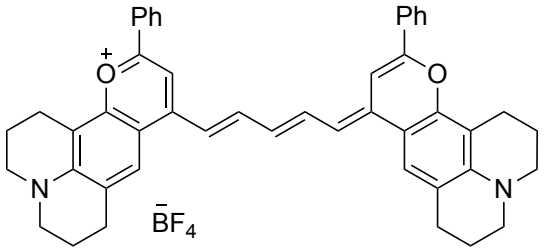

11-phenyl-9-((1*E*,3*E*,5*E*)-5-(11-phenyl-2,3,6,7-tetrahydro-1*H*,5*H*,9*H*-pyrano[2,3-*f*]pyrido[3,2,1-*ij*]quinolin-9-ylidene)penta-1,3-dien-1-yl)-2,3,6,7-tetrahydro-1*H*,5*H*-pyrano[2,3-*f*]pyrido[3,2,1-*ij*]quinolin-12-ium tetrafluoroborate (**4**, JuloFlav5): Flavylium **S5b** (see Ref. **Error! Bookmark not defined.** for synthesis) (150 mg, 0.372 mmol, 1.00 equiv.), malonaldehyde bis(phenylimine) monohydrochloride (47.2 mg, 0.182 mmol, 0.490 equiv.) and sodium acetate (92.6 mg, 1.13 mmol, 3.03 equiv.) were added to a 25 mL Schlenk tube under a N_2 atmosphere. Acetic anhydride (4.0 mL) was added and the solution was freeze-pump-thawed x3 before heating to 100 ºC for 60 min. The reaction was cooled, ~10 mL of toluene was added, and the product was collected by vacuum filtration. The product was rinsed with toluene until filtrate runs clear, followed by a water rinse. The product was further purified by column chromatography, after dry-loading onto silica, in a three-way gradient of 1:1 toluene/DCM plus 1% EtOH to 0:1 toluene/DCM plus 20% EtOH. An iridescent red solid resulted (97.9 mg, 0.130 mmol, 71%). ^{1}H NMR (500 MHz, DMSO-d_6) δ 8.15 (t, J = 13.0 Hz, 2H), 8.13 – 8.08 (m, 4H), 7.70 – 7.58 (m, 10H), 7.05 (d, J = 13.4 Hz, 2H), 6.79 (t, J = 12.4 Hz, 1H), 3.41 – 3.38 (m, 8H), 2.92 (t, J = 6.5 Hz, 4H), 2.78 (t, J = 6.5 Hz, 4H), 1.98 (p, J = 5.7 Hz, 4H), 1.91 (p, J = 5.8 Hz, 4H). ^{13}C NMR (126 MHz, DMSO-d_6) δ 154.9, 150.4, 147.6, 144.2, 131.5, 131.2, 129.1, 125.6, 122.6, 121.6, 114.5, 110.4, 105.5, 100.9, 49.6, 49.0, 27.1, 20.5, 19.8, 19.6. HRMS (ESI$^+$) calcd for $C_{47}H_{43}N_2O_2^+$ [M]$^+$: 667.3319; found: 667.3296. IR (film): 2928, 2849, 1631, 1431, 1091, 1038, 916 cm^{-1}. Absorbance (CH_2Cl_2): 588, 805, 897 nm. Emission (CH_2Cl_2, ex. 755 nm): 925 nm.

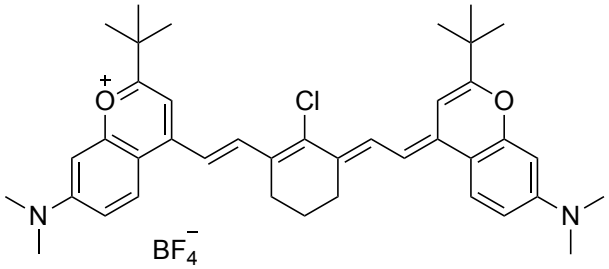

2-(*tert*-butyl)-4-((*E*)-2-((*E*)-3-(2-((*E*)-2-(*tert*-butyl)-7-(dimethylamino)-4*H*-chromen-4-ylidene)ethylidene)-2-chlorocyclohex-1-en-1-yl)vinyl)-7-(dimethylamino)chromenylium tetrafluoroborate (**5**, Chrom7): Chromenylium **S4a** (300 mg, 0.900 mmol, 1.00 equiv.), *N*-[(3-(anilinomethylene)-2-chloro-1-cyclohexen-1-yl)methylene]aniline hydrochloride (153 mg, 0.426 mmol, 0.47 equiv.) and 2,6-di-*tert*-butyl-4-methyl pyridine (555 mg, 2.70 mmol, 2.98 equiv.) were added to a flame-dried 50 mL Schlenk tube under a N_2 atmosphere. Toluene (2.1 mL) and *n*-butanol (4.8 mL) were added and the solution was freeze-pump-thawed x3 before heating to 100 ºC for 3 h. The reaction was cooled and evaporated. The product was precipitated in toluene and collected by vacuum filtration, washing with ~200 mL toluene, ~50 mL trifluorotoluene, ~50 mL cold THF. The product was further purified by column chromatography after dry-loading onto silica in DCM plus a gradient of 0.5–5% EtOH. After a second column in a three-way gradient of 3:7 toluene/DCM plus 0.5 % EtOH to 0:1 toluene/DCM plus 5% EtOH, the procedure resulted in a red iridescent product (108 mg, 0.152 mmol, 36%). ^{1}H NMR (500 MHz, Acetonitrile-d_3) δ 8.00 (d, J = 13.8 Hz, 2H), 7.82 (d, J = 9.3 Hz, 2H), 6.86 (dd, J = 9.4, 2.6 Hz, 2H), 6.79 (s, 2H), 6.73 (d, J = 13.8 Hz, 2H), 6.50 (d, J = 2.5 Hz, 2H), 3.04 (s, 12H), 2.71 (t, J = 6.3 Hz, 4H), 1.89 (p, J = 6.2 Hz, 2H), 1.42 (s, 18H). ^{13}C NMR (126 MHz, Acetonitrile-d_3) δ 170.8, 157.2, 155.3, 146.8, 146.1, 139.1, 130.5, 126.3, 113.9, 112.9, 112.3, 100.4, 98.0, 40.5, 37.4, 28.2, 27.6, 21.8. HRMS (ESI$^+$) calcd for

$C_{40}H_{48}ClN_2O_2^+$ $[M]^+$: 623.3399; found: 623.3383. IR (film): 2964, 2927, 2872, 2811, 1627, 1377, 1227, 1155, 982, 934, 884 cm^{-1}. Absorbance (CH_2Cl_2): 499, 562, 975 nm. Emission (CH_2Cl_2, ex. 885 nm): 996 nm.

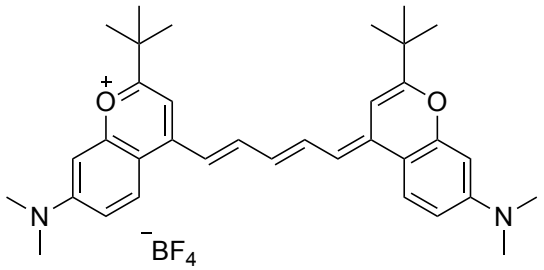

2-(*tert*-butyl)-4-((1*E*,3*E*)-5-((*E*)-2-(*tert*-butyl)-7-(dimethylamino)-4*H*-chromen-4-ylidene)penta-1,3-dien-1-yl)-7-(dimethylamino)chromenylium tetrafluoroborate (**6**, Chrom5): Chromenylium **S4a** (150 mg, 0.45 mmol, 1.0 equiv.), malonaldehyde bis(phenylimine) monohydrochloride (57.3 mg, 0.221 mmol, 0.490 equiv.), and sodium acetate (117 mg, 1.43 mmol, 3.16 equiv.) were added to a 25 mL Schlenk tube under a N_2 atmosphere. Acetic anhydride (3.5 mL) was added and the solution was freeze-pump-thawed x3 before heating to 120 ºC for 60 min. The reaction was cooled, ~14 mL of toluene was added, and the product was collected by vacuum filtration. The product was rinsed with toluene until filtrate runs clear, followed by a water rinse. The product was further purified by column chromatography, after dry-loading onto silica, in a three-way gradient of 1:1 toluene/DCM plus 1% EtOH to 0:1 toluene/DCM plus 12% EtOH. An iridescent dark purple solid resulted (76.6 mg, 0.125 mmol, 57%). ^{1}H NMR (500 MHz, Acetonitrile-d_3) δ 7.93 (t, J = 13.0 Hz, 2H), 7.87 (d, J = 9.4 Hz, 2H), 6.91 (dd, J = 9.3, 2.6 Hz, 2H), 6.86 (s, 2H), 6.83 (d, J = 13.5 Hz, 2H), 6.68 (t, J = 12.5 Hz, 1H), 6.61 (d, J = 2.6 Hz, 2H), 3.10 (s, 12H), 1.40 (s, 18H). ^{13}C NMR (126 MHz, Acetonitrile-d_3) δ 171.3, 157.5, 155.6, 150.1, 148.2, 128.3, 126.5, 114.5, 114.0, 112.0, 100.3, 98.1, 40.6, 37.5, 28.2. HRMS (ESI$^+$) calcd for $C_{35}H_{43}N_2O_2^+$ $[M]^+$: 523.3319; found: 523.3312. IR (film): 2961, 2923, 2870, 1631, 1457, 124, 977, 929, 882 cm^{-1}. Absorbance (CH_2Cl_2): 521, 741, 819 nm. Emission (CH_2Cl_2, ex. 755 nm): 836 nm.

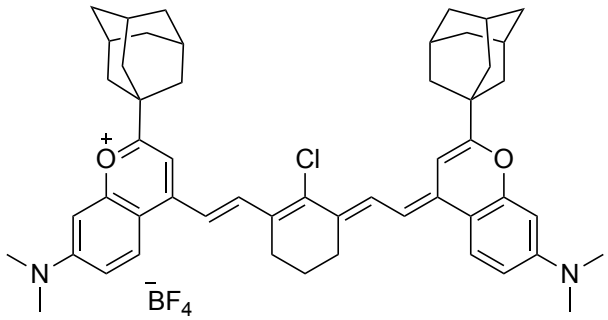

2-((3*r*,5*r*,7*r*)-adamantan-1-yl)-4-((*E*)-2-((*E*)-3-(2-((*E*)-2-((3*r*,5*r*,7*r*)-adamantan-1-yl)-7-(dimethylamino)-4*H*-chromen-4-ylidene)ethylidene)-2-chlorocyclohex-1-en-1-yl)vinyl)-7-(dimethylamino)chromenylium tetrafluoroborate (**7**): Chromenylium **S4b** (30.5 mg, 0.0745 mmol, 1.00 equiv.), *N*-[(3-(anilinomethylene)- 2-chloro-1-cyclohexen-1-yl)methylene]aniline hydrochloride (11.9 mg, 0.0331 mmol, 0.440 equiv.) and 2,6-di-*tert*-butyl-4-methyl pyridine (46.1 mg, 0.225 mmol, 3.01 equiv.) were added to a flame-dried 25 mL Schlenk tube under a N_2 atmosphere. Toluene (0.20 mL) and *n*-butanol (0.50 mL) were added and the solution was freeze-pump-thawed x3 before heating to 100 ºC for 6.5 h. The reaction was cooled and evaporated. The crude product was purified by column chromatography after dry-loading onto silica in DCM plus a gradient of 0.5–4% EtOH. After a second column in a three-way gradient of 3:7 toluene/DCM plus 0.4% EtOH to 0:1 toluene/DCM plus 7% EtOH, the procedure resulted in a dark blue product (9.2 mg, 0.011 mmol, 32%). ^{1}H NMR (500 MHz, DMSO-d_6) δ 8.15 (d, J = 9.6 Hz, 2H), 7.93 (d, J = 13.6 Hz, 2H), 7.14 – 6.90 (m, 4H), 6.71 (s, 2H), 6.68 (d, J = 2.5 Hz, 2H), 3.07 (s, 12H), 2.76 (m,

4H), 2.13 – 2.11 (m, 6H), 2.03 – 2.02 (m, *J* = 12H), 1.86 – 1.76 (m, 14H). ^{13}C NMR (126 MHz, DMSO-d_6) δ 169.0, 155.8, 154.2, 145.0, 144.4, 137.7, 129.4, 126.2, 113.3, 111.84, 111.81, 99.2, 97.0, {two peaks at 40.4–38.8, beneath DMSO-d_6 solvent peak} 37.9, 35.9, 27.6, 26.5, 20.8. HRMS (ESI$^+$) calcd for $C_{52}H_{60}ClN_2O_2^+$ [M]$^+$: 779.4338; found: 779.4307. IR (film): 2902, 2850, 1634, 1363, 1230, 1143, 987, 932, 885 cm^{-1}. Absorbance (CH_2Cl_2): 500, 562, 876, 977 nm. Emission (CH_2Cl_2, ex. 885 nm): 997 nm.

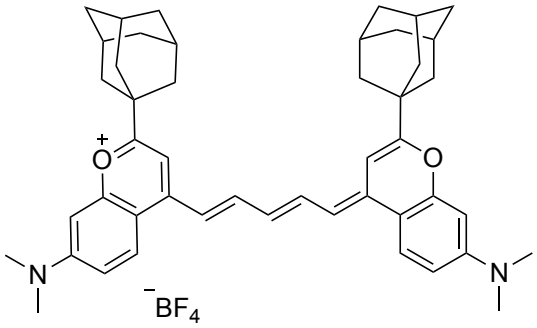

2-((3*r*,5*r*,7*r*)-adamantan-1-yl)-4-((1*E*,3*E*)-5-((*E*)-2-((3*r*,5*r*,7*r*)-adamantan-1-yl)-7-(dimethylamino)-4*H*-chromen-4-ylidene)penta-1,3-dien-1-yl)-7-(dimethylamino)chromenylium tetrafluoroborate (**8**). Chromenylium **S4b** (15.1 mg, 0.0369 mmol, 1.00 equiv.), malonaldehyde bis(phenylimine) monohydrochloride (4.5 mg, 0.020 mmol, 0.47 equiv.), and sodium acetate (10.2 mg, 0.124 mmol, 3.37 equiv.) were added to a 25 mL Schlenk tube under a N_2 atmosphere. Acetic anhydride (0.41 mL) was added and the solution was freeze-pump-thawed x3 before heating to 100 ºC for 70 min. The reaction was cooled, ~5 mL of toluene was added, and the product was collected by vacuum filtration. An iridescent dark purple solid resulted (10.5 mg, 0.0137 mmol, 79%). ^{1}H NMR (500 MHz, Methylene Chloride-d_2) δ 7.87 (d, *J* = 9.4 Hz, 2H), 7.80 (t, *J* = 12.9 Hz, 2H), 6.91 (dd, *J* = 9.3, 2.6 Hz, 2H), 6.82 (d, *J* = 13.4 Hz, 2H), 6.76-6.71 (m, 3H), 6.57 (d, *J* = 2.6 Hz, 2H), 3.16 (s, 12H), 2.16 (t, *J* = 3.1 Hz, 6H), 2.05 (d, *J* = 2.8 Hz, 12H), 1.89 – 1.75 (m, 12H). ^{13}C NMR (126 MHz, Methylene Chloride-d_2) δ 170.9, 157.1, 154.8, 148.9, 147.9, 127.3, 125.8, 113.5, 113.3, 111.7, 99.9, 97.6, 40.6, 40.2, 39.0, 36.8, 28.6. HRMS (ESI$^+$) calcd for $C_{47}H_{55}N_2O_2^+$ [M]$^+$: 679.4258; found: 679.4240. IR (film): 2905, 2851, 1631, 1463, 1122, 984, 929, 884. Absorbance (CH_2Cl_2): 521, 742, 818 nm. Emission (CH_2Cl_2, ex. 755 nm): 837 nm.

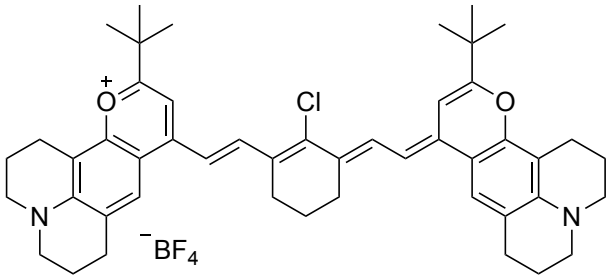

11-(Tert-butyl)-9-((E)-2-((E)-3-((E)-2-(11-(tert-butyl)-2,3,6,7-tetrahydro-1H,5H,9H-pyrano[2,3-f]pyrido[3,2,1-ij]quinolin-9-ylidene)ethylidene)-2-chlorocyclohex-1-en-1-yl)vinyl)-2,3,6,7-tetrahydro-1H,5H-pyrano[2,3-f]pyrido[3,2,1-ij]quinolin-12-ium tetrafluoroborate (9, JuloChrom7**).** Chromenylium **S4c** (52 mg, 0.13 mmol, 1.0 equiv.), *N*-[(3-(anilinomethylene)- 2-chloro-1-cyclohexen-1-yl)methylene]aniline hydrochloride (22 mg, 0.062 mmol, 0.48 equiv.), and 2,6-di-*tert*-butyl-4-methyl pyridine (80 mg, 0.4 mmol, 3 equiv.) were dissolved in a mixture of *n*-butanol (820 µL) and toluene (350 µL) in a 25 mL Schlenk flask and heated to 105 °C for 7 hours. The solution was cooled to rt and evaporated onto silica gel. The crude product was purified via silica gel chromatography, eluting with a DCM/toluene/EtOH solvent gradient of 7:3 + 0.2% EtOH, increasing up to 10% EtOH gradually, followed by a trituration with ice cold THF. The procedure gave a dark purple solid (30. mg, 0.036 mmol, 28 %). ^{1}H NMR (500 MHz, Methylene Chloride-d_2) δ 8.15 (d, J = 13.8 Hz, 2H), 7.48 (s, 2H), 6.79 (s, 4H), 3.39 (s,

8H), 2.89 (s, 8H), 2.77 (s, 4H), 2.02 (d, J = 7.2 Hz, 8H), 1.41 (s, 18H), 0.08 (s, 2H). HRMS (ESI^+) calcd for $C_{48}H_{56}ClN_2O_2^{++}$ $[M]^+$: 727.4025; found: 727.4003. IR (film): 2925, 2854, 1628, 1234, 1144, 1048, 960, 929, 895 cm^{-1}. Absorbance (CH_2Cl_2): 524, 563, 608, 1008 nm. Emission (CH_2Cl_2): 1033 nm.

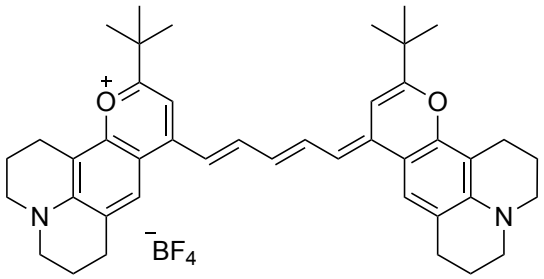

11-(*tert*-butyl)-9-((1*E*,3*E*,5*E*)-5-(11-(*tert*-butyl)-2,3,6,7-tetrahydro-1*H*,5*H*,9*H*-pyrano[2,3-*f*]pyrido[3,2,1-*ij*]quinolin-9-ylidene)penta-1,3-dien-1-yl)-2,3,6,7-tetrahydro-1*H*,5*H*-pyrano[2,3-*f*]pyrido[3,2,1-*ij*]quinolin-12-ium tetrafluoroborate (**10,** JuloChrom5). Chromenylium **S4c** (150 mg, 0.39 mmol, 1.0 equiv.), malonaldehyde bis(phenylimine) monohydrochloride (49.7 mg, 0.192 mmol, 0.490 equiv.), and sodium acetate (99.1 mg, 1.21 mmol, 3.09 equiv.) were added to a 25 mL Schlenk tube under a N_2 atmosphere. Acetic anhydride (3.5 mL) was added and the solution was freeze-pump-thawed x3 before heating to 100 ºC for 60 min. The reaction was cooled, ~10 mL of toluene was added, and the product was collected by vacuum filtration. A bronze solid resulted (111 mg, 0.155 mmol, 81%). ^1H NMR (500 MHz, Acetonitrile-d_3) δ 7.85 (t, J = 13.0 Hz, 2H), 7.51 (s, 2H), 6.81 (s, 2H), 6.78 (d, J = 13.6 Hz, 2H), 6.61 (t, J = 12.5 Hz, 1H), 3.36 (q, J = 6.5 Hz, 8H), 2.85 (t, J = 6.4 Hz, 4H), 2.81 (t, J = 6.1 Hz, 4H), 1.99 – 1.96 (m, 8H), 1.39 (s, 18H). ^{13}C NMR (126 MHz, Acetonitrile-d_3) δ 170.0, 152.6, 149.1, 148.4, 146.9, 127.3, 124.1, 122.3, 113.7, 111.6, 107.0, 99.7, 50.9, 50.4, 37.6, 28.5, 28.4, 21.8, 20.91, 20.87. HRMS (ESI^+) calcd for $C_{43}H_{51}N_2O_2^+$ $[M]^+$: 627.3945; found: 627.3927. IR (film): 2955, 2847, 1633, 1439, 1091, 951, 925, 886 cm^{-1}. Absorbance (CH_2Cl_2): 560, 771, 852 nm. Emission (CH_2Cl_2, ex. 755 nm): 872 nm.

^{1}H NMRs

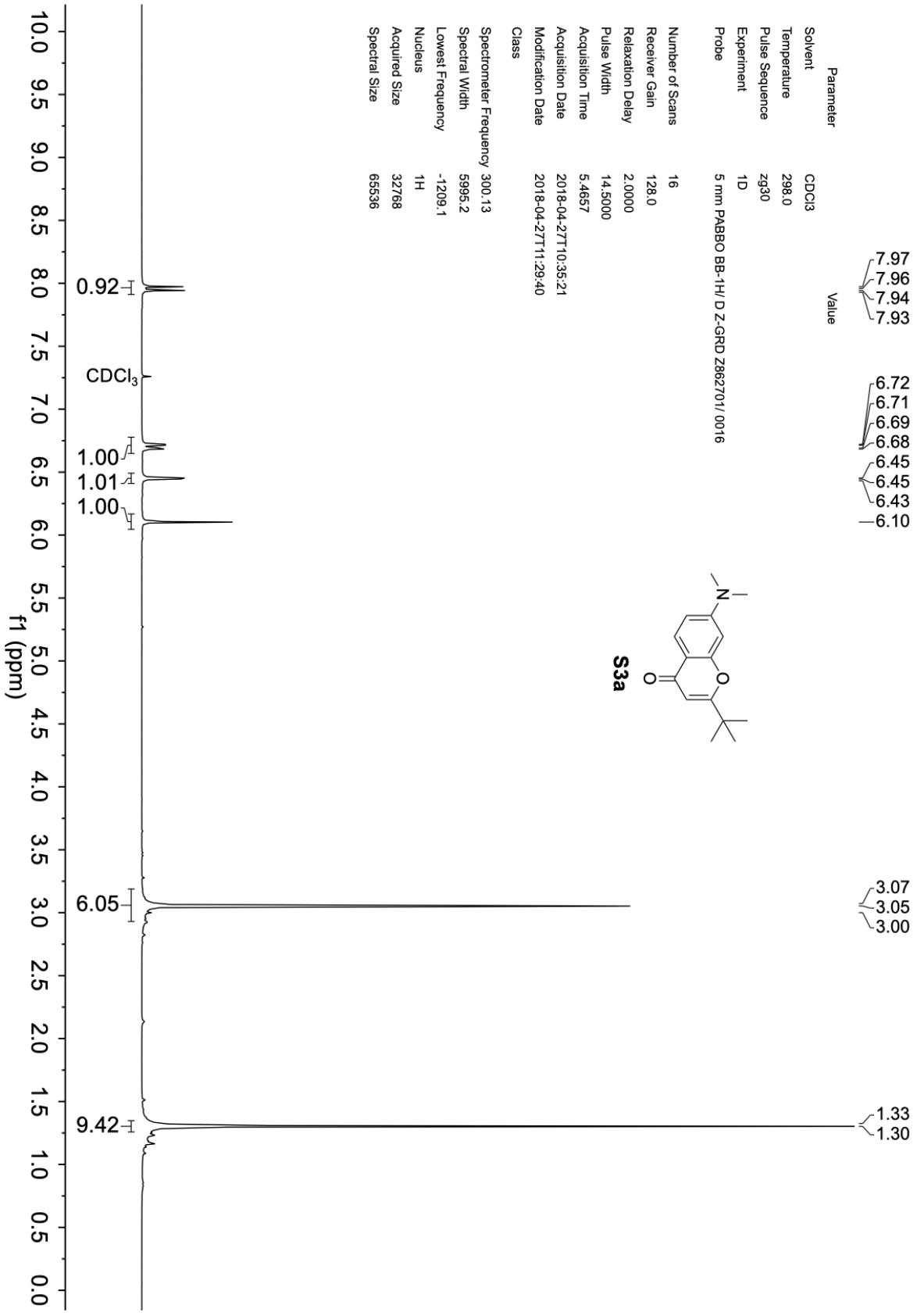
Parameter
Value
Solvent
CDCl3
Temperature
298.0
Pulse Sequence
zg30
Experiment
1D
Probe
5 mm PABBO BB-1H/ D Z-GRD Z862701/ 0016
Number of Scans
16
Receiver Gain
128.0
Relaxation Delay
2.0000
Pulse Width
14.5000
Acquisition Time
5.4657
Acquisition Date
2018-04-27T10:35:21
Modification Date
2018-04-27T11:29:40
Class
Spectrometer Frequency
300.13
Spectral Width
5995.2
Lowest Frequency
-1209.1
Nucleus
1H
Acquired Size
32768
Spectral Size
65536
S3a
7.97
7.96
7.94
7.93
6.72
6.71
6.69
6.68
6.45
6.45
6.43
6.10
3.07
3.05
3.00
1.33
1.30
0.92
CDCl3
1.00
1.01
1.00
6.05
9.42
f1 (ppm)

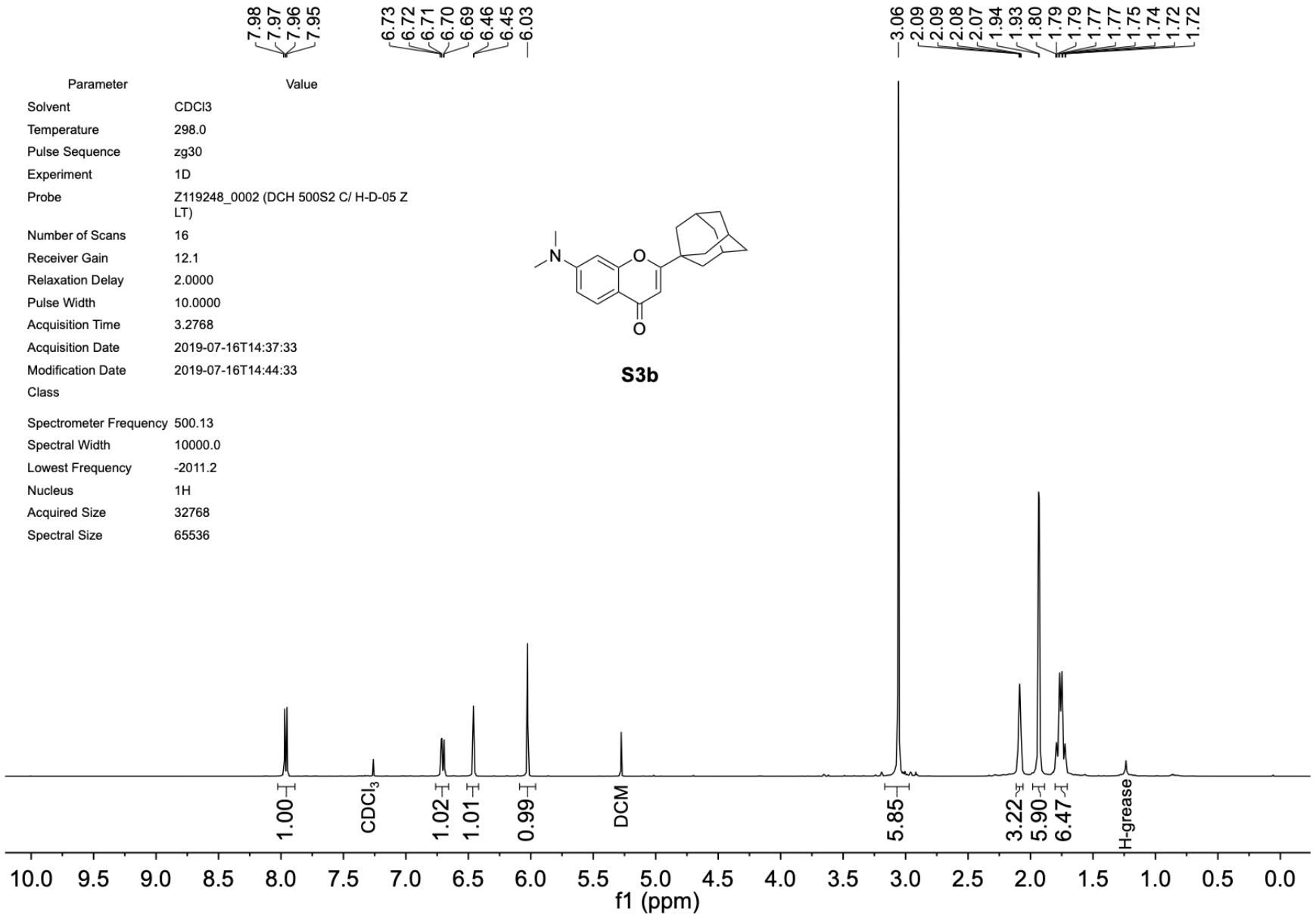
7.98
7.97
7.96
7.95
6.73
6.72
6.71
6.70
6.69
6.46
6.45
6.03
3.06
2.09
2.09
2.08
2.07
1.94
1.93
1.80
1.79
1.79
1.77
1.77
1.75
1.74
1.72
1.72
Parameter Value
Solvent CDCl3
Temperature 298.0
Pulse Sequence zg30
Experiment 1D
Probe Z119248_0002 (DCH 500S2 C/ H-D-05 Z LT)
Number of Scans 16
Receiver Gain 12.1
Relaxation Delay 2.0000
Pulse Width 10.0000
Acquisition Time 3.2768
Acquisition Date 2019-07-16T14:37:33
Modification Date 2019-07-16T14:44:33
Class
Spectrometer Frequency 500.13
Spectral Width 10000.0
Lowest Frequency -2011.2
Nucleus 1H
Acquired Size 32768
Spectral Size 65536
N
O
O
S3b
1.00
CDCl3
1.02
1.01
0.99
DCM
5.85
3.22
5.90
6.47
H-grease
10.0 9.5 9.0 8.5 8.0 7.5 7.0 6.5 6.0 5.5 5.0 4.5 4.0 3.5 3.0 2.5 2.0 1.5 1.0 0.5 0.0
f1 (ppm)

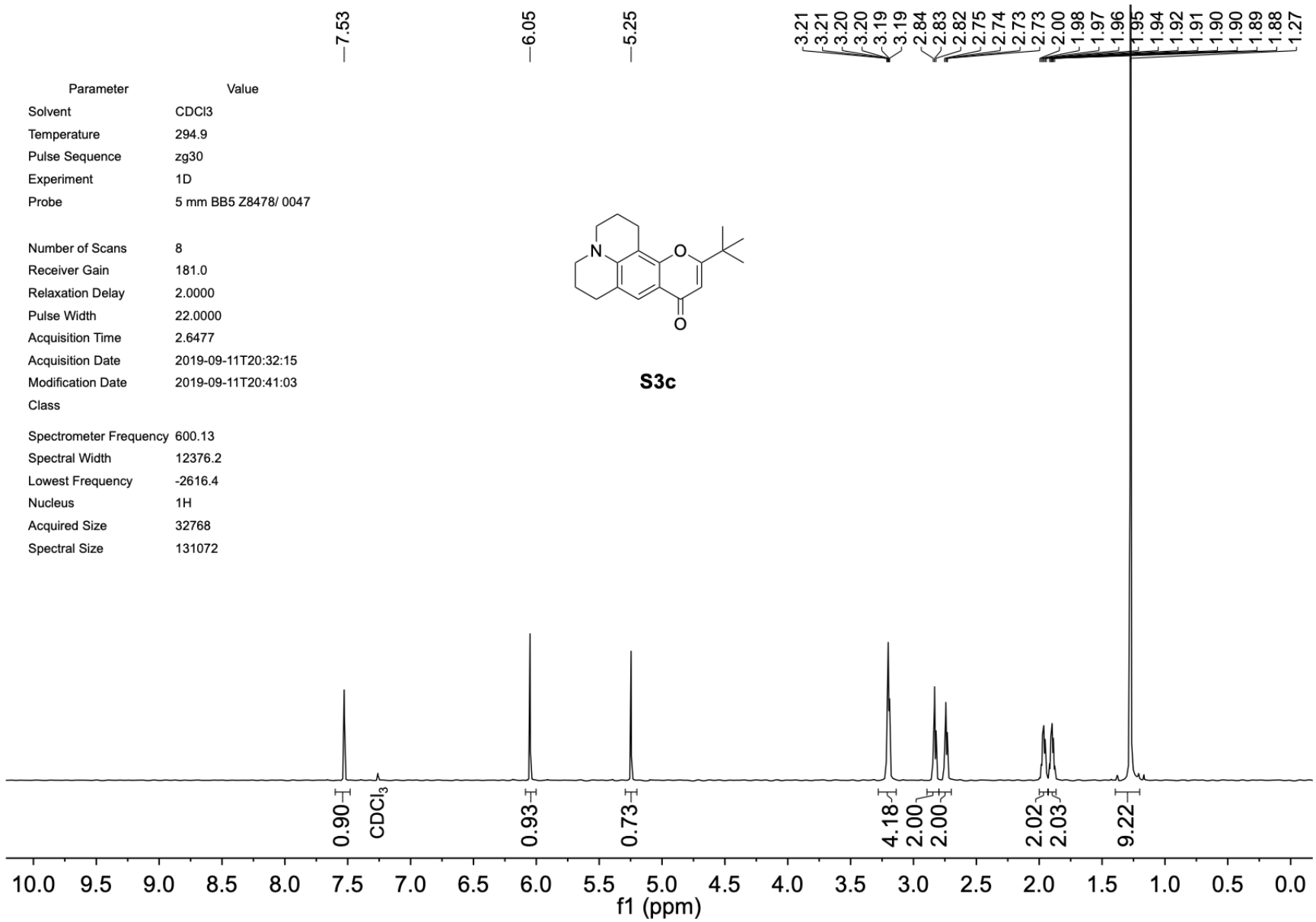
7.53
6.05
5.25
3.21
3.21
3.20
3.20
3.19
3.19
2.84
2.83
2.82
2.75
2.74
2.73
2.73
2.00
1.98
1.97
1.96
1.95
1.94
1.92
1.91
1.90
1.90
1.89
1.88
1.27
Parameter Value
Solvent CDCl3
Temperature 294.9
Pulse Sequence zg30
Experiment 1D
Probe 5 mm BB5 Z8478/ 0047
Number of Scans 8
Receiver Gain 181.0
Relaxation Delay 2.0000
Pulse Width 22.0000
Acquisition Time 2.6477
Acquisition Date 2019-09-11T20:32:15
Modification Date 2019-09-11T20:41:03
Class
Spectrometer Frequency 600.13
Spectral Width 12376.2
Lowest Frequency -2616.4
Nucleus 1H
Acquired Size 32768
Spectral Size 131072
N
O
O
S3c
0.90
CDCl3
0.93
0.73
4.18
2.00
2.00
2.02
2.03
9.22
10.0 9.5 9.0 8.5 8.0 7.5 7.0 6.5 6.0 5.5 5.0 4.5 4.0 3.5 3.0 2.5 2.0 1.5 1.0 0.5 0.0
f1 (ppm)

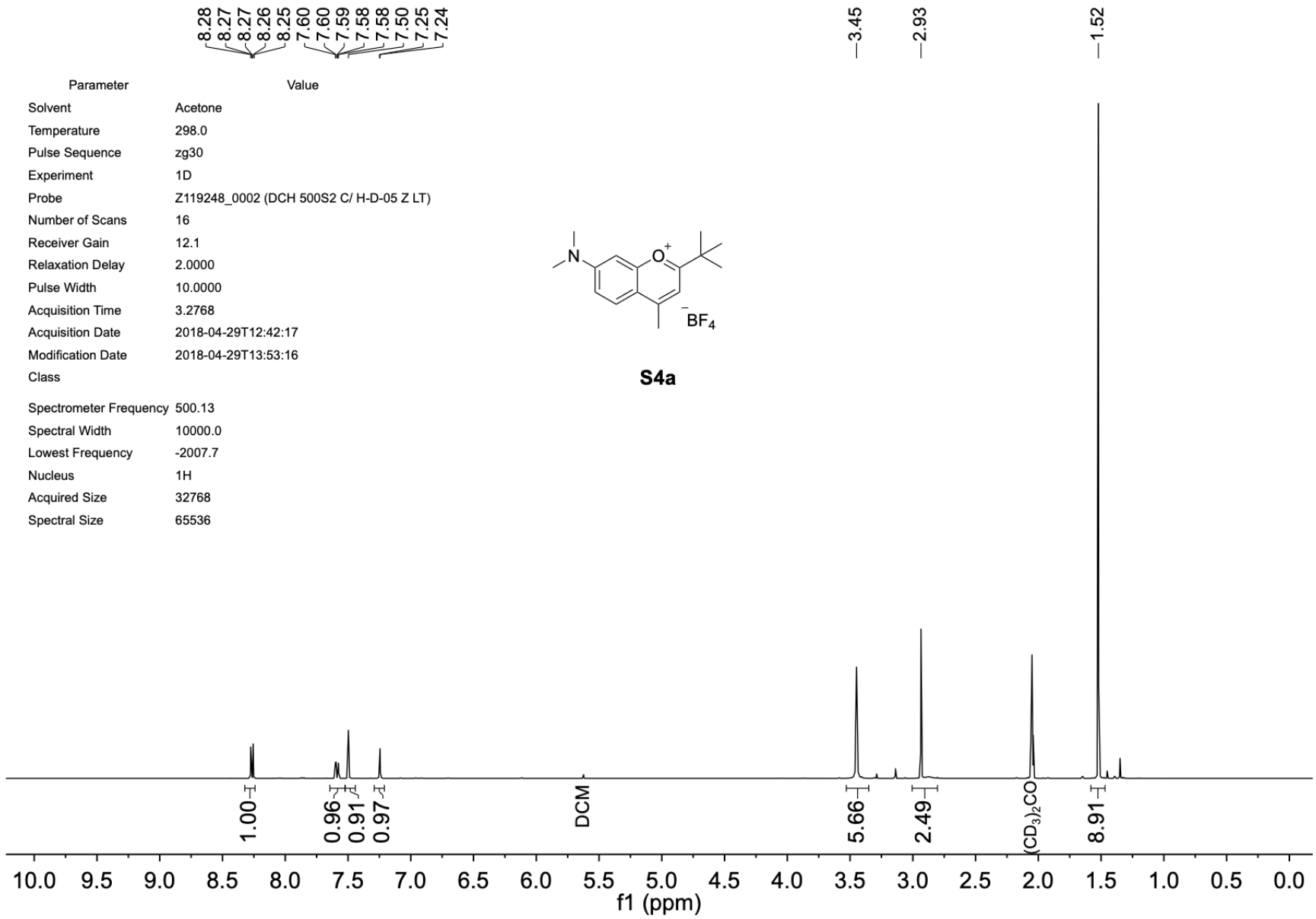
8.28
8.27
8.27
8.26
8.25
7.60
7.60
7.59
7.58
7.58
7.50
7.25
7.24
3.45
2.93
1.52
Parameter Value
Solvent Acetone
Temperature 298.0
Pulse Sequence zg30
Experiment 1D
Probe Z119248_0002 (DCH 500S2 C/ H-D-05 Z LT)
Number of Scans 16
Receiver Gain 12.1
Relaxation Delay 2.0000
Pulse Width 10.0000
Acquisition Time 3.2768
Acquisition Date 2018-04-29T12:42:17
Modification Date 2018-04-29T13:53:16
Class
Spectrometer Frequency 500.13
Spectral Width 10000.0
Lowest Frequency -2007.7
Nucleus 1H
Acquired Size 32768
Spectral Size 65536
N
O+
BF4
S4a
1.00
0.96
0.91
0.97
DCM
5.66
2.49
(CD3)2CO
8.91
10.0 9.5 9.0 8.5 8.0 7.5 7.0 6.5 6.0 5.5 5.0 4.5 4.0 3.5 3.0 2.5 2.0 1.5 1.0 0.5 0.0
f1 (ppm)

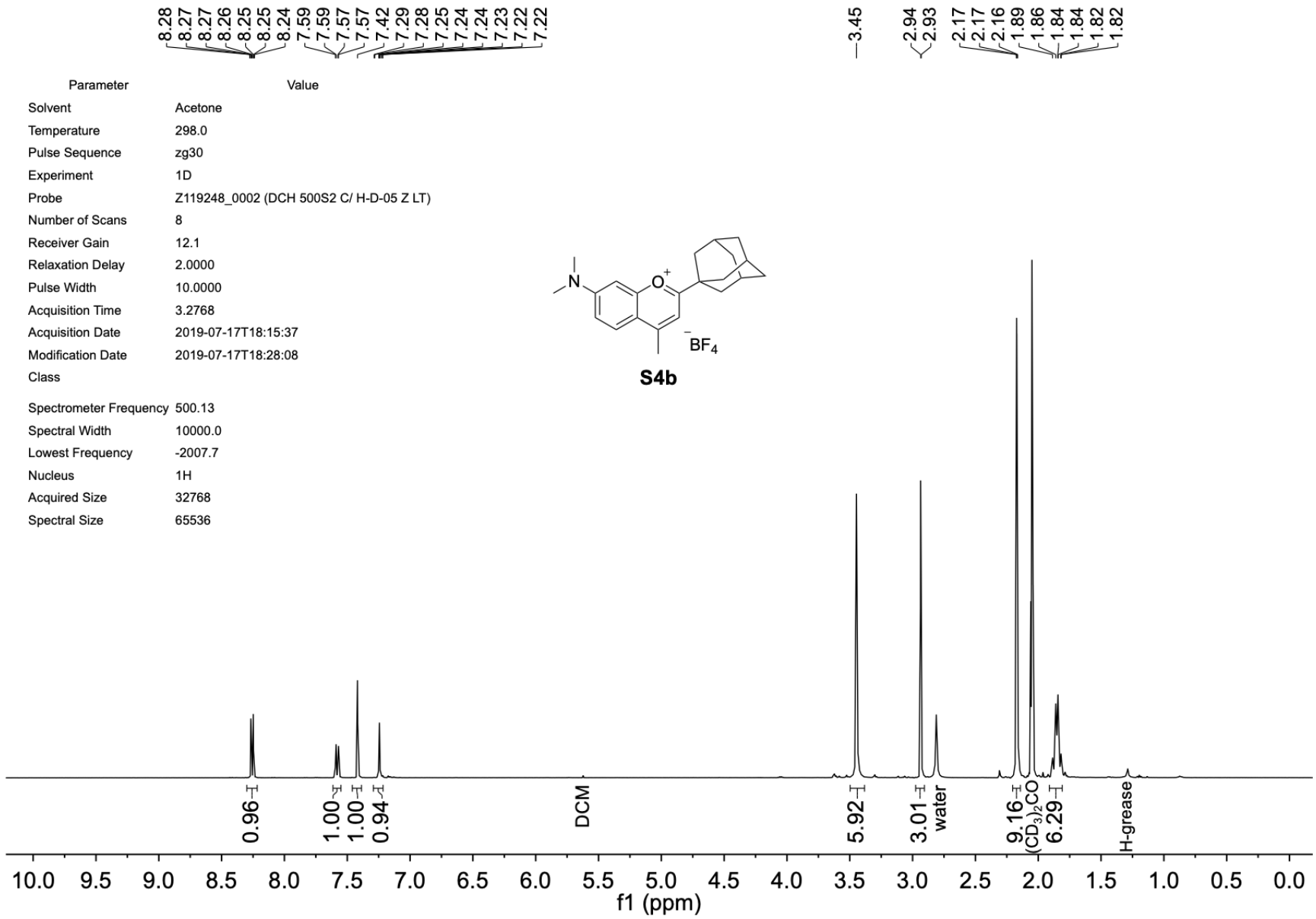
8.28
8.27
8.27
8.26
8.25
8.25
8.24
7.59
7.59
7.57
7.57
7.42
7.29
7.28
7.25
7.24
7.24
7.23
7.22
7.22
3.45
2.94
2.93
2.17
2.17
2.16
1.89
1.86
1.84
1.84
1.82
1.82
Parameter Value
Solvent Acetone
Temperature 298.0
Pulse Sequence zg30
Experiment 1D
Probe Z119248_0002 (DCH 500S2 C/ H-D-05 Z LT)
Number of Scans 8
Receiver Gain 12.1
Relaxation Delay 2.0000
Pulse Width 10.0000
Acquisition Time 3.2768
Acquisition Date 2019-07-17T18:15:37
Modification Date 2019-07-17T18:28:08
Class
Spectrometer Frequency 500.13
Spectral Width 10000.0
Lowest Frequency -2007.7
Nucleus 1H
Acquired Size 32768
Spectral Size 65536
N
O+
BF4
S4b
0.96
1.00
1.00
0.94
DCM
5.92
3.01
water
9.16
(CD3)2CO
6.29
H-grease
10.0 9.5 9.0 8.5 8.0 7.5 7.0 6.5 6.0 5.5 5.0 4.5 4.0 3.5 3.0 2.5 2.0 1.5 1.0 0.5 0.0
f1 (ppm)

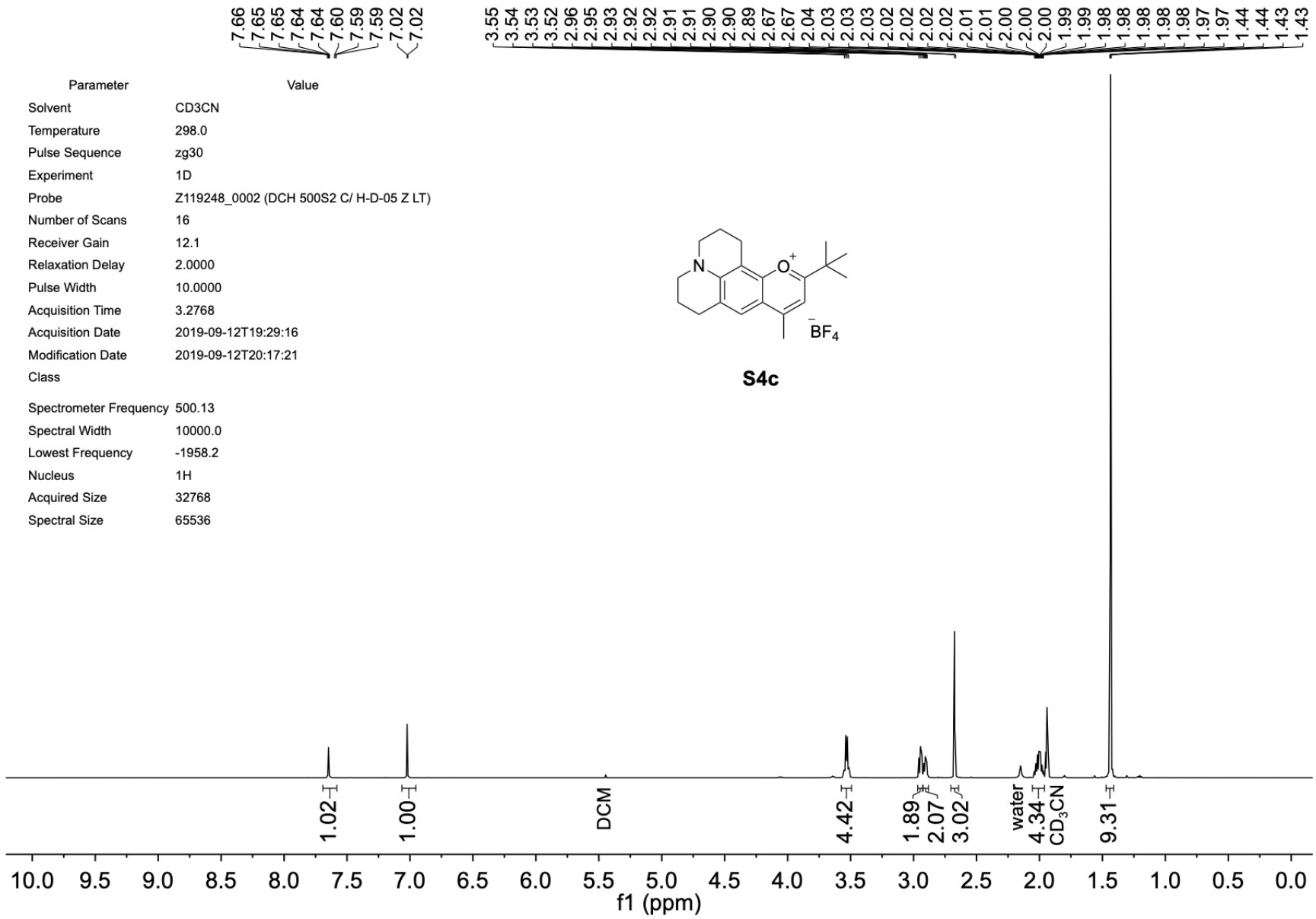
7.66 7.65 7.65 7.64 7.64 7.60 7.59 7.59 7.02 7.02
3.55 3.54 3.53 3.52 2.96 2.95 2.93 2.92 2.92 2.91 2.91 2.90 2.90 2.89 2.67 2.67 2.04 2.03 2.03 2.03 2.02 2.02 2.02 2.02 2.01 2.01 2.00 2.00 2.00 1.99 1.99 1.98 1.98 1.98 1.98 1.98 1.97 1.97 1.44 1.44 1.43 1.43
Parameter Value
Solvent CD3CN
Temperature 298.0
Pulse Sequence zg30
Experiment 1D
Probe Z119248_0002 (DCH 500S2 C/ H-D-05 Z LT)
Number of Scans 16
Receiver Gain 12.1
Relaxation Delay 2.0000
Pulse Width 10.0000
Acquisition Time 3.2768
Acquisition Date 2019-09-12T19:29:16
Modification Date 2019-09-12T20:17:21
Class
Spectrometer Frequency 500.13
Spectral Width 10000.0
Lowest Frequency -1958.2
Nucleus 1H
Acquired Size 32768
Spectral Size 65536
N
O+
BF4
S4c
1.02
1.00
DCM
4.42
1.89
2.07
3.02
water
4.34
CD3CN
9.31
10.0 9.5 9.0 8.5 8.0 7.5 7.0 6.5 6.0 5.5 5.0 4.5 4.0 3.5 3.0 2.5 2.0 1.5 1.0 0.5 0.0
f1 (ppm)

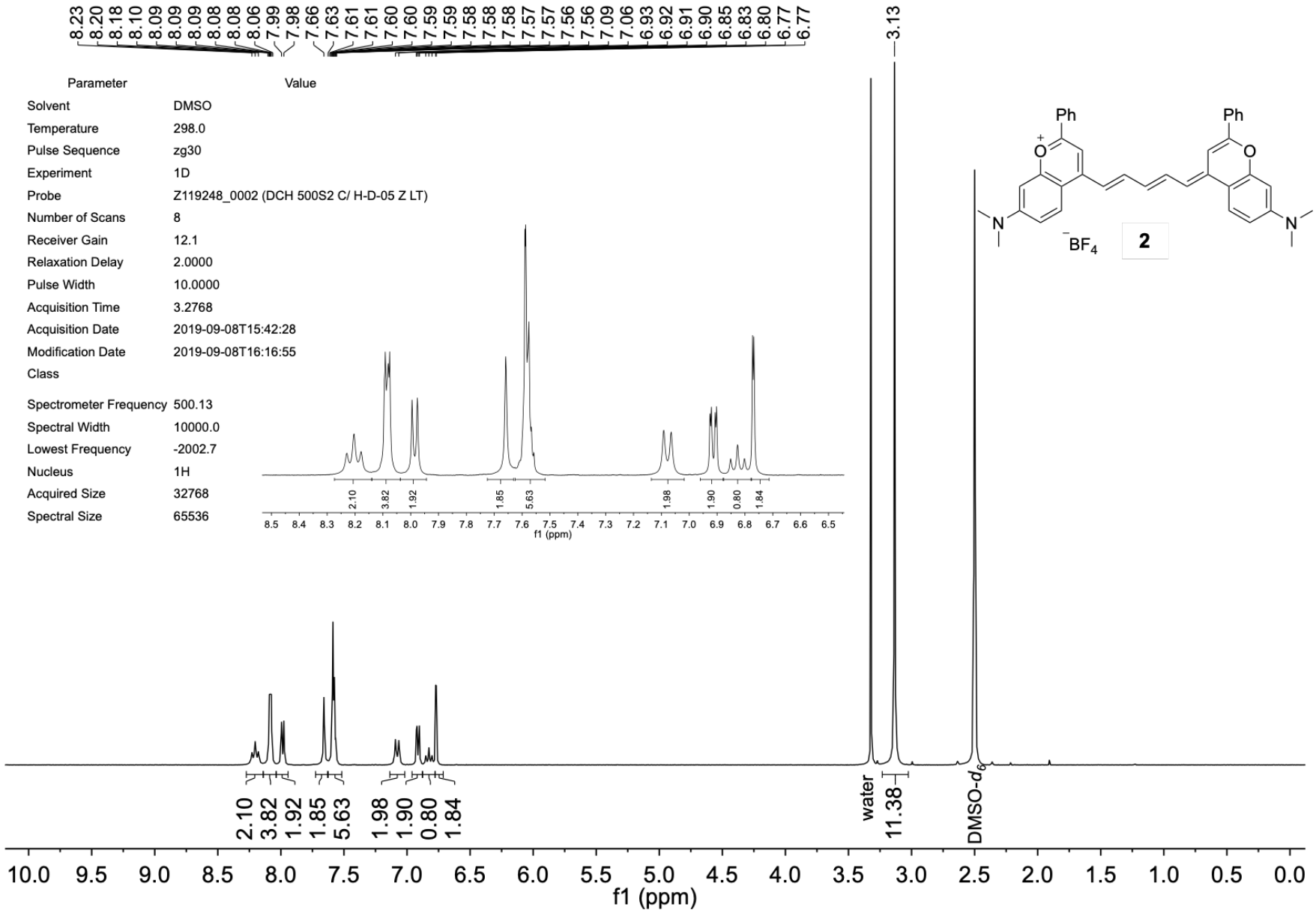
8.23 8.20 8.18 8.10 8.09 8.09 8.09 8.08 8.08 8.06 7.99 7.98 7.66 7.63 7.61 7.61 7.60 7.60 7.59 7.59 7.58 7.58 7.58 7.57 7.57 7.56 7.56 7.09 7.06 6.93 6.92 6.91 6.90 6.85 6.83 6.80 6.77 6.77
3.13
Parameter Value
Solvent DMSO
Temperature 298.0
Pulse Sequence zg30
Experiment 1D
Probe Z119248_0002 (DCH 500S2 C/ H-D-05 Z LT)
Number of Scans 8
Receiver Gain 12.1
Relaxation Delay 2.0000
Pulse Width 10.0000
Acquisition Time 3.2768
Acquisition Date 2019-09-08T15:42:28
Modification Date 2019-09-08T16:16:55
Class
Spectrometer Frequency 500.13
Spectral Width 10000.0
Lowest Frequency -2002.7
Nucleus 1H
Acquired Size 32768
Spectral Size 65536
2.10 3.82 1.92 1.85 5.63 1.98 1.90 0.80 1.84
f1 (ppm)
Ph
Ph
O
O
N
N
$^{-}BF_4$
2
water
DMSO-d_6
11.38
2.10 3.82 1.92 1.85 5.63 1.98 1.90 0.80 1.84
10.0 9.5 9.0 8.5 8.0 7.5 7.0 6.5 6.0 5.5 5.0 4.5 4.0 3.5 3.0 2.5 2.0 1.5 1.0 0.5 0.0
f1 (ppm)

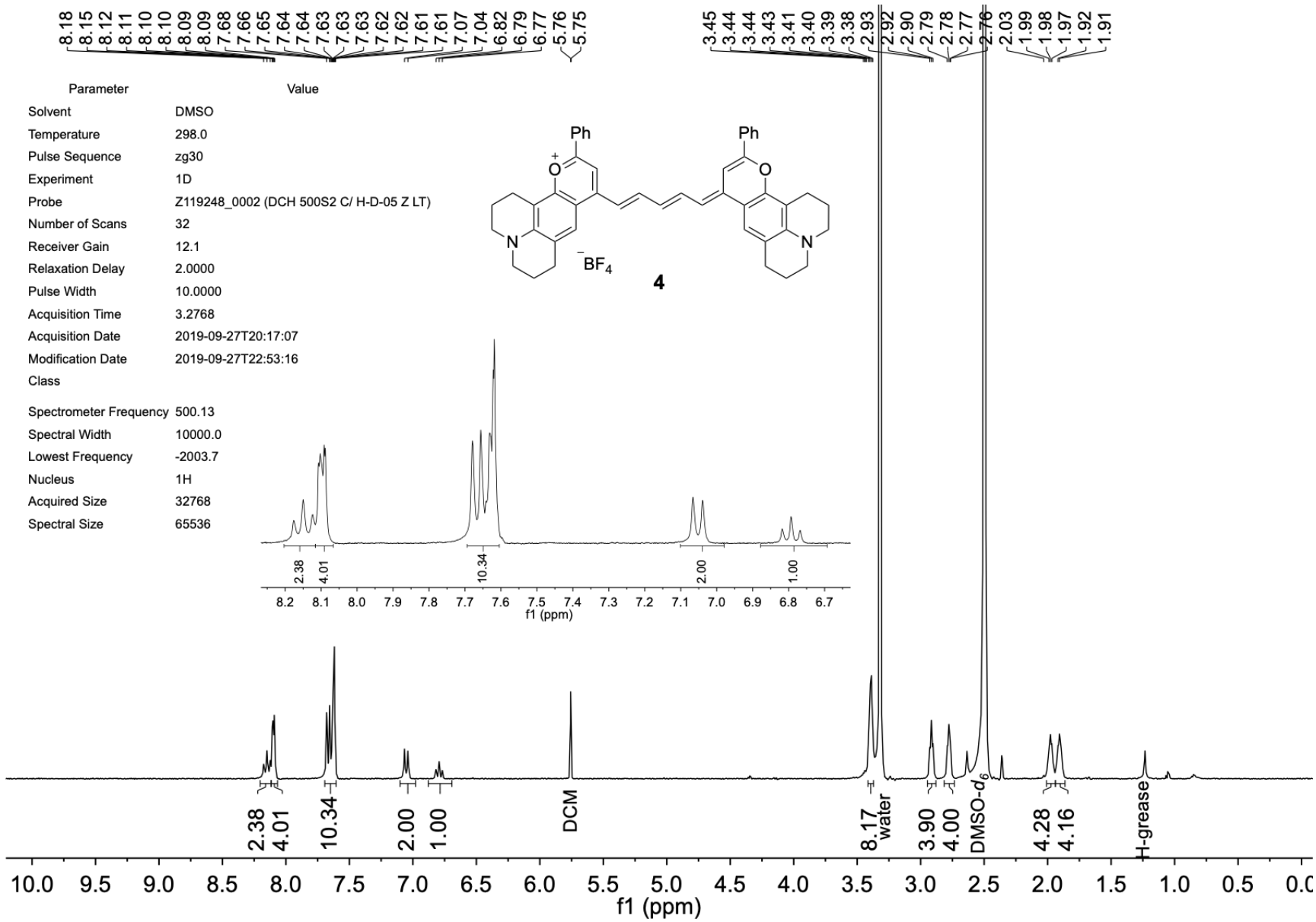
8.18 8.15 8.12 8.11 8.10 8.10 8.09 8.09 7.68 7.66 7.65 7.64 7.64 7.63 7.63 7.63 7.62 7.62 7.61 7.61 7.07 7.04 6.82 6.79 6.77 5.76 5.75
3.45 3.44 3.44 3.43 3.41 3.40 3.39 3.38 2.93 2.92 2.90 2.79 2.78 2.77 2.76 2.03 1.99 1.98 1.97 1.92 1.91
Parameter Value
Solvent DMSO
Temperature 298.0
Pulse Sequence zg30
Experiment 1D
Probe Z119248_0002 (DCH 500S2 C/ H-D-05 Z LT)
Number of Scans 32
Receiver Gain 12.1
Relaxation Delay 2.0000
Pulse Width 10.0000
Acquisition Time 3.2768
Acquisition Date 2019-09-27T20:17:07
Modification Date 2019-09-27T22:53:16
Class
Spectrometer Frequency 500.13
Spectral Width 10000.0
Lowest Frequency -2003.7
Nucleus 1H
Acquired Size 32768
Spectral Size 65536
Ph
Ph
O
N
N
BF4
4
2.38
4.01
10.34
2.00
1.00
8.2 8.1 8.0 7.9 7.8 7.7 7.6 7.5 7.4 7.3 7.2 7.1 7.0 6.9 6.8 6.7
f1 (ppm)
2.38
4.01
10.34
2.00
1.00
DCM
8.17
water
3.90
4.00
DMSO-d6
4.28
4.16
H-grease
10.0 9.5 9.0 8.5 8.0 7.5 7.0 6.5 6.0 5.5 5.0 4.5 4.0 3.5 3.0 2.5 2.0 1.5 1.0 0.5 0.0
f1 (ppm)

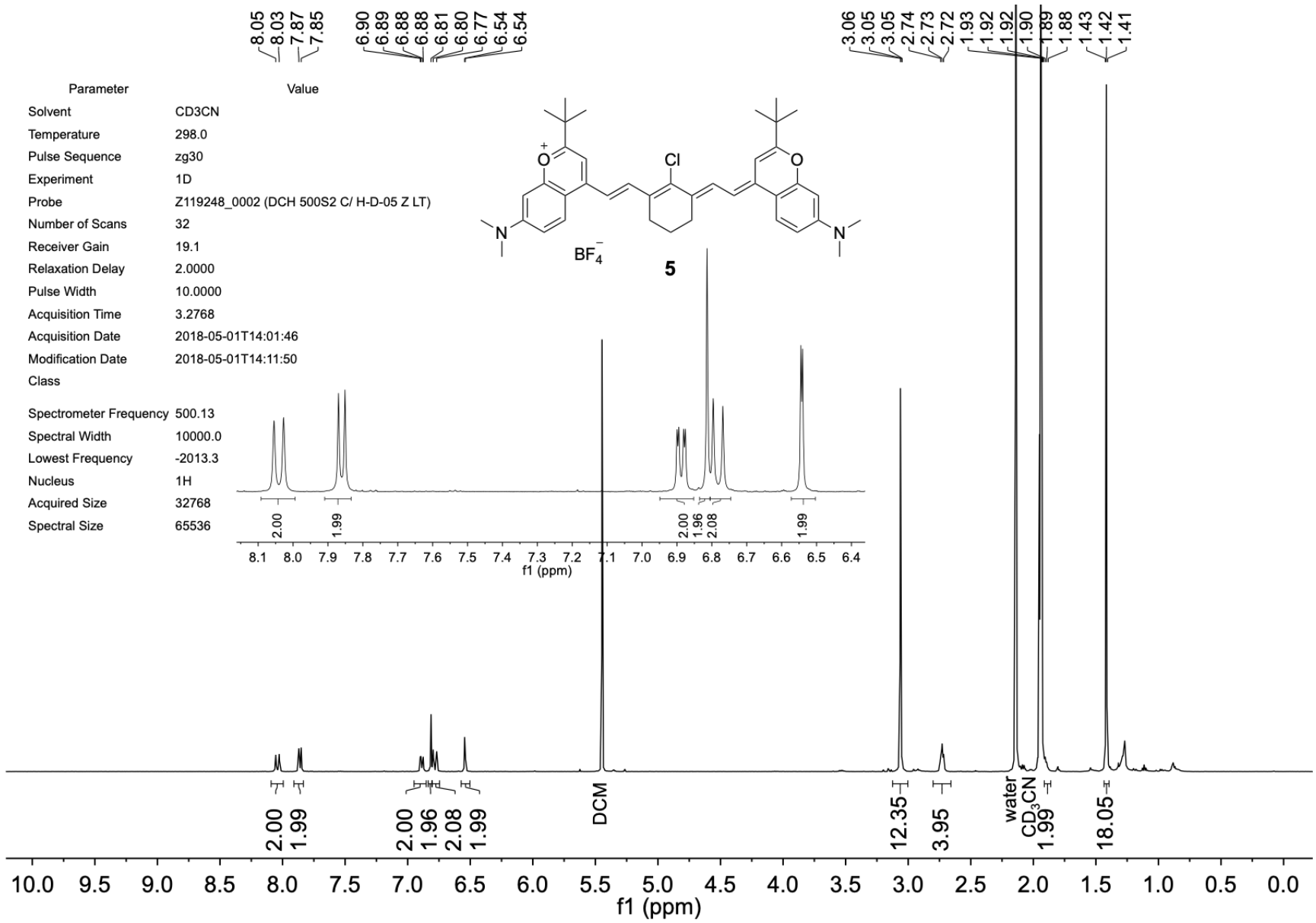
8.05
8.03
7.87
7.85
6.90
6.89
6.88
6.88
6.81
6.80
6.77
6.54
6.54
3.06
3.05
3.05
2.74
2.73
2.72
1.93
1.92
1.92
1.90
1.89
1.88
1.43
1.42
1.41
Parameter Value
Solvent CD3CN
Temperature 298.0
Pulse Sequence zg30
Experiment 1D
Probe Z119248_0002 (DCH 500S2 C/ H-D-05 Z LT)
Number of Scans 32
Receiver Gain 19.1
Relaxation Delay 2.0000
Pulse Width 10.0000
Acquisition Time 3.2768
Acquisition Date 2018-05-01T14:01:46
Modification Date 2018-05-01T14:11:50
Class
Spectrometer Frequency 500.13
Spectral Width 10000.0
Lowest Frequency -2013.3
Nucleus 1H
Acquired Size 32768
Spectral Size 65536
Cl
O
O
N
N
BF4−
5
2.00
1.99
2.00
1.96
2.08
1.99
f1 (ppm)
2.00
1.99
2.00
1.96
2.08
1.99
DCM
12.35
3.95
water
CD3CN
1.99
18.05
f1 (ppm)

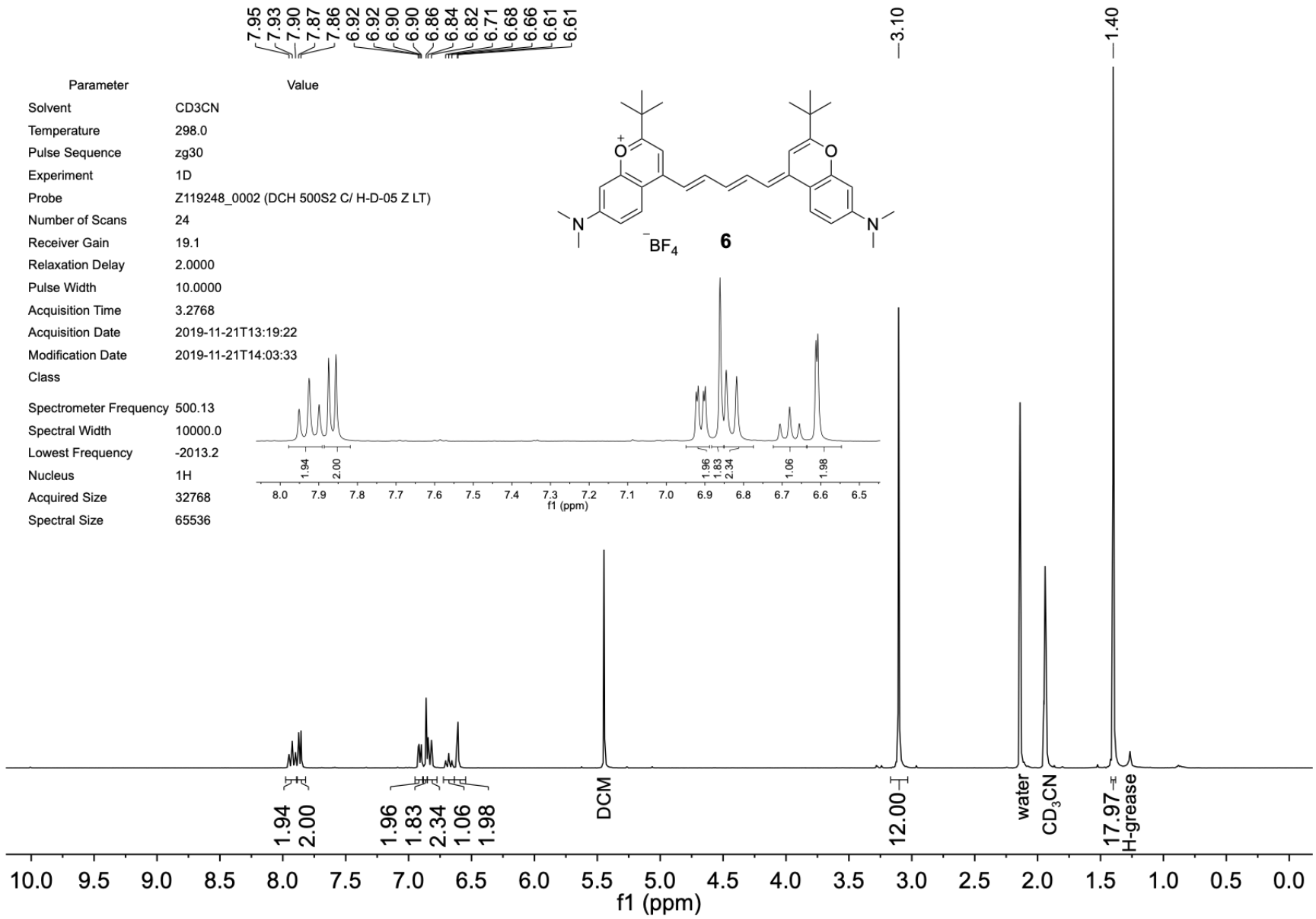
7.95
7.93
7.90
7.87
7.86
6.92
6.92
6.90
6.90
6.86
6.84
6.82
6.71
6.68
6.66
6.61
6.61
3.10
1.40
Parameter Value
Solvent CD3CN
Temperature 298.0
Pulse Sequence zg30
Experiment 1D
Probe Z119248_0002 (DCH 500S2 C/ H-D-05 Z LT)
Number of Scans 24
Receiver Gain 19.1
Relaxation Delay 2.0000
Pulse Width 10.0000
Acquisition Time 3.2768
Acquisition Date 2019-11-21T13:19:22
Modification Date 2019-11-21T14:03:33
Class
Spectrometer Frequency 500.13
Spectral Width 10000.0
Lowest Frequency -2013.2
Nucleus 1H
Acquired Size 32768
Spectral Size 65536
$^{-}BF_4$
6
1.94
2.00
1.96
1.83
2.34
1.06
1.98
f1 (ppm)
DCM
12.00
water
CD_3CN
17.97
H-grease
f1 (ppm)

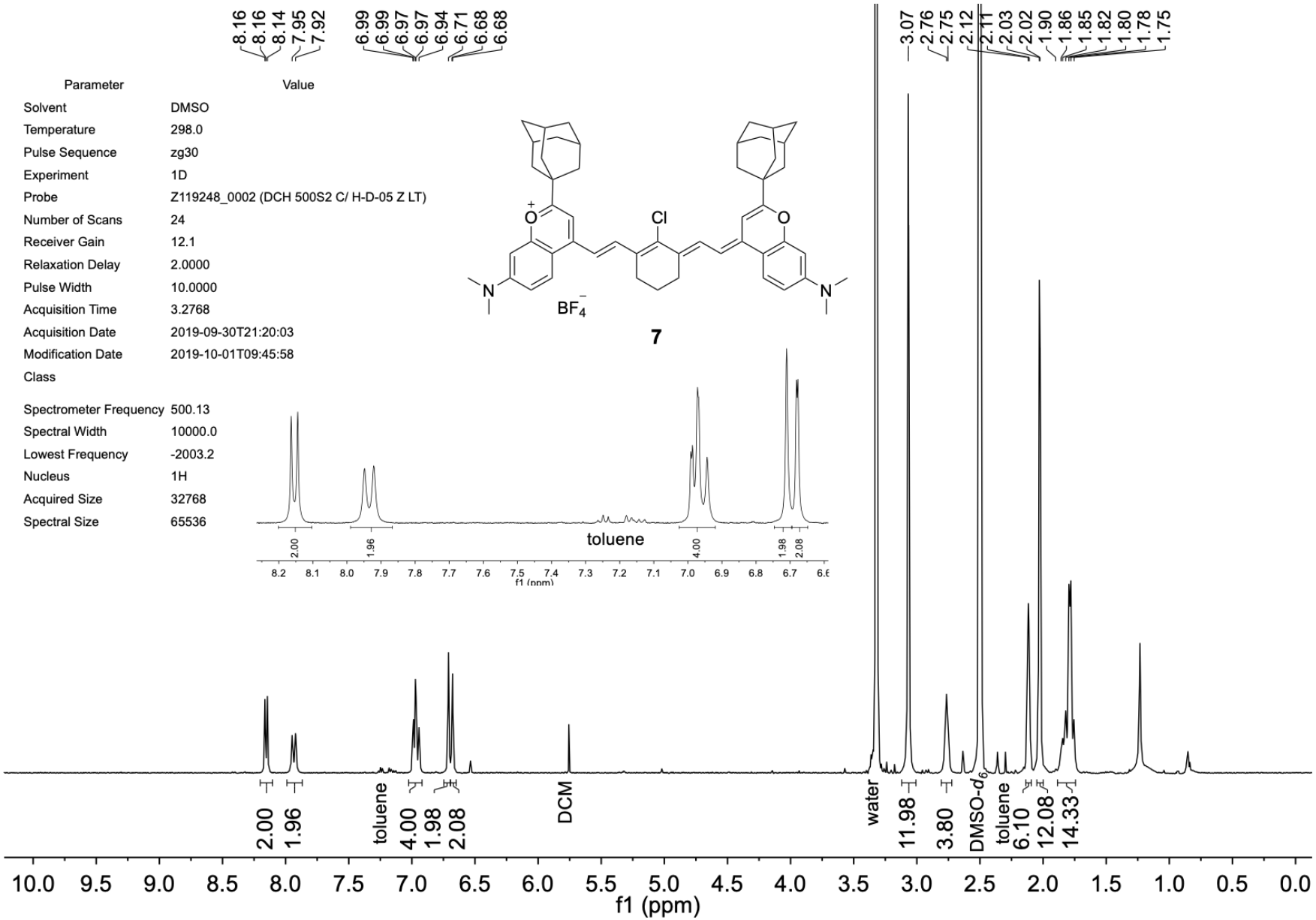
8.16
8.16
8.14
7.95
7.92
6.99
6.99
6.97
6.97
6.94
6.71
6.68
6.68
3.07
2.76
2.75
2.12
2.11
2.03
2.02
1.90
1.86
1.85
1.82
1.80
1.78
1.75
Parameter
Value
Solvent DMSO
Temperature 298.0
Pulse Sequence zg30
Experiment 1D
Probe Z119248_0002 (DCH 500S2 C/ H-D-05 Z LT)
Number of Scans 24
Receiver Gain 12.1
Relaxation Delay 2.0000
Pulse Width 10.0000
Acquisition Time 3.2768
Acquisition Date 2019-09-30T21:20:03
Modification Date 2019-10-01T09:45:58
Class
Spectrometer Frequency 500.13
Spectral Width 10000.0
Lowest Frequency -2003.2
Nucleus 1H
Acquired Size 32768
Spectral Size 65536
Cl
O
N
BF4
7
toluene
2.00
1.96
4.00
1.98
2.08
f1 (ppm)
2.00
1.96
toluene
4.00
1.98
2.08
DCM
water
11.98
3.80
DMSO-d6
toluene
6.10
12.08
14.33
f1 (ppm)

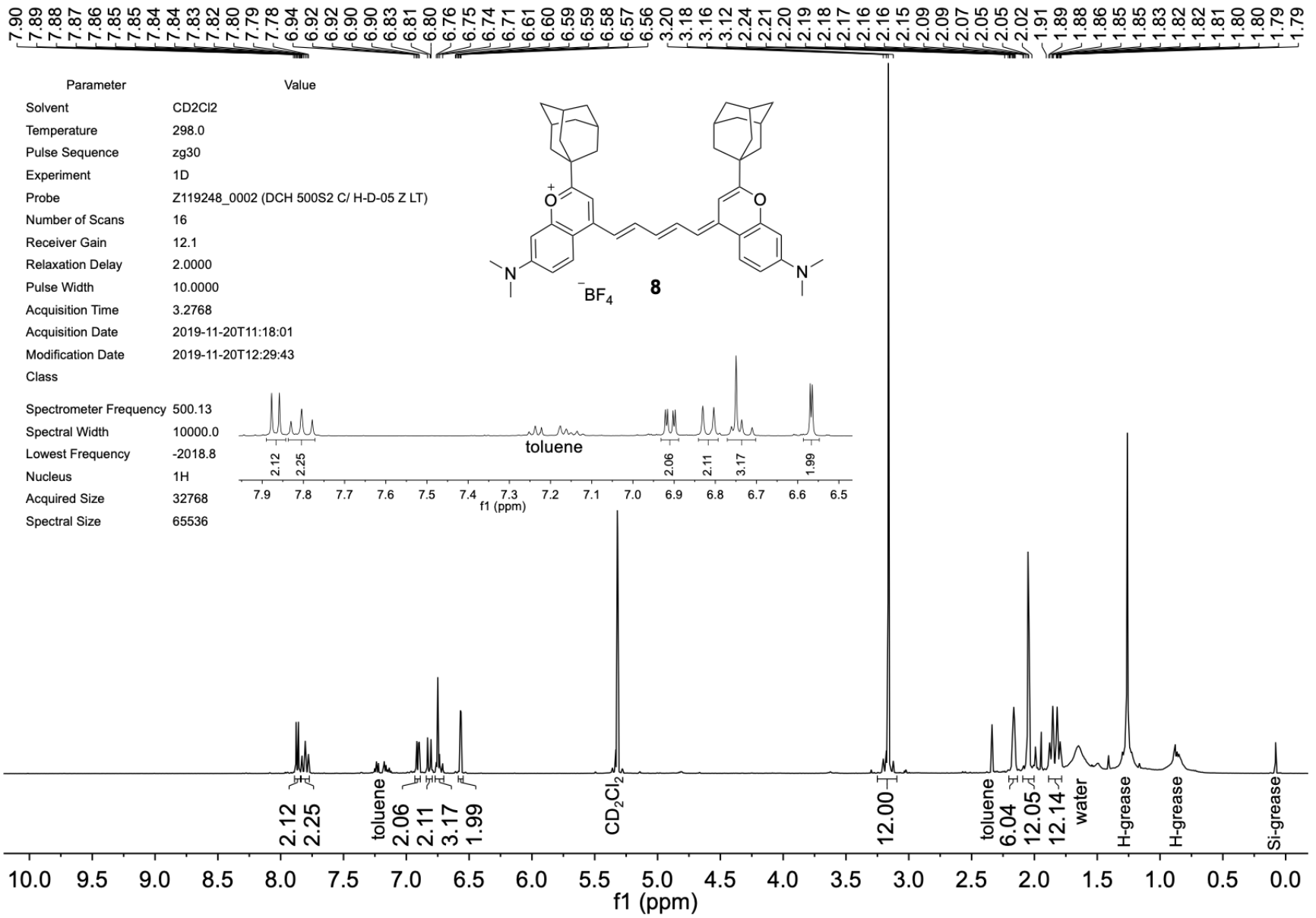
Parameter Value
Solvent CD2Cl2
Temperature 298.0
Pulse Sequence zg30
Experiment 1D
Probe Z119248_0002 (DCH 500S2 C/ H-D-05 Z LT)
Number of Scans 16
Receiver Gain 12.1
Relaxation Delay 2.0000
Pulse Width 10.0000
Acquisition Time 3.2768
Acquisition Date 2019-11-20T11:18:01
Modification Date 2019-11-20T12:29:43
Class
Spectrometer Frequency 500.13
Spectral Width 10000.0
Lowest Frequency -2018.8
Nucleus 1H
Acquired Size 32768
Spectral Size 65536
8
toluene
f1 (ppm)
2.12
2.25
toluene
2.06
2.11
3.17
1.99
CD2Cl2
12.00
toluene
6.04
12.05
12.14
water
H-grease
H-grease
Si-grease
f1 (ppm)

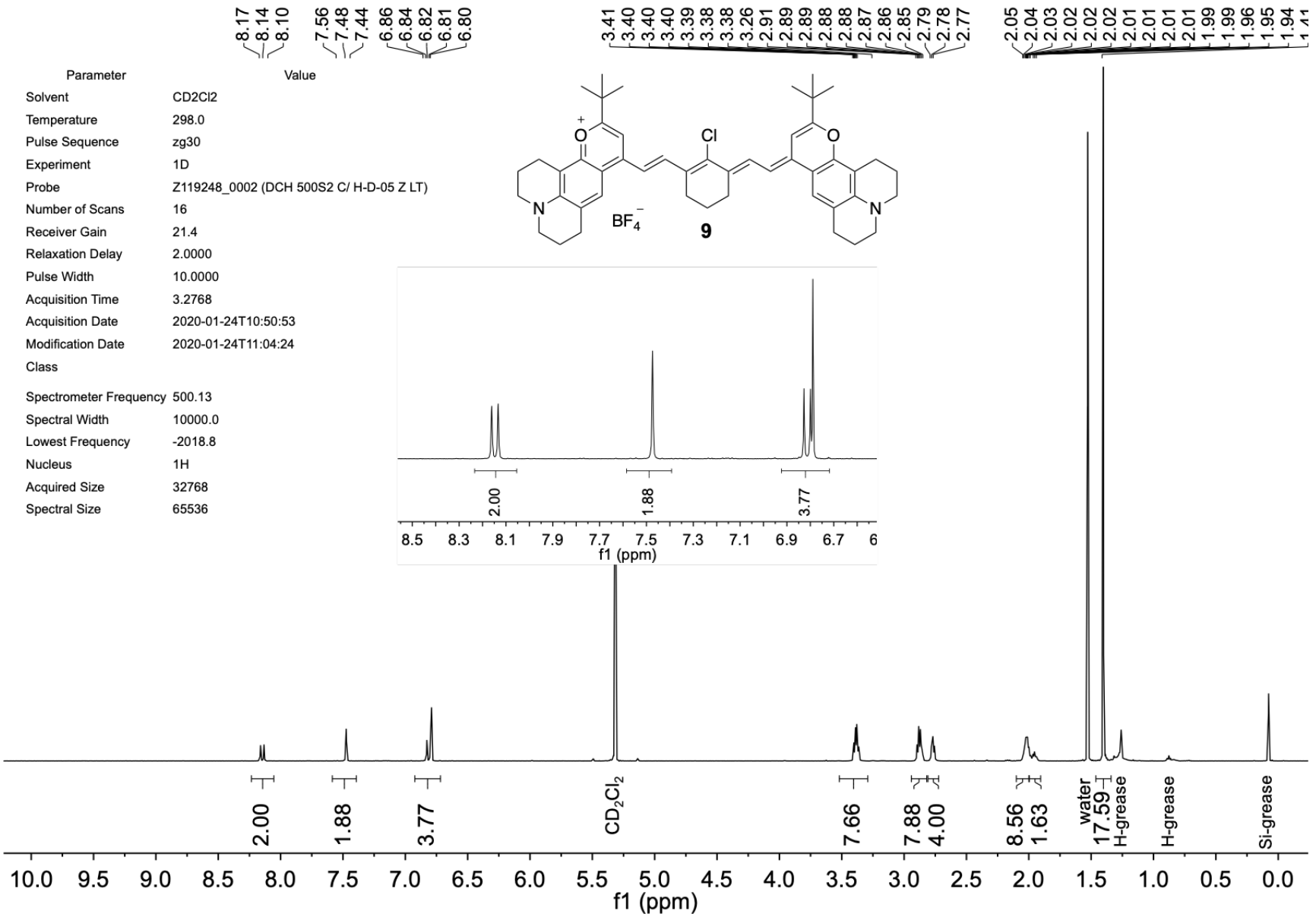
8.17 8.14 8.10 7.56 7.48 7.44 6.86 6.84 6.82 6.81 6.80
3.41 3.40 3.40 3.39 3.38 3.38 3.26 2.91 2.89 2.89 2.88 2.88 2.87 2.86 2.85 2.79 2.78 2.77
2.05 2.04 2.03 2.02 2.02 2.02 2.01 2.01 2.01 2.01 1.99 1.99 1.96 1.95 1.94
Parameter Value
Solvent CD2Cl2
Temperature 298.0
Pulse Sequence zg30
Experiment 1D
Probe Z119248_0002 (DCH 500S2 C/ H-D-05 Z LT)
Number of Scans 16
Receiver Gain 21.4
Relaxation Delay 2.0000
Pulse Width 10.0000
Acquisition Time 3.2768
Acquisition Date 2020-01-24T10:50:53
Modification Date 2020-01-24T11:04:24
Class
Spectrometer Frequency 500.13
Spectral Width 10000.0
Lowest Frequency -2018.8
Nucleus 1H
Acquired Size 32768
Spectral Size 65536
Cl
O
N
BF4−
9
2.00 1.88 3.77
8.5 8.3 8.1 7.9 7.7 7.5 7.3 7.1 6.9 6.7
f1 (ppm)
2.00 1.88 3.77 CD2Cl2 7.66 7.88 4.00 8.56 1.63 water 17.59 H-grease H-grease Si-grease
10.0 9.5 9.0 8.5 8.0 7.5 7.0 6.5 6.0 5.5 5.0 4.5 4.0 3.5 3.0 2.5 2.0 1.5 1.0 0.5 0.0
f1 (ppm)

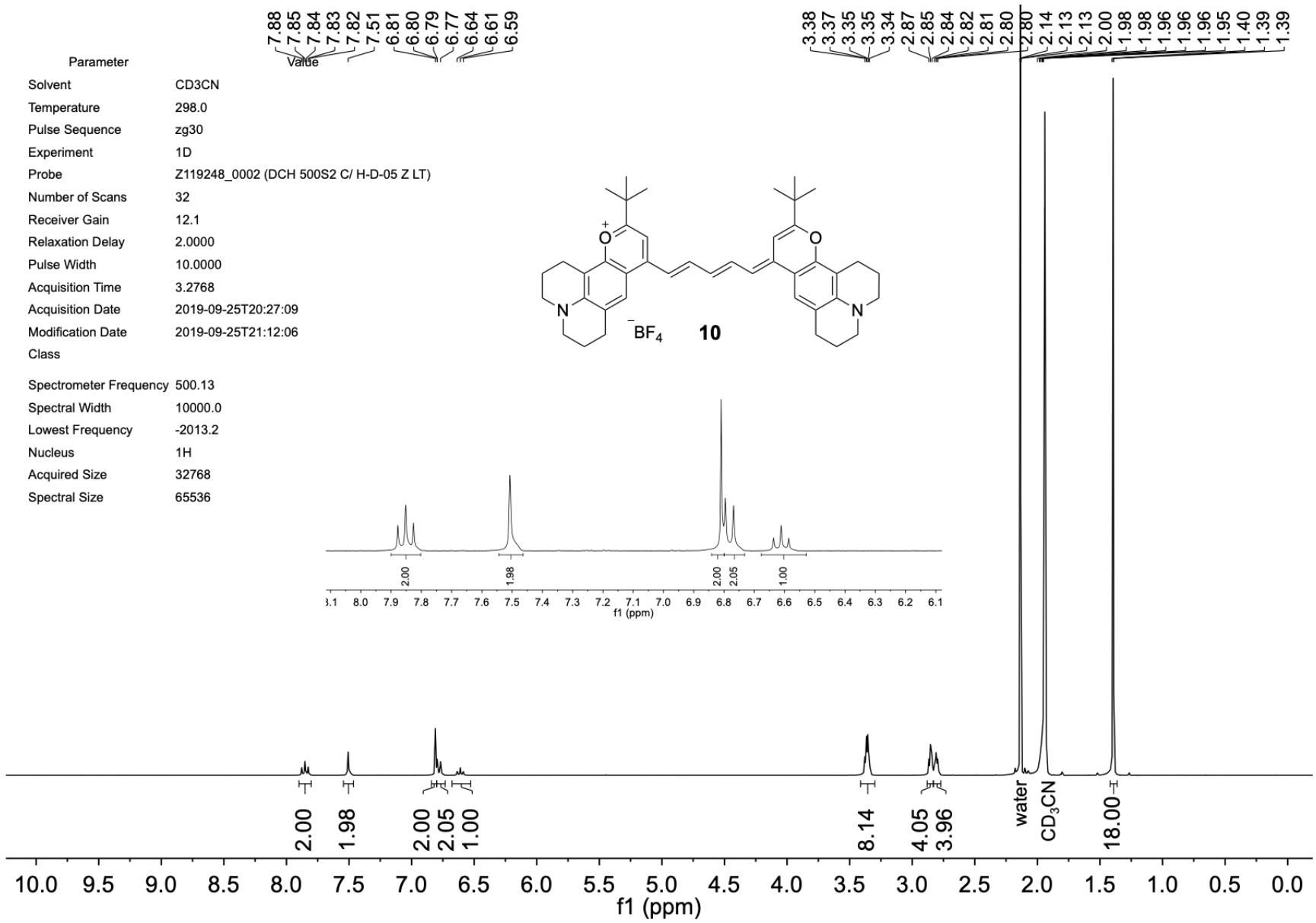
7.88 7.85 7.84 7.83 7.82 7.51 6.81 6.80 6.79 6.77 6.64 6.61 6.59
3.38 3.37 3.35 3.35 3.34 2.87 2.85 2.84 2.82 2.81 2.80 2.80 2.14 2.13 2.13 2.00 1.98 1.98 1.96 1.96 1.96 1.95 1.40 1.39 1.39
Parameter Value
Solvent CD3CN
Temperature 298.0
Pulse Sequence zg30
Experiment 1D
Probe Z119248_0002 (DCH 500S2 C/ H-D-05 Z LT)
Number of Scans 32
Receiver Gain 12.1
Relaxation Delay 2.0000
Pulse Width 10.0000
Acquisition Time 3.2768
Acquisition Date 2019-09-25T20:27:09
Modification Date 2019-09-25T21:12:06
Class
Spectrometer Frequency 500.13
Spectral Width 10000.0
Lowest Frequency -2013.2
Nucleus 1H
Acquired Size 32768
Spectral Size 65536
O
N
O
N
$^{-}BF_4$
10
2.00 1.98 2.00 2.05 1.00
f1 (ppm)
2.00 1.98 2.00 2.05 1.00
8.14 4.05 3.96
water
CD_3CN
18.00
10.0 9.5 9.0 8.5 8.0 7.5 7.0 6.5 6.0 5.5 5.0 4.5 4.0 3.5 3.0 2.5 2.0 1.5 1.0 0.5 0.0
f1 (ppm)

^{13}C NMRs

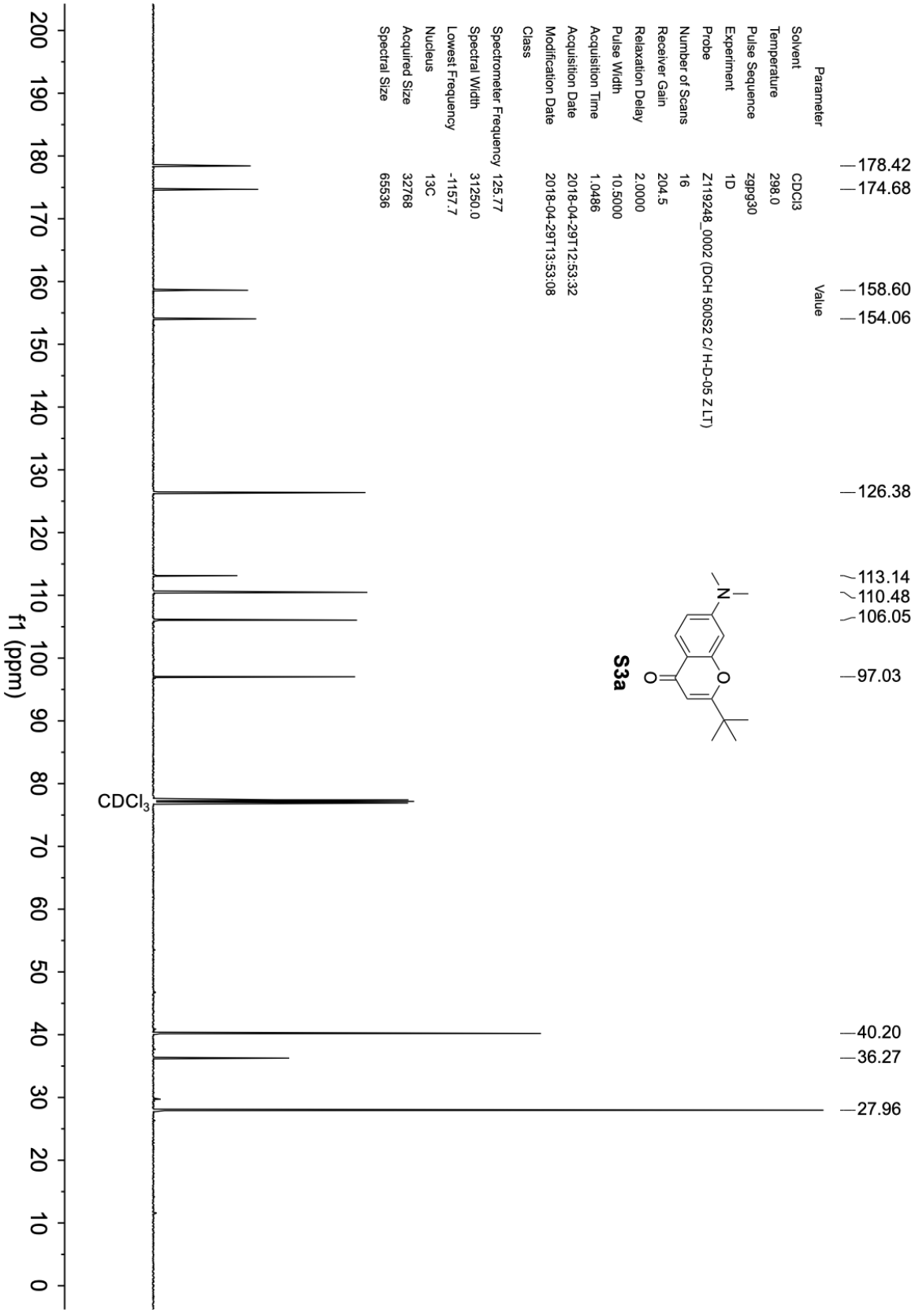
Parameter
Value
Solvent
CDCl3
Temperature
298.0
Pulse Sequence
zgpg30
Experiment
1D
Probe
Z119248_0002 (DCH 500S2 C/ H-D-05 Z LT)
Number of Scans
16
Receiver Gain
204.5
Relaxation Delay
2.0000
Pulse Width
10.5000
Acquisition Time
1.0486
Acquisition Date
2018-04-29T12:53:32
Modification Date
2018-04-29T13:53:08
Class
Spectrometer Frequency
125.77
Spectral Width
31250.0
Lowest Frequency
-1157.7
Nucleus
13C
Acquired Size
32768
Spectral Size
65536
178.42
174.68
158.60
154.06
126.38
113.14
110.48
106.05
97.03
40.20
36.27
27.96
CDCl3
S3a
f1 (ppm)

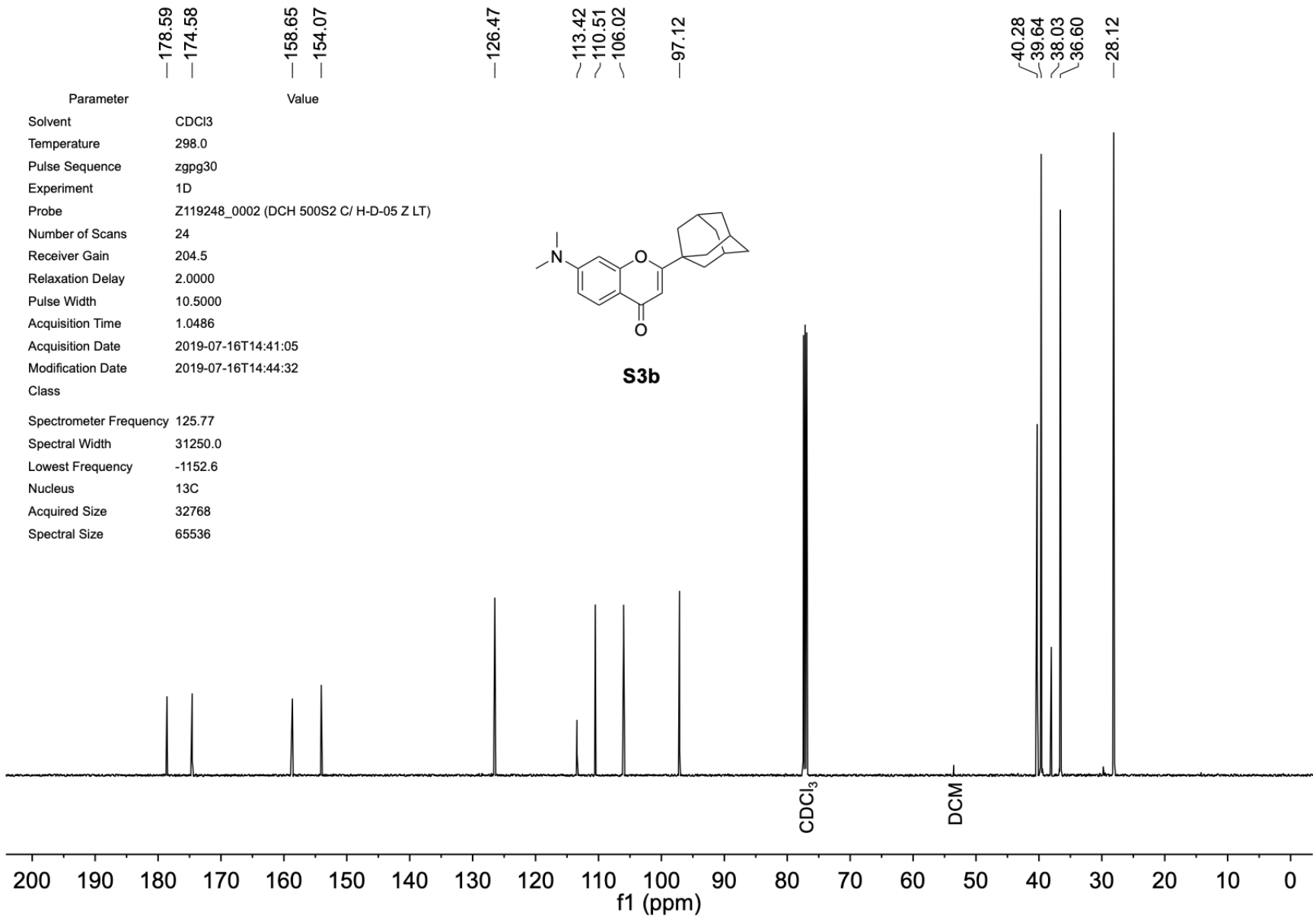
178.59
174.58
158.65
154.07
126.47
113.42
110.51
106.02
97.12
40.28
39.64
38.03
36.60
28.12
Parameter
Value
Solvent
CDCl3
Temperature
298.0
Pulse Sequence
zgpg30
Experiment
1D
Probe
Z119248_0002 (DCH 500S2 C/ H-D-05 Z LT)
Number of Scans
24
Receiver Gain
204.5
Relaxation Delay
2.0000
Pulse Width
10.5000
Acquisition Time
1.0486
Acquisition Date
2019-07-16T14:41:05
Modification Date
2019-07-16T14:44:32
Class
Spectrometer Frequency
125.77
Spectral Width
31250.0
Lowest Frequency
-1152.6
Nucleus
13C
Acquired Size
32768
Spectral Size
65536
N
O
O
S3b
CDCl3
DCM
200
190
180
170
160
150
140
130
120
110
100
90
80
70
60
50
40
30
20
10
0
f1 (ppm)

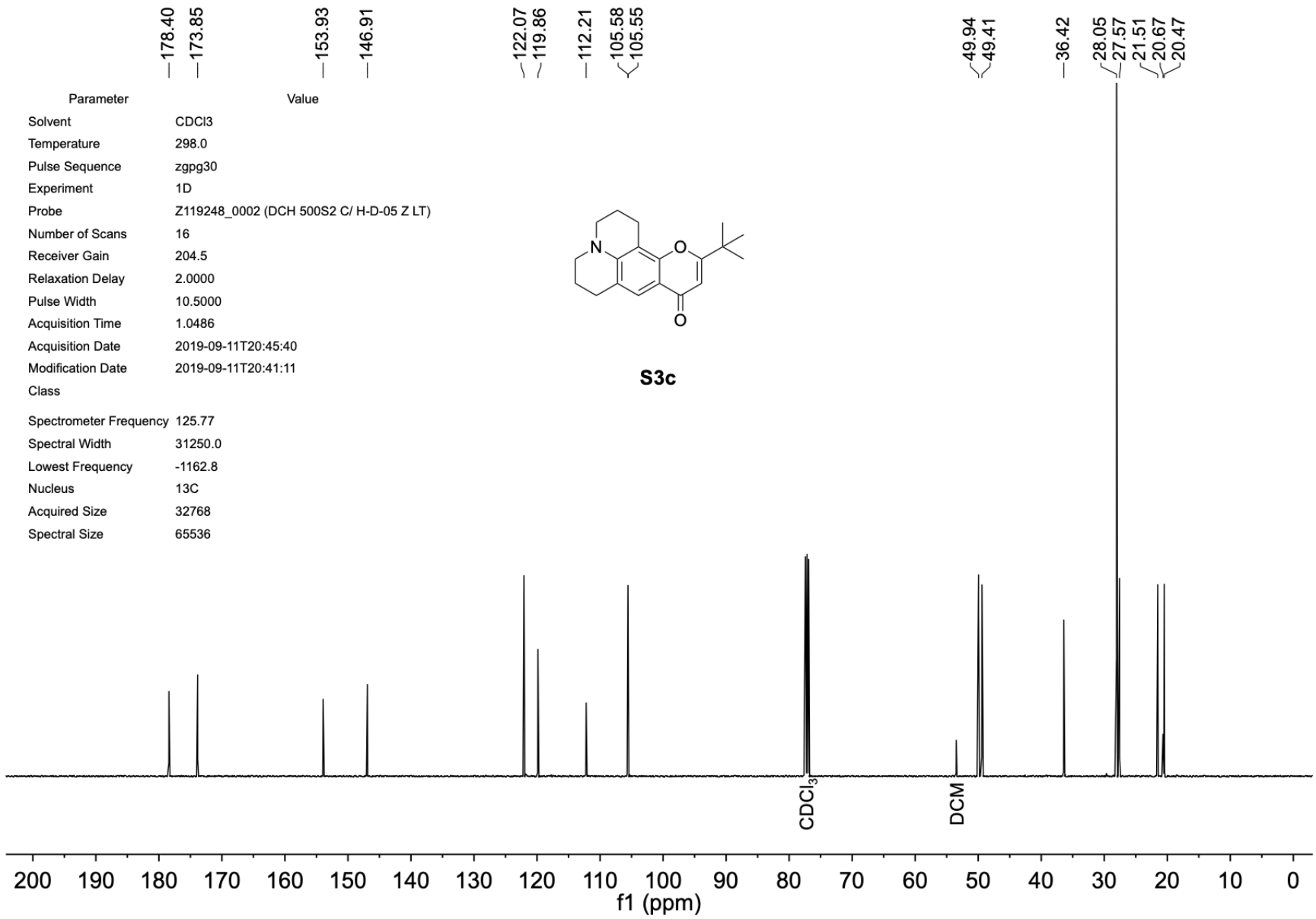
178.40
173.85
153.93
146.91
122.07
119.86
112.21
105.58
105.55
49.94
49.41
36.42
28.05
27.57
21.51
20.67
20.47
Parameter Value
Solvent CDCl3
Temperature 298.0
Pulse Sequence zgpg30
Experiment 1D
Probe Z119248_0002 (DCH 500S2 C/ H-D-05 Z LT)
Number of Scans 16
Receiver Gain 204.5
Relaxation Delay 2.0000
Pulse Width 10.5000
Acquisition Time 1.0486
Acquisition Date 2019-09-11T20:45:40
Modification Date 2019-09-11T20:41:11
Class
Spectrometer Frequency 125.77
Spectral Width 31250.0
Lowest Frequency -1162.8
Nucleus 13C
Acquired Size 32768
Spectral Size 65536
N
O
O
S3c
CDCl3
DCM
200 190 180 170 160 150 140 130 120 110 100 90 80 70 60 50 40 30 20 10 0
f1 (ppm)

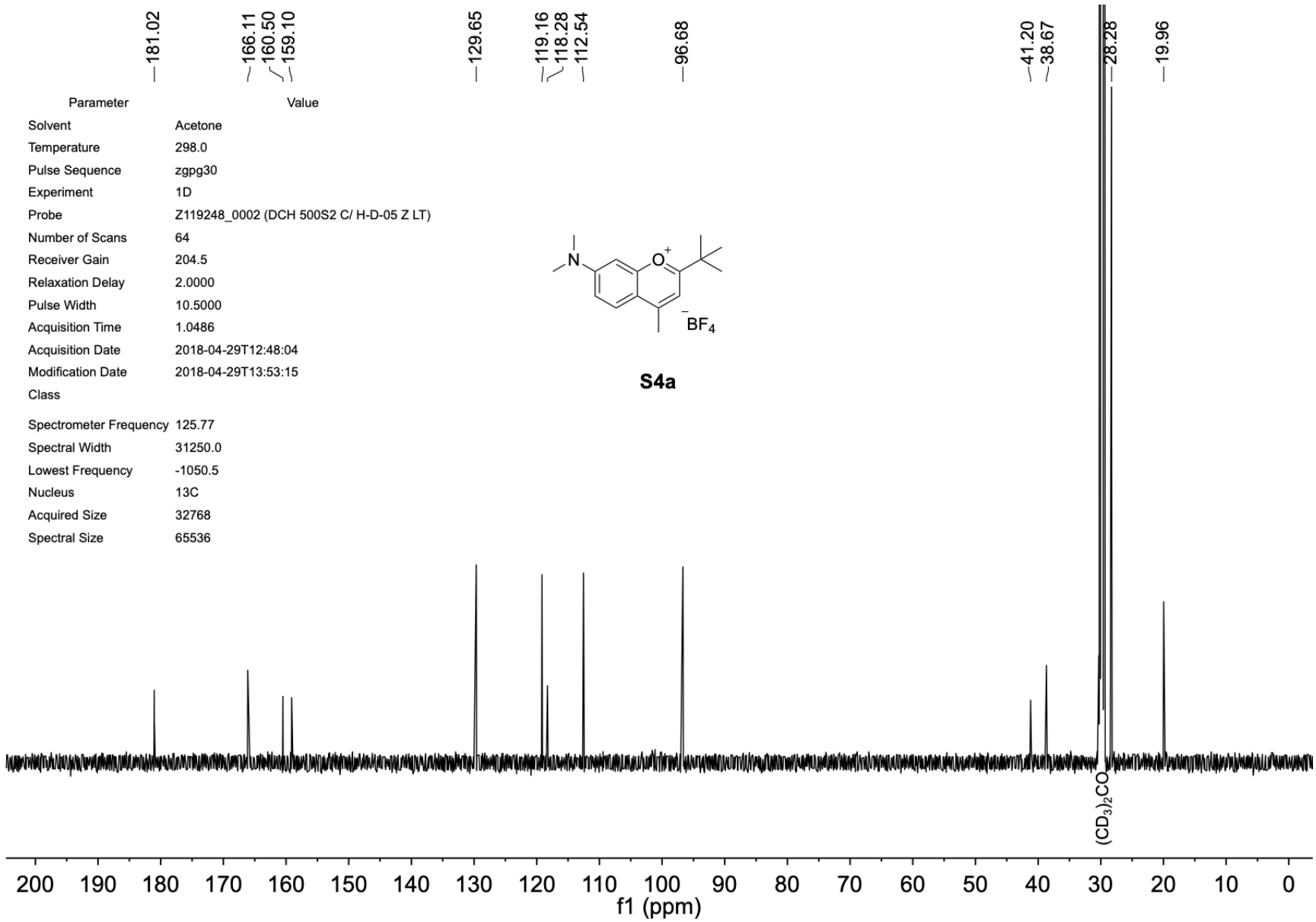
181.02
166.11
160.50
159.10
129.65
119.16
118.28
112.54
96.68
41.20
38.67
28.28
19.96
Parameter Value
Solvent Acetone
Temperature 298.0
Pulse Sequence zgpg30
Experiment 1D
Probe Z119248_0002 (DCH 500S2 C/ H-D-05 Z LT)
Number of Scans 64
Receiver Gain 204.5
Relaxation Delay 2.0000
Pulse Width 10.5000
Acquisition Time 1.0486
Acquisition Date 2018-04-29T12:48:04
Modification Date 2018-04-29T13:53:15
Class
Spectrometer Frequency 125.77
Spectral Width 31250.0
Lowest Frequency -1050.5
Nucleus 13C
Acquired Size 32768
Spectral Size 65536
N
O+
BF4
S4a
(CD3)2CO
200 190 180 170 160 150 140 130 120 110 100 90 80 70 60 50 40 30 20 10 0
f1 (ppm)

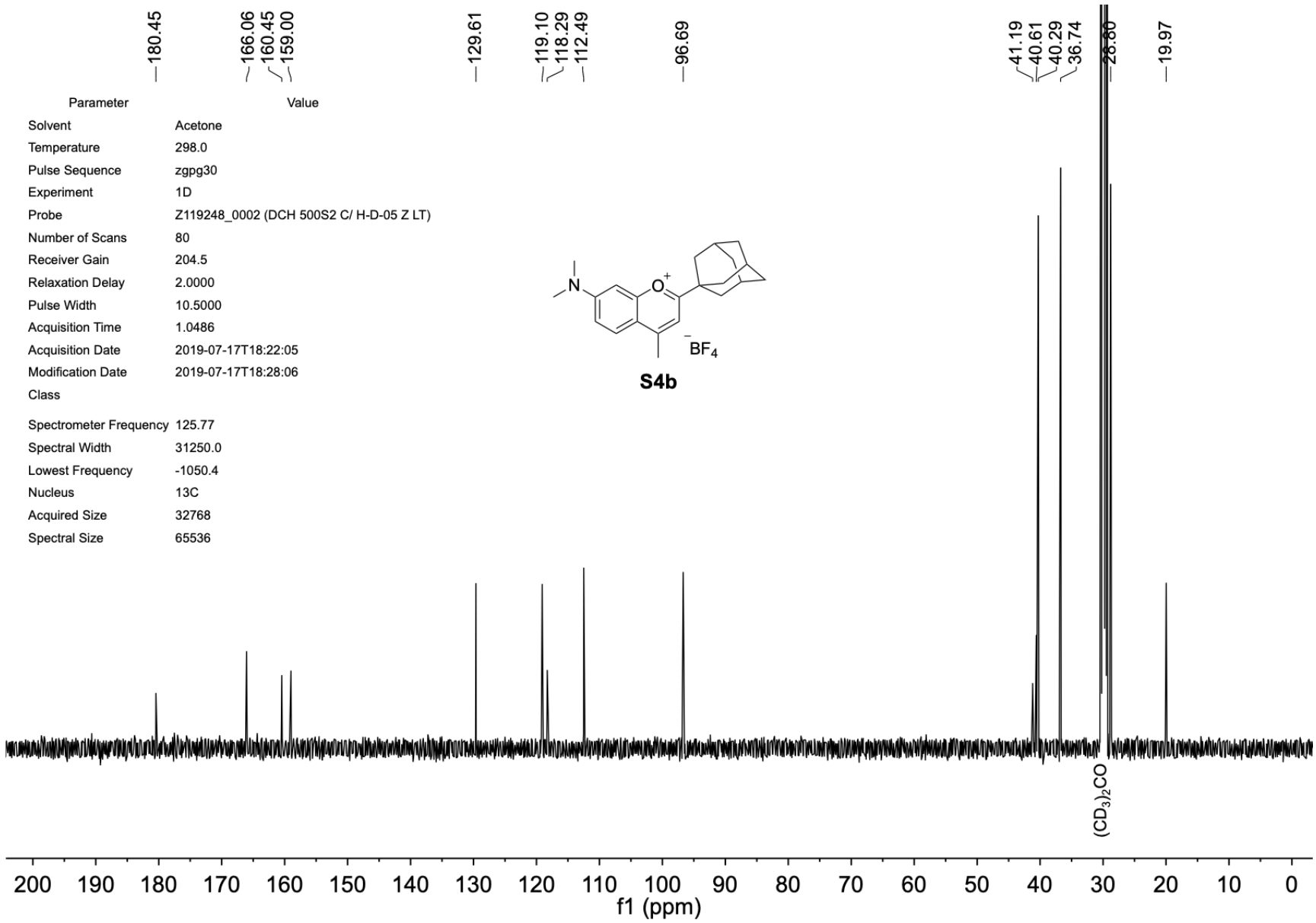
180.45
166.06
160.45
159.00
129.61
119.10
118.29
112.49
96.69
41.19
40.61
40.29
36.74
28.80
19.97
Parameter Value
Solvent Acetone
Temperature 298.0
Pulse Sequence zgpg30
Experiment 1D
Probe Z119248_0002 (DCH 500S2 C/ H-D-05 Z LT)
Number of Scans 80
Receiver Gain 204.5
Relaxation Delay 2.0000
Pulse Width 10.5000
Acquisition Time 1.0486
Acquisition Date 2019-07-17T18:22:05
Modification Date 2019-07-17T18:28:06
Class
Spectrometer Frequency 125.77
Spectral Width 31250.0
Lowest Frequency -1050.4
Nucleus 13C
Acquired Size 32768
Spectral Size 65536
N
O+
BF4
S4b
(CD3)2CO
200 190 180 170 160 150 140 130 120 110 100 90 80 70 60 50 40 30 20 10 0
f1 (ppm)

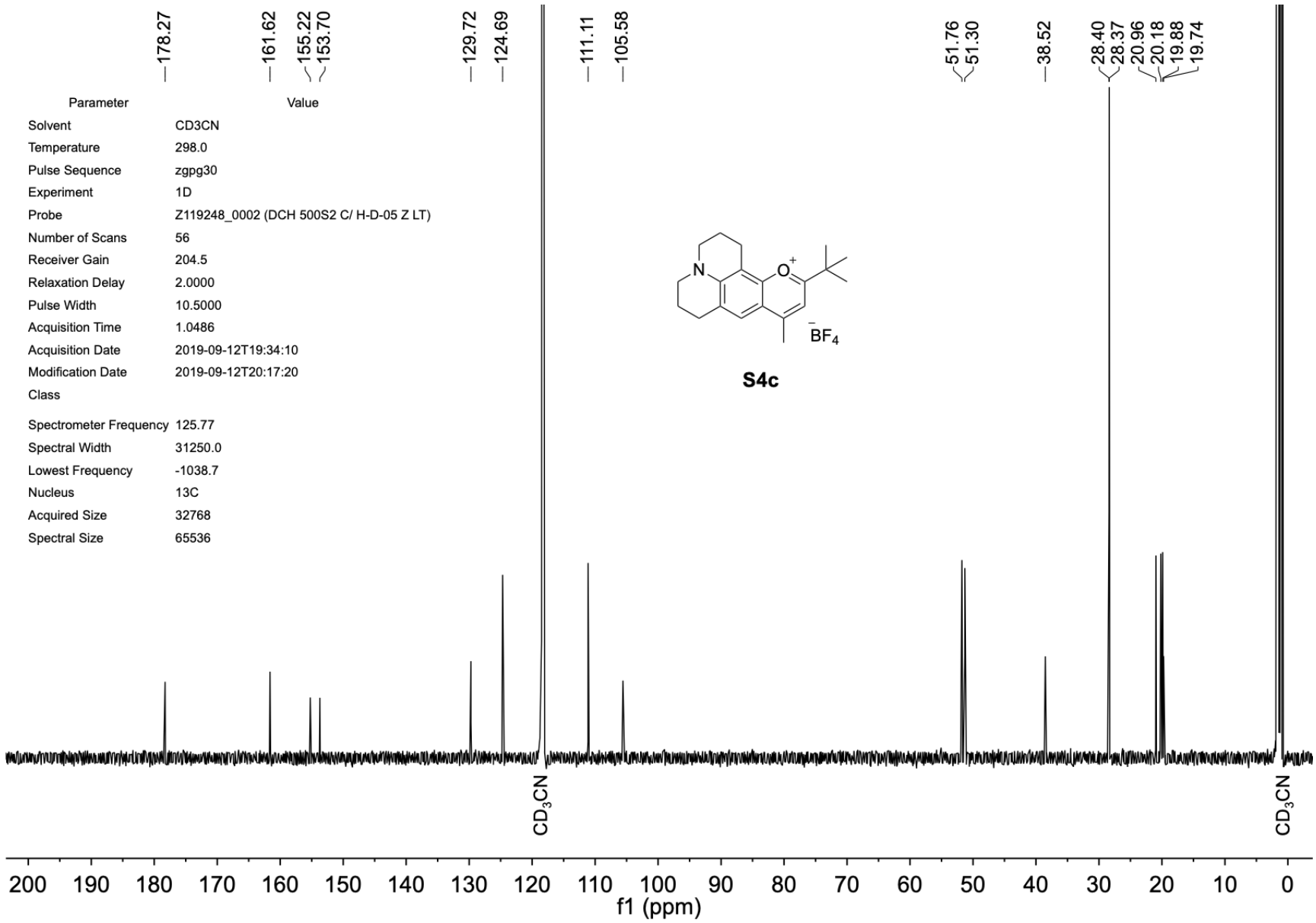
178.27
161.62
155.22
153.70
129.72
124.69
111.11
105.58
51.76
51.30
38.52
28.40
28.37
20.96
20.18
19.88
19.74
Parameter Value
Solvent CD3CN
Temperature 298.0
Pulse Sequence zgpg30
Experiment 1D
Probe Z119248_0002 (DCH 500S2 C/ H-D-05 Z LT)
Number of Scans 56
Receiver Gain 204.5
Relaxation Delay 2.0000
Pulse Width 10.5000
Acquisition Time 1.0486
Acquisition Date 2019-09-12T19:34:10
Modification Date 2019-09-12T20:17:20
Class
Spectrometer Frequency 125.77
Spectral Width 31250.0
Lowest Frequency -1038.7
Nucleus 13C
Acquired Size 32768
Spectral Size 65536
N
O+
BF4
S4c
CD3CN
CD3CN
200 190 180 170 160 150 140 130 120 110 100 90 80 70 60 50 40 30 20 10 0
f1 (ppm)

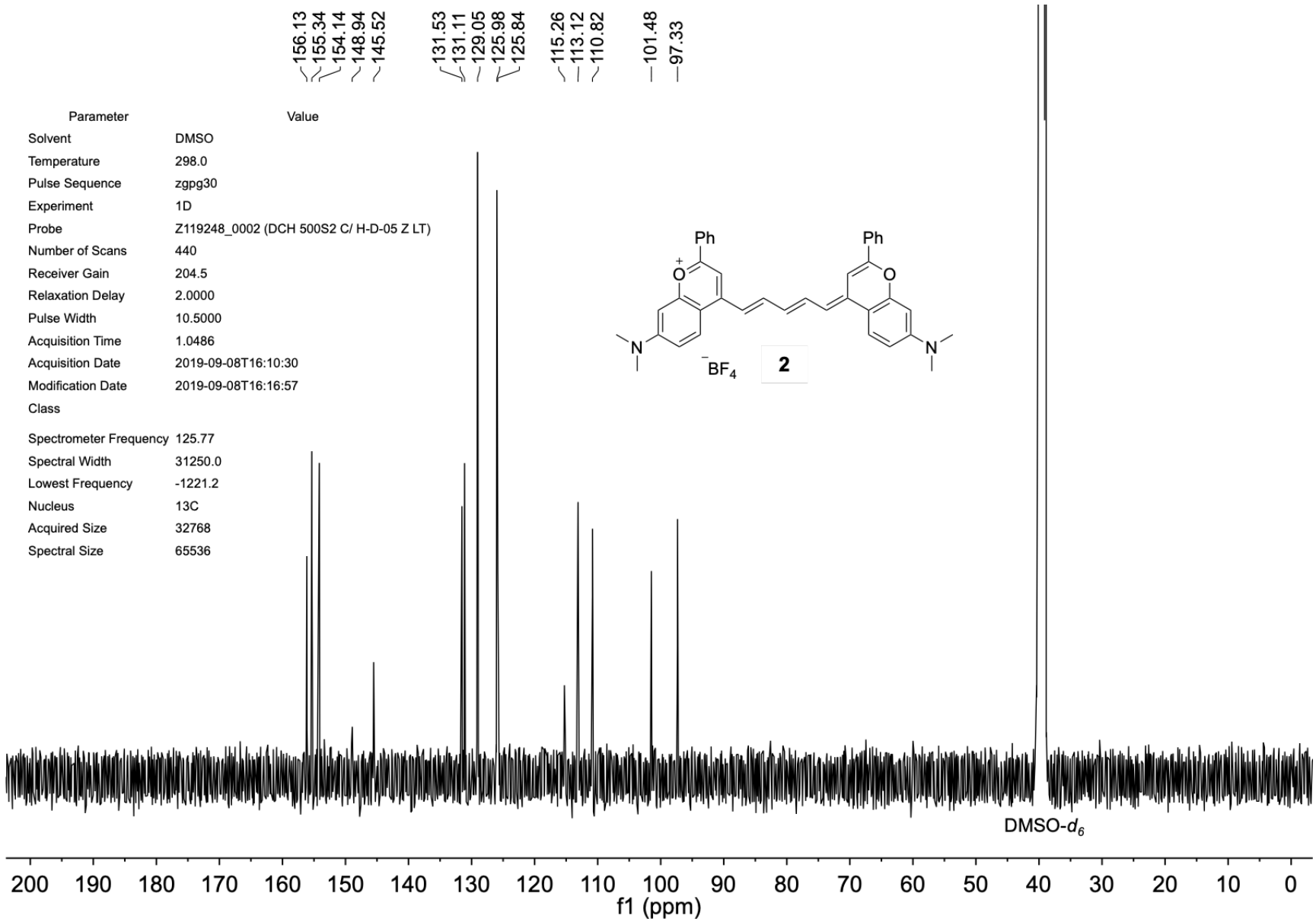
156.13
155.34
154.14
148.94
145.52
131.53
131.11
129.05
125.98
125.84
115.26
113.12
110.82
101.48
97.33
Parameter Value
Solvent DMSO
Temperature 298.0
Pulse Sequence zgpg30
Experiment 1D
Probe Z119248_0002 (DCH 500S2 C/ H-D-05 Z LT)
Number of Scans 440
Receiver Gain 204.5
Relaxation Delay 2.0000
Pulse Width 10.5000
Acquisition Time 1.0486
Acquisition Date 2019-09-08T16:10:30
Modification Date 2019-09-08T16:16:57
Class
Spectrometer Frequency 125.77
Spectral Width 31250.0
Lowest Frequency -1221.2
Nucleus 13C
Acquired Size 32768
Spectral Size 65536
Ph
Ph
O
O
N
N
BF4
2
DMSO-d6
200 190 180 170 160 150 140 130 120 110 100 90 80 70 60 50 40 30 20 10 0
f1 (ppm)

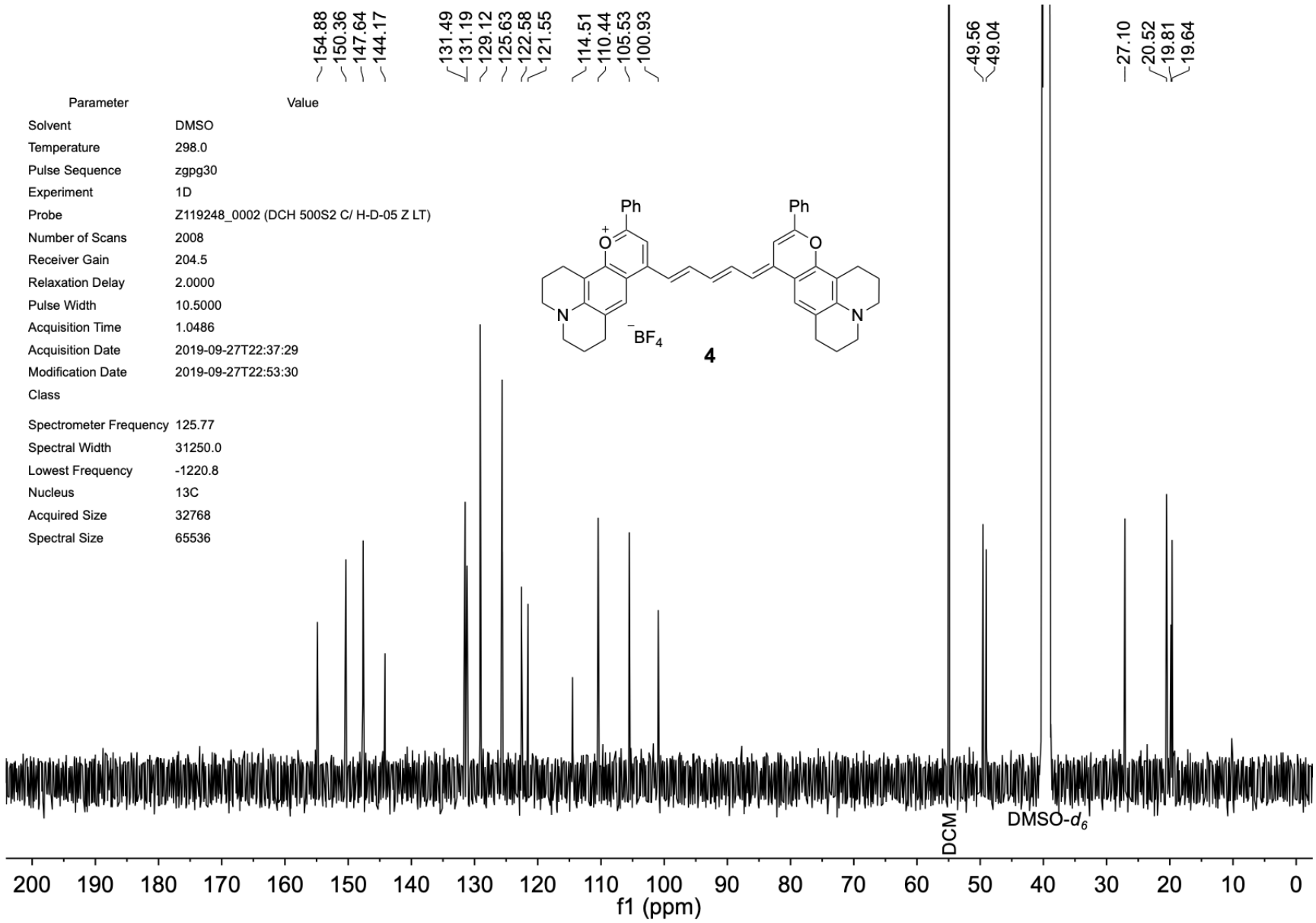
154.88
150.36
147.64
144.17
131.49
131.19
129.12
125.63
122.58
121.55
114.51
110.44
105.53
100.93
49.56
49.04
27.10
20.52
19.81
19.64
Parameter Value
Solvent DMSO
Temperature 298.0
Pulse Sequence zgpg30
Experiment 1D
Probe Z119248_0002 (DCH 500S2 C/ H-D-05 Z LT)
Number of Scans 2008
Receiver Gain 204.5
Relaxation Delay 2.0000
Pulse Width 10.5000
Acquisition Time 1.0486
Acquisition Date 2019-09-27T22:37:29
Modification Date 2019-09-27T22:53:30
Class
Spectrometer Frequency 125.77
Spectral Width 31250.0
Lowest Frequency -1220.8
Nucleus 13C
Acquired Size 32768
Spectral Size 65536
Ph
Ph
O
O
N
N
BF4
4
DCM
DMSO-d6
200 190 180 170 160 150 140 130 120 110 100 90 80 70 60 50 40 30 20 10 0
f1 (ppm)

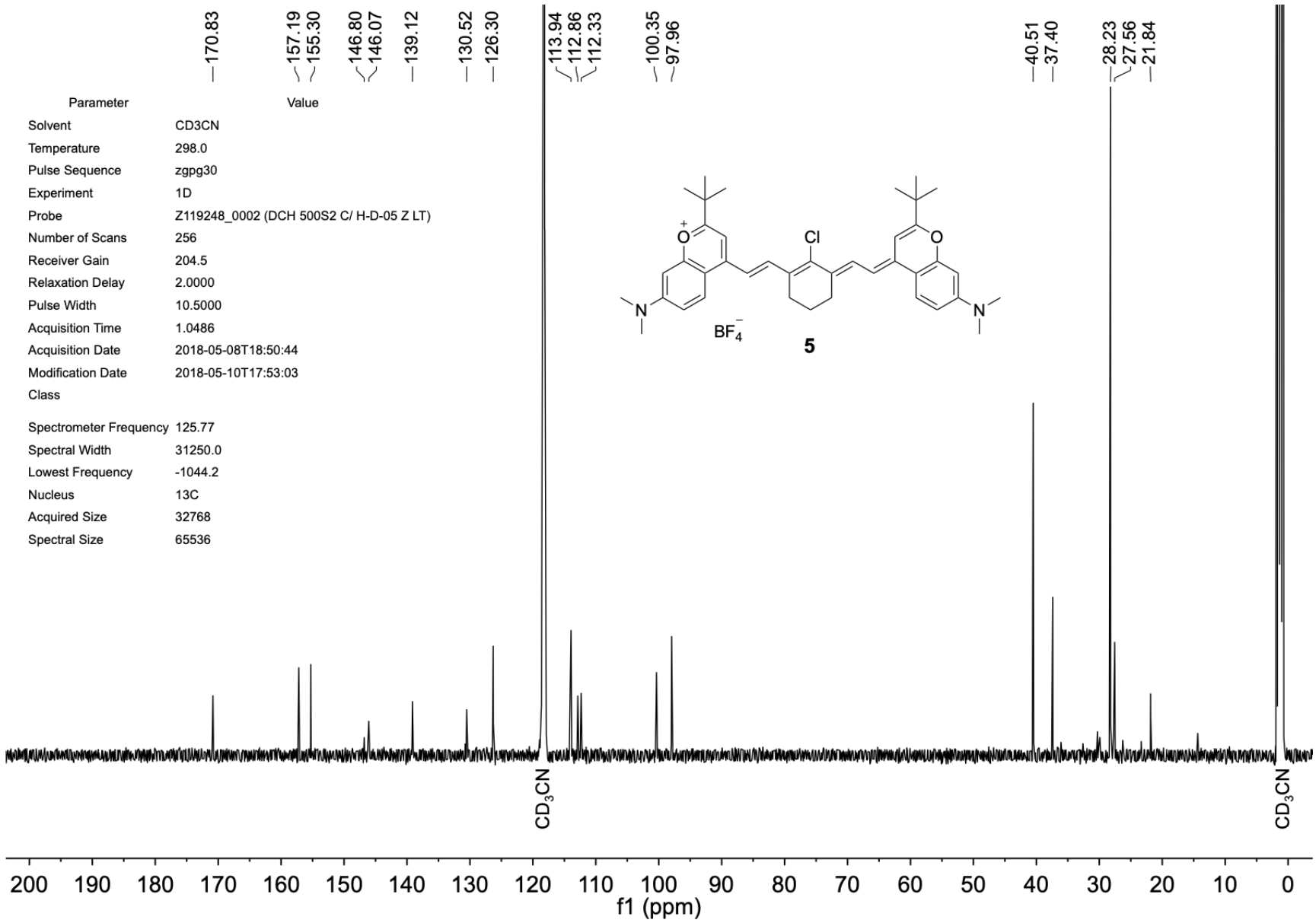
170.83
157.19
155.30
146.80
146.07
139.12
130.52
126.30
113.94
112.86
112.33
100.35
97.96
40.51
37.40
28.23
27.56
21.84
Parameter Value
Solvent CD3CN
Temperature 298.0
Pulse Sequence zgpg30
Experiment 1D
Probe Z119248_0002 (DCH 500S2 C/ H-D-05 Z LT)
Number of Scans 256
Receiver Gain 204.5
Relaxation Delay 2.0000
Pulse Width 10.5000
Acquisition Time 1.0486
Acquisition Date 2018-05-08T18:50:44
Modification Date 2018-05-10T17:53:03
Class
Spectrometer Frequency 125.77
Spectral Width 31250.0
Lowest Frequency -1044.2
Nucleus 13C
Acquired Size 32768
Spectral Size 65536
Cl
O
N
BF4−
5
CD3CN
CD3CN
200 190 180 170 160 150 140 130 120 110 100 90 80 70 60 50 40 30 20 10 0
f1 (ppm)

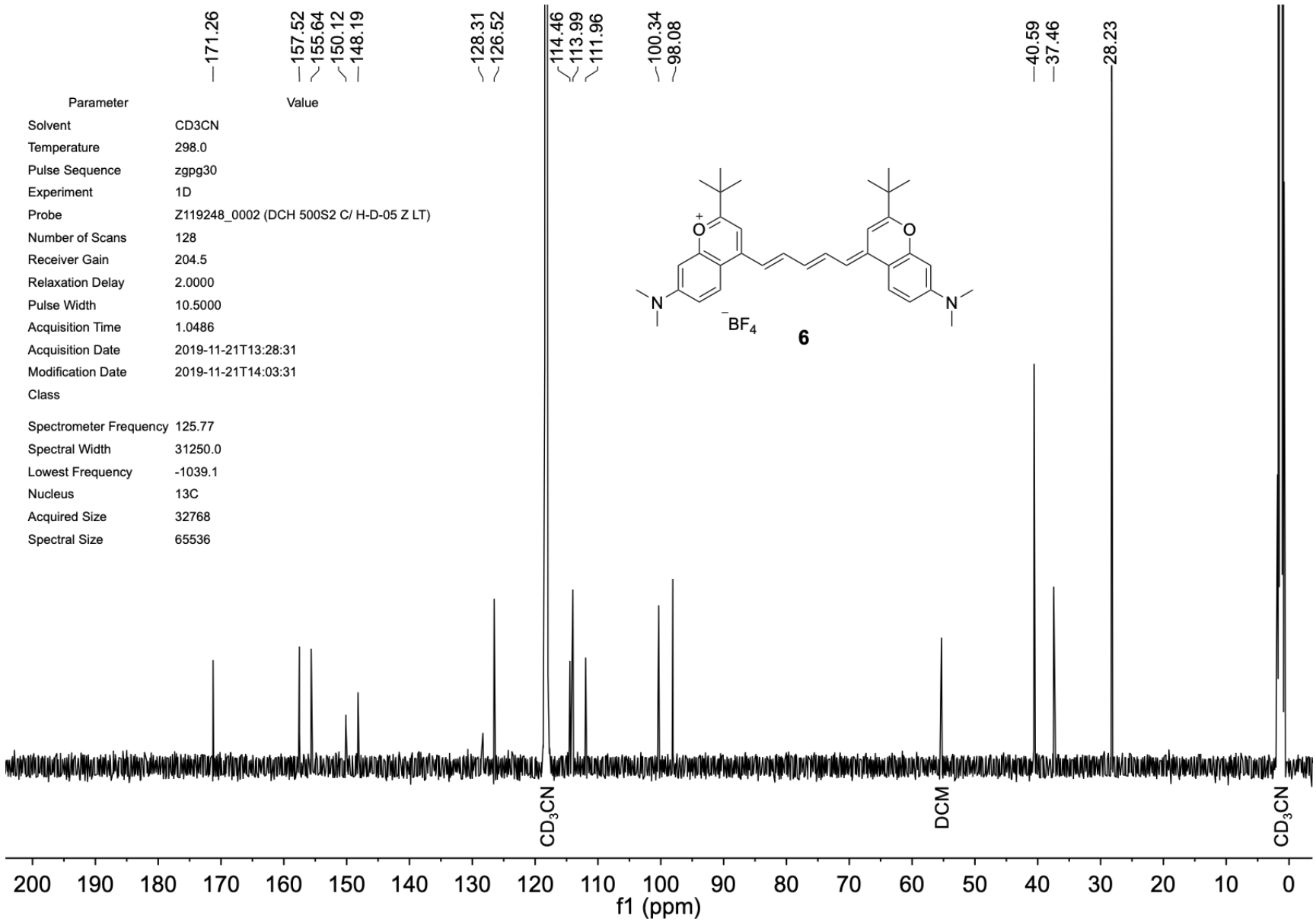
171.26
157.52
155.64
150.12
148.19
128.31
126.52
114.46
113.99
111.96
100.34
98.08
40.59
37.46
28.23
Parameter Value
Solvent CD3CN
Temperature 298.0
Pulse Sequence zgpg30
Experiment 1D
Probe Z119248_0002 (DCH 500S2 C/ H-D-05 Z LT)
Number of Scans 128
Receiver Gain 204.5
Relaxation Delay 2.0000
Pulse Width 10.5000
Acquisition Time 1.0486
Acquisition Date 2019-11-21T13:28:31
Modification Date 2019-11-21T14:03:31
Class
Spectrometer Frequency 125.77
Spectral Width 31250.0
Lowest Frequency -1039.1
Nucleus 13C
Acquired Size 32768
Spectral Size 65536
$^{-}BF_4$
6
CD_3CN
DCM
CD_3CN
200 190 180 170 160 150 140 130 120 110 100 90 80 70 60 50 40 30 20 10 0
f1 (ppm)

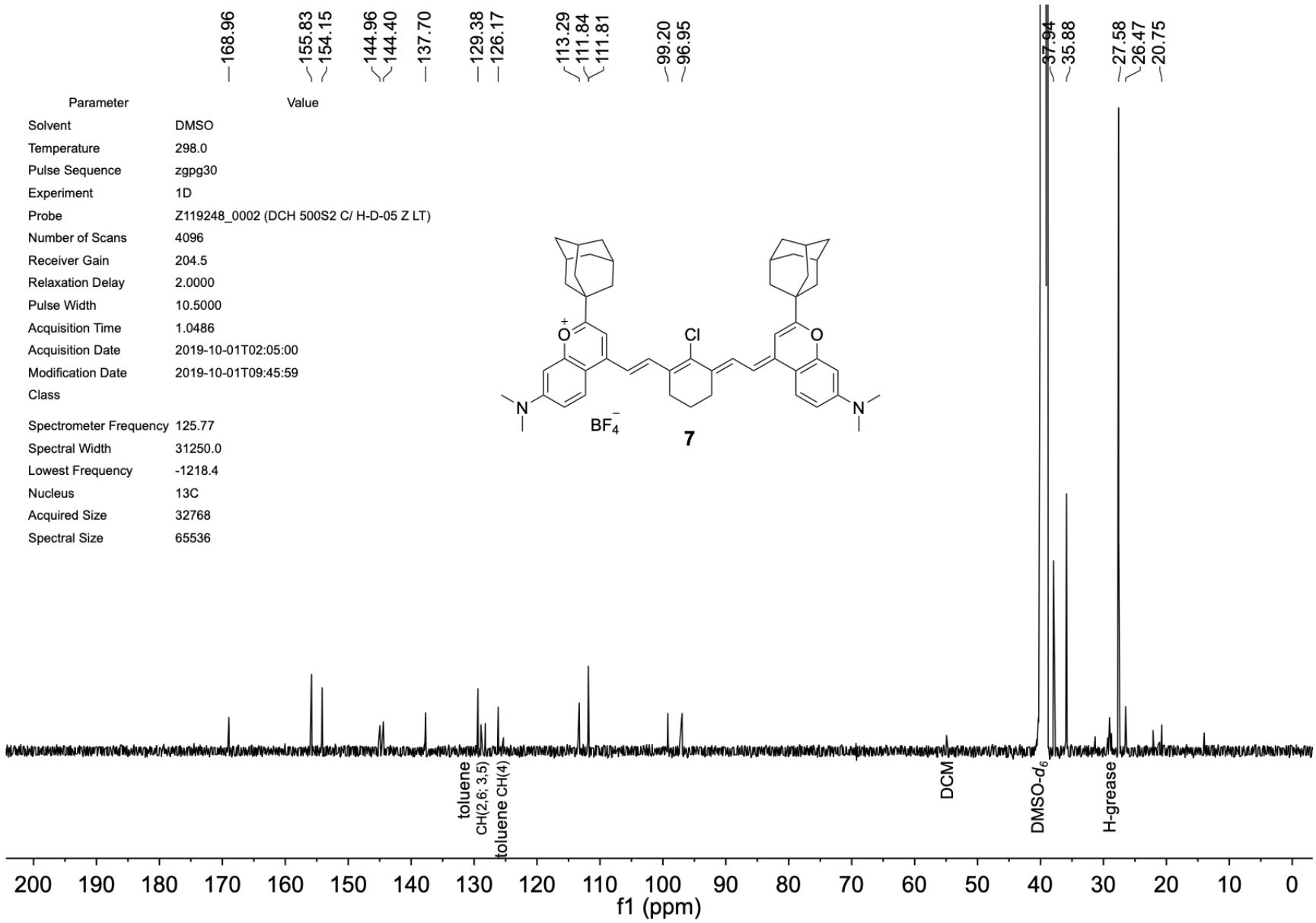
168.96
155.83
154.15
144.96
144.40
137.70
129.38
126.17
113.29
111.84
111.81
99.20
96.95
37.94
35.88
27.58
26.47
20.75
Parameter Value
Solvent DMSO
Temperature 298.0
Pulse Sequence zgpg30
Experiment 1D
Probe Z119248_0002 (DCH 500S2 C/ H-D-05 Z LT)
Number of Scans 4096
Receiver Gain 204.5
Relaxation Delay 2.0000
Pulse Width 10.5000
Acquisition Time 1.0486
Acquisition Date 2019-10-01T02:05:00
Modification Date 2019-10-01T09:45:59
Class
Spectrometer Frequency 125.77
Spectral Width 31250.0
Lowest Frequency -1218.4
Nucleus 13C
Acquired Size 32768
Spectral Size 65536
Cl
BF4
7
toluene
CH(2,6; 3,5)
toluene CH(4)
DCM
DMSO-d6
H-grease
200 190 180 170 160 150 140 130 120 110 100 90 80 70 60 50 40 30 20 10 0
f1 (ppm)

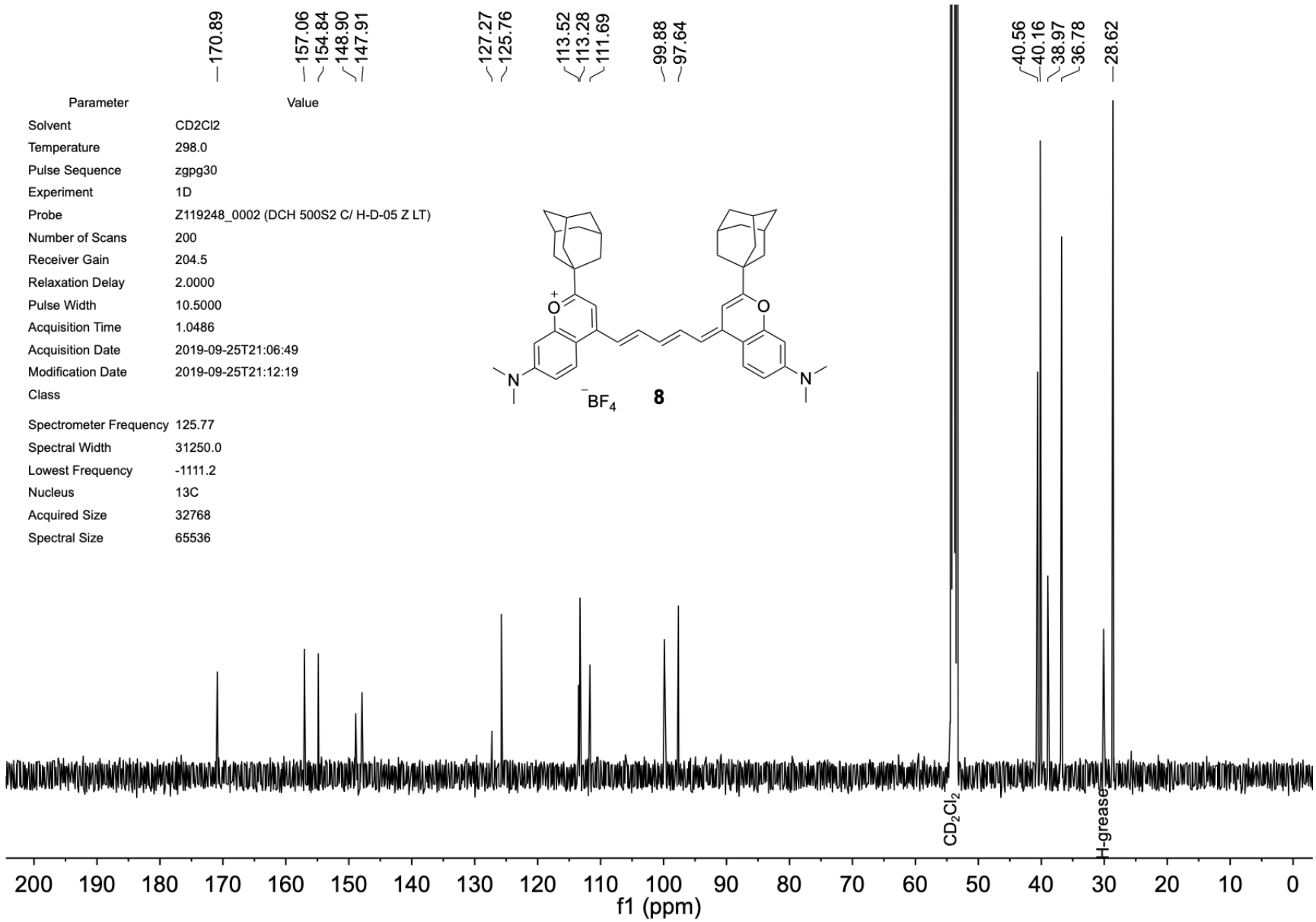
170.89
157.06
154.84
148.90
147.91
127.27
125.76
113.52
113.28
111.69
99.88
97.64
40.56
40.16
38.97
36.78
28.62
Parameter Value
Solvent CD2Cl2
Temperature 298.0
Pulse Sequence zgpg30
Experiment 1D
Probe Z119248_0002 (DCH 500S2 C/ H-D-05 Z LT)
Number of Scans 200
Receiver Gain 204.5
Relaxation Delay 2.0000
Pulse Width 10.5000
Acquisition Time 1.0486
Acquisition Date 2019-09-25T21:06:49
Modification Date 2019-09-25T21:12:19
Class
Spectrometer Frequency 125.77
Spectral Width 31250.0
Lowest Frequency -1111.2
Nucleus 13C
Acquired Size 32768
Spectral Size 65536
O
O
N
N
BF4
8
CD2Cl2
H-grease
200 190 180 170 160 150 140 130 120 110 100 90 80 70 60 50 40 30 20 10 0
f1 (ppm)

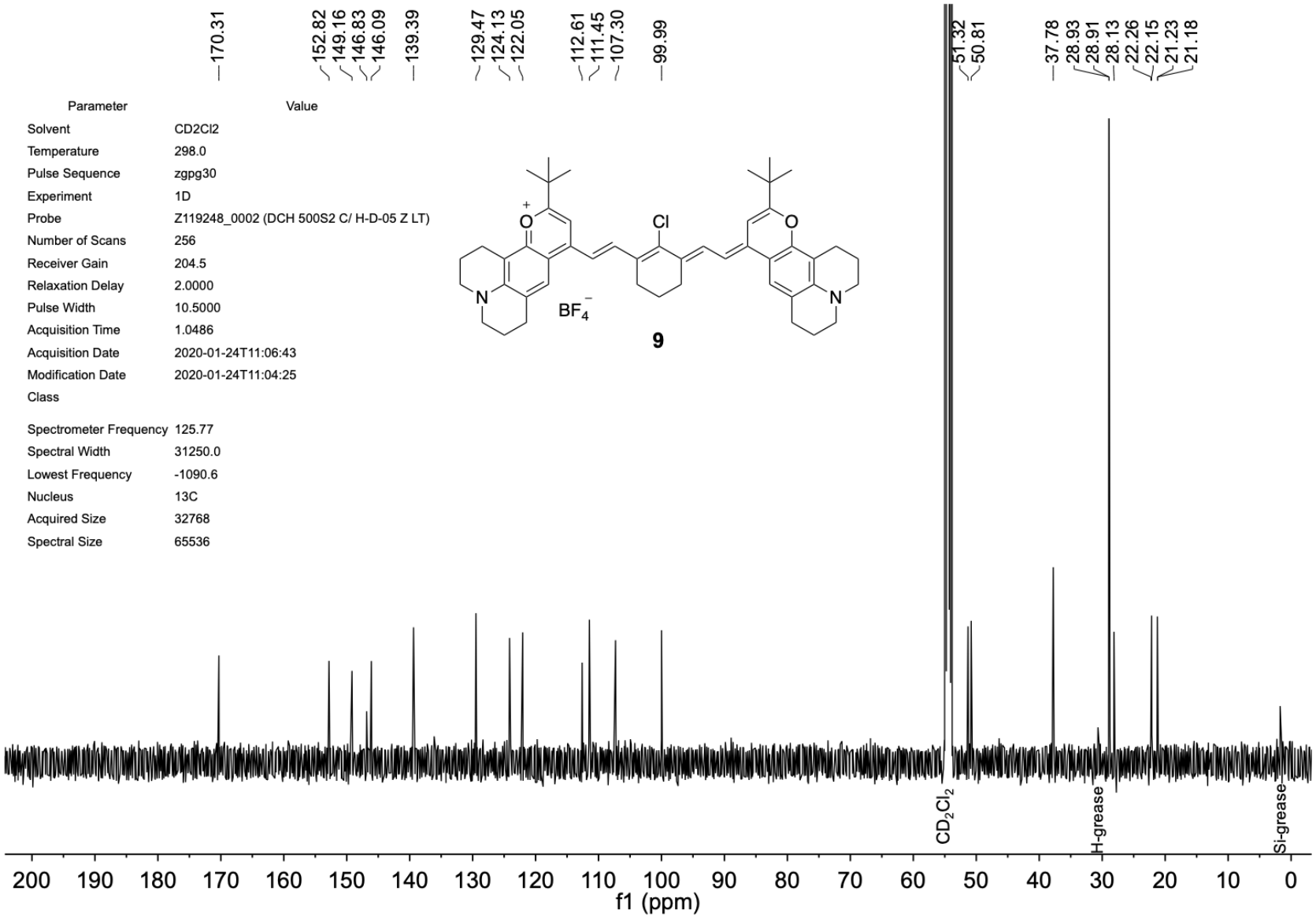
170.31
152.82
149.16
146.83
146.09
139.39
129.47
124.13
122.05
112.61
111.45
107.30
99.99
51.32
50.81
37.78
28.93
28.91
28.13
22.26
22.15
21.23
21.18
Parameter Value
Solvent CD2Cl2
Temperature 298.0
Pulse Sequence zgpg30
Experiment 1D
Probe Z119248_0002 (DCH 500S2 C/ H-D-05 Z LT)
Number of Scans 256
Receiver Gain 204.5
Relaxation Delay 2.0000
Pulse Width 10.5000
Acquisition Time 1.0486
Acquisition Date 2020-01-24T11:06:43
Modification Date 2020-01-24T11:04:25
Class
Spectrometer Frequency 125.77
Spectral Width 31250.0
Lowest Frequency -1090.6
Nucleus 13C
Acquired Size 32768
Spectral Size 65536
Cl
O
N
BF4−
9
CD2Cl2
H-grease
Si-grease
200 190 180 170 160 150 140 130 120 110 100 90 80 70 60 50 40 30 20 10 0
f1 (ppm)

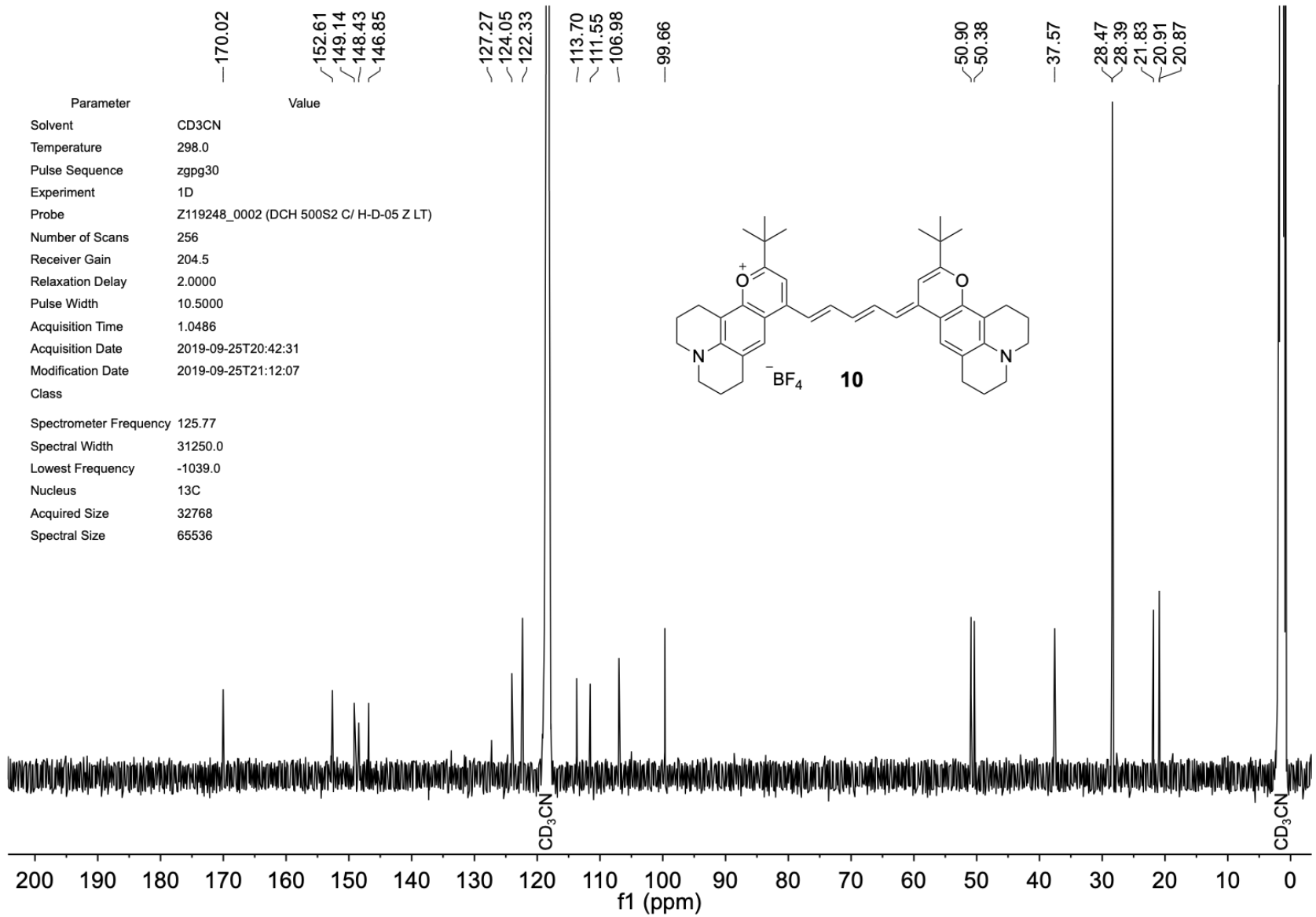
170.02
152.61
149.14
148.43
146.85
127.27
124.05
122.33
113.70
111.55
106.98
99.66
50.90
50.38
37.57
28.47
28.39
21.83
20.91
20.87
Parameter Value
Solvent CD3CN
Temperature 298.0
Pulse Sequence zgpg30
Experiment 1D
Probe Z119248_0002 (DCH 500S2 C/ H-D-05 Z LT)
Number of Scans 256
Receiver Gain 204.5
Relaxation Delay 2.0000
Pulse Width 10.5000
Acquisition Time 1.0486
Acquisition Date 2019-09-25T20:42:31
Modification Date 2019-09-25T21:12:07
Class
Spectrometer Frequency 125.77
Spectral Width 31250.0
Lowest Frequency -1039.0
Nucleus 13C
Acquired Size 32768
Spectral Size 65536
BF4
10
CD3CN
CD3CN
200 190 180 170 160 150 140 130 120 110 100 90 80 70 60 50 40 30 20 10 0
f1 (ppm)

FT-IR spectra

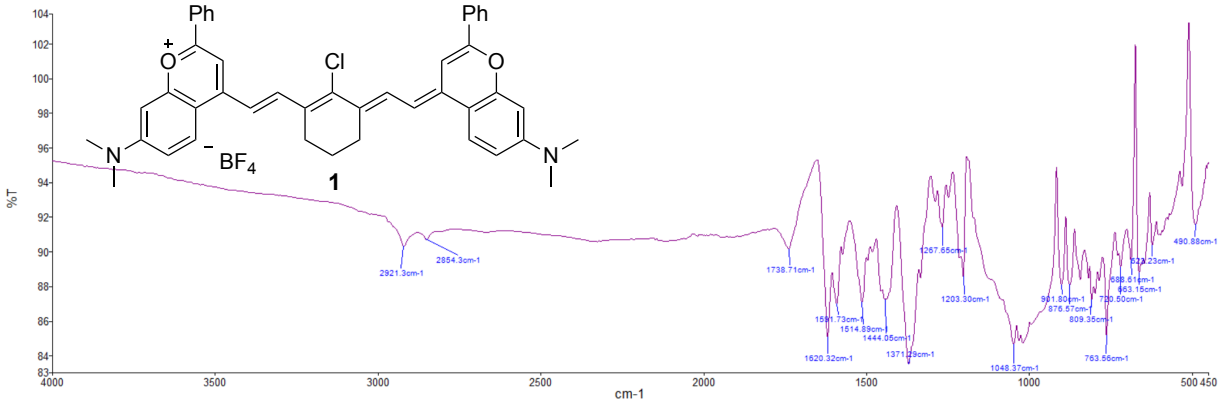

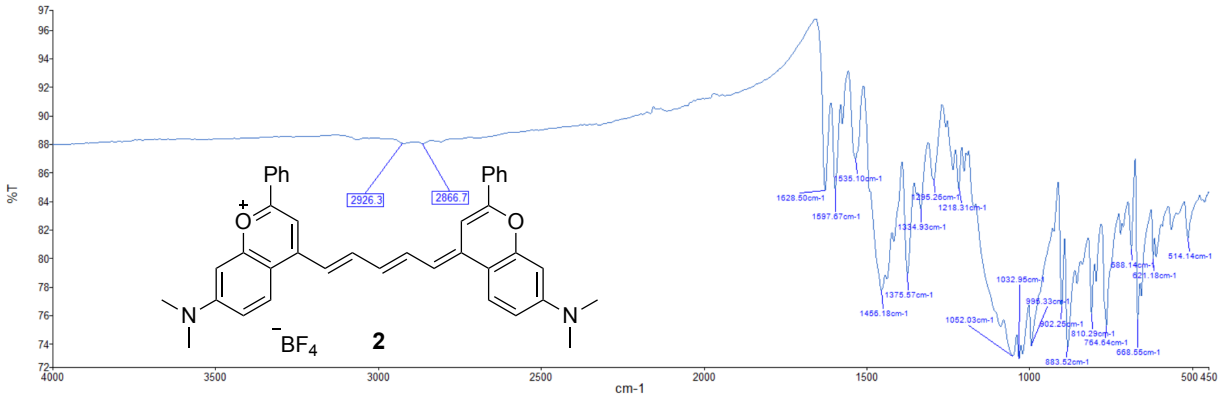

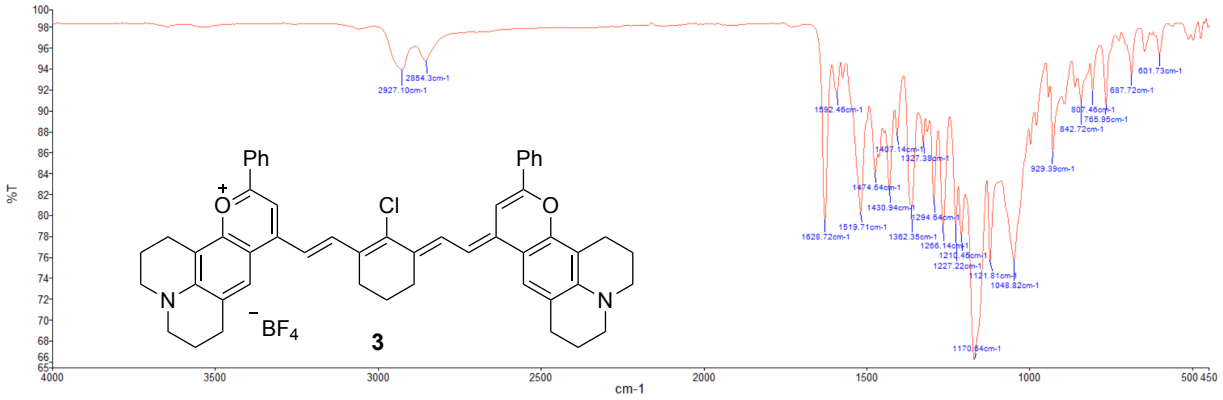

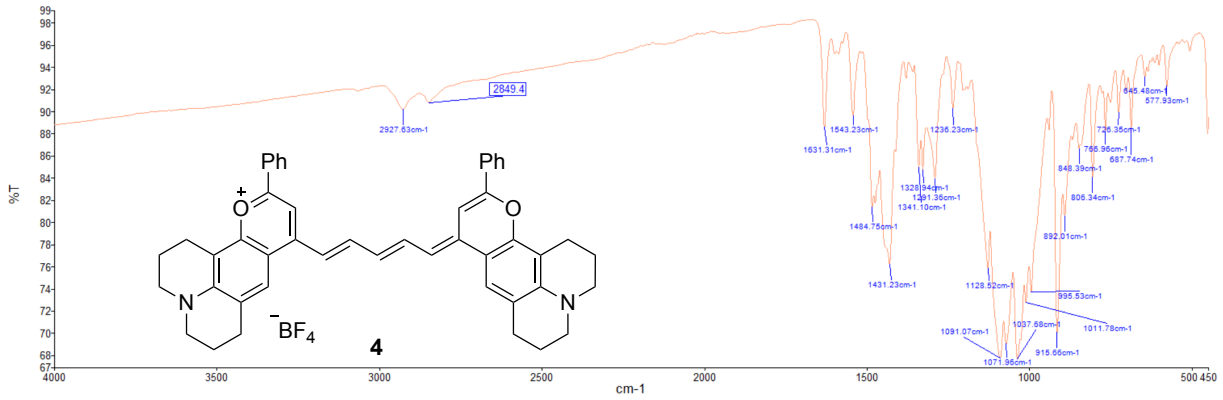
Ph
Ph
O
O
N
N
BF_4^-
4
%T
cm-1
2927.63cm-1
2849.4
1631.31cm-1
1543.23cm-1
1484.75cm-1
1431.23cm-1
1341.10cm-1
1328.94cm-1
1391.36cm-1
1236.23cm-1
1128.52cm-1
1071.96cm-1
1091.07cm-1
1037.68cm-1
995.53cm-1
1011.78cm-1
915.66cm-1
892.01cm-1
848.39cm-1
806.34cm-1
765.96cm-1
726.35cm-1
687.74cm-1
645.48cm-1
577.93cm-1

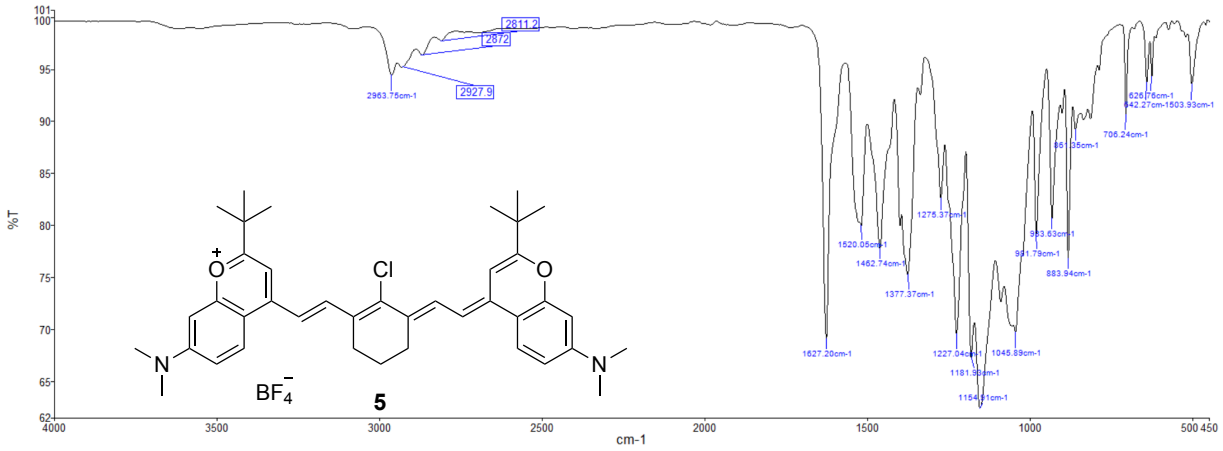
Cl
O
O
N
N
BF_4^-
5
%T
cm-1
2963.75cm-1
2927.9
2872
2811.2
1627.20cm-1
1520.05cm-1
1462.74cm-1
1377.37cm-1
1275.37cm-1
1227.04cm-1
1181.38cm-1
1154.91cm-1
1045.89cm-1
963.63cm-1
931.79cm-1
883.94cm-1
706.24cm-1
661.35cm-1
626.76cm-1
542.27cm-1
503.93cm-1

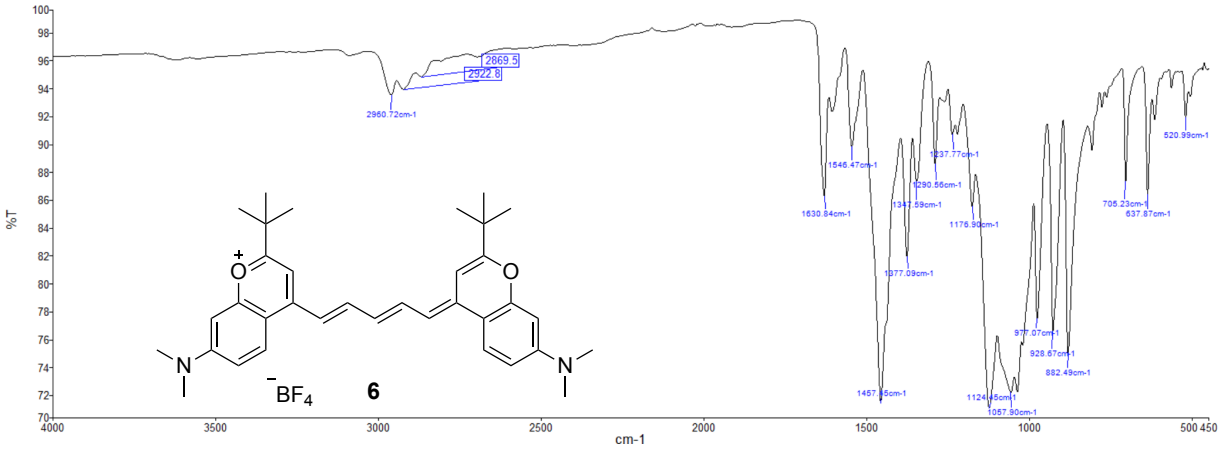
O
O
N
N
BF_4^-
6
%T
cm-1
2960.72cm-1
2922.6
2869.5
1630.84cm-1
1546.47cm-1
1457.18cm-1
1377.09cm-1
1347.59cm-1
1290.56cm-1
1237.77cm-1
1176.96cm-1
1124.45cm-1
1057.90cm-1
977.07cm-1
928.67cm-1
882.49cm-1
705.23cm-1
637.87cm-1
520.99cm-1

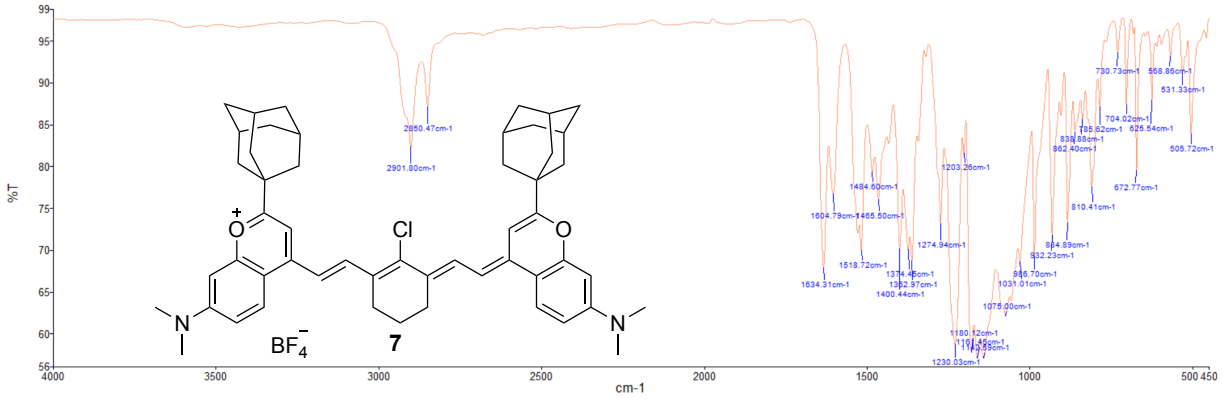
%T
cm-1
2850.47cm-1
2901.80cm-1
1634.31cm-1
1604.79cm-1
1518.72cm-1
1484.60cm-1
1465.50cm-1
1400.44cm-1
1374.45cm-1
1352.97cm-1
1274.94cm-1
1203.26cm-1
1180.12cm-1
1161.46cm-1
1143.89cm-1
1230.03cm-1
1075.00cm-1
1031.01cm-1
966.70cm-1
932.23cm-1
884.89cm-1
862.40cm-1
838.86cm-1
810.41cm-1
785.62cm-1
730.73cm-1
704.02cm-1
672.77cm-1
625.54cm-1
568.85cm-1
531.33cm-1
505.72cm-1
Cl
O
N
BF4
7

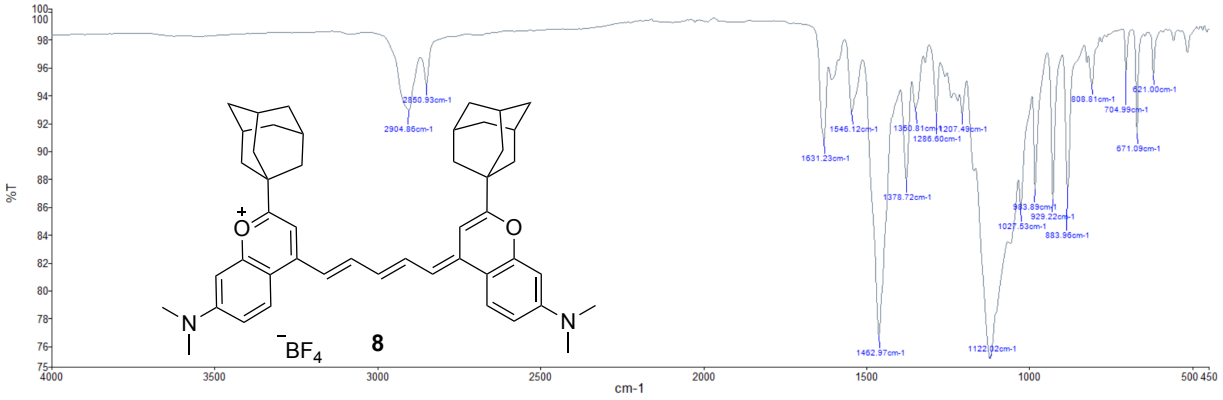
%T
cm-1
2850.93cm-1
2904.86cm-1
1631.23cm-1
1546.12cm-1
1462.97cm-1
1378.72cm-1
1350.81cm-1
1286.60cm-1
1207.49cm-1
1122.02cm-1
1027.53cm-1
983.89cm-1
929.22cm-1
883.96cm-1
808.81cm-1
704.99cm-1
671.09cm-1
621.00cm-1
O
N
BF4
8

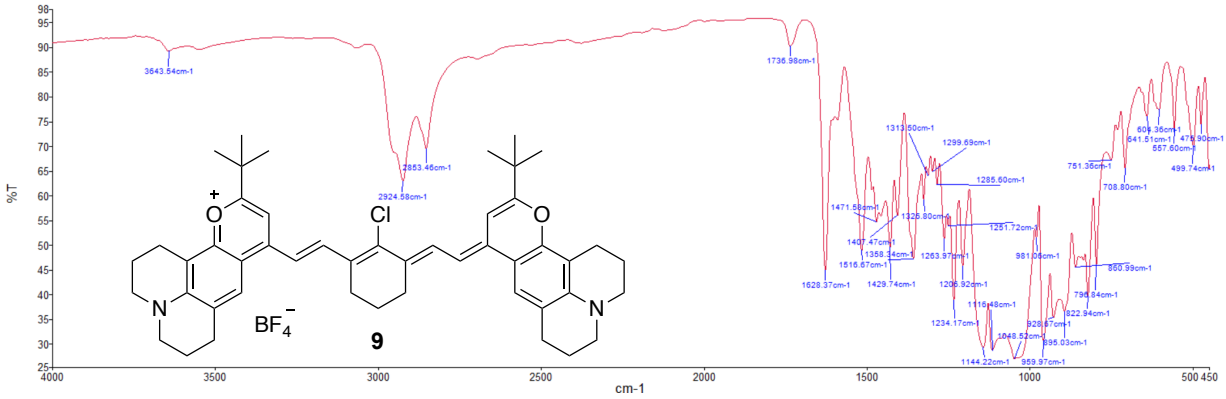
%T
cm-1
3643.54cm-1
2853.46cm-1
2924.58cm-1
1736.98cm-1
1628.37cm-1
1516.67cm-1
1471.58cm-1
1429.74cm-1
1407.47cm-1
1358.34cm-1
1328.80cm-1
1313.50cm-1
1299.69cm-1
1285.60cm-1
1263.97cm-1
1251.72cm-1
1206.92cm-1
1144.22cm-1
1116.48cm-1
1048.52cm-1
1234.17cm-1
981.06cm-1
959.97cm-1
926.67cm-1
895.03cm-1
860.99cm-1
822.94cm-1
796.84cm-1
751.36cm-1
708.80cm-1
609.36cm-1
641.51cm-1
557.60cm-1
499.74cm-1
O
N
BF4
9

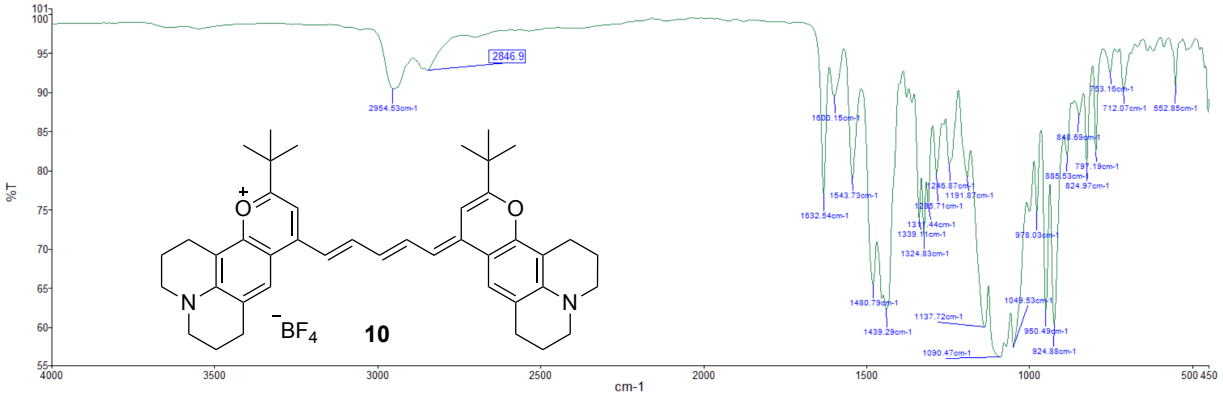
%T
cm-1
2954.53cm-1
2846.9
1632.54cm-1
1600.15cm-1
1543.73cm-1
1480.79cm-1
1439.29cm-1
1339.11cm-1
1324.83cm-1
1137.72cm-1
1090.47cm-1
978.03cm-1
950.49cm-1
924.88cm-1
885.53cm-1
824.97cm-1
797.19cm-1
753.15cm-1
712.07cm-1
552.85cm-1
BF4
10

Absorption coefficient and emission spectra

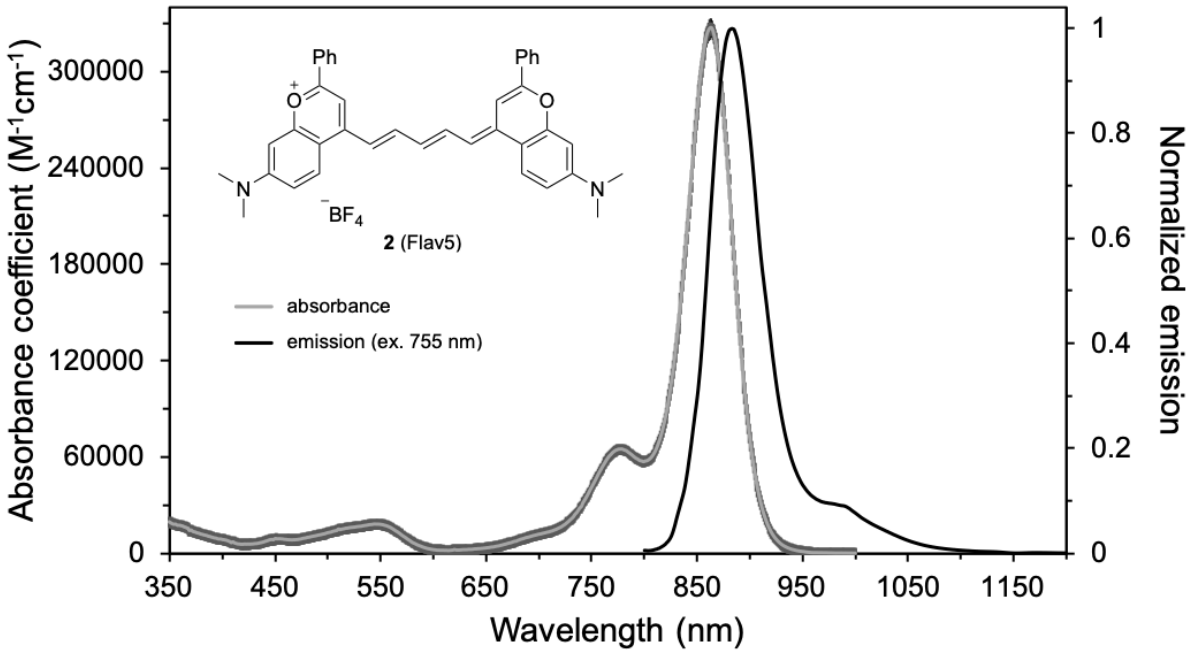

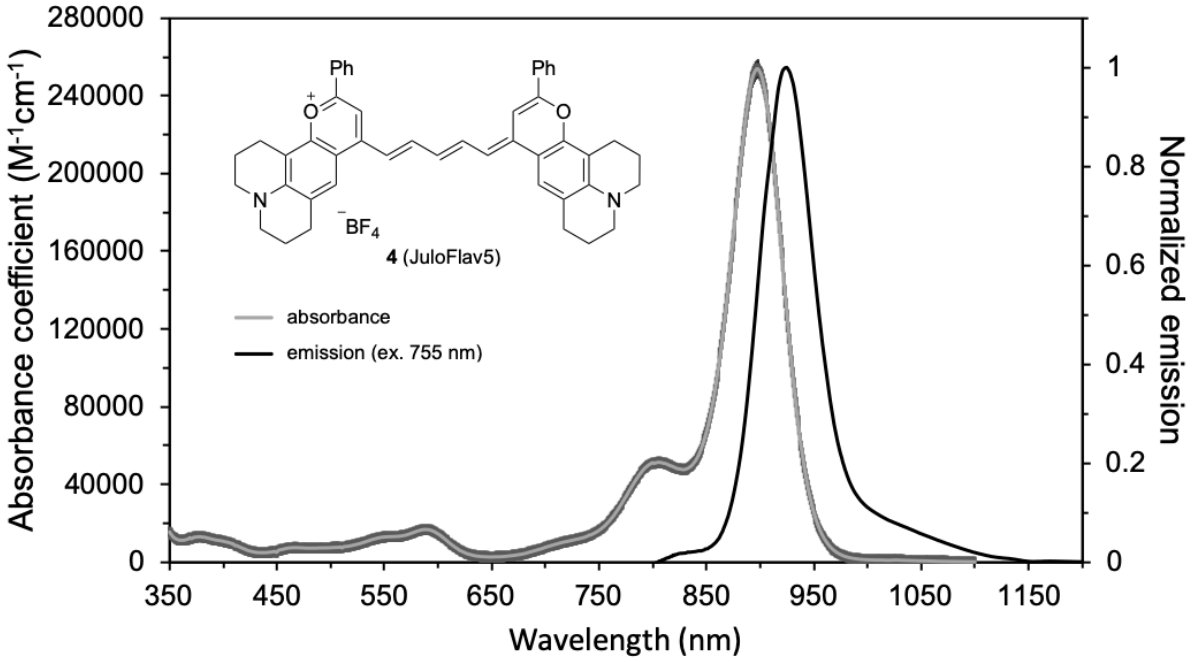

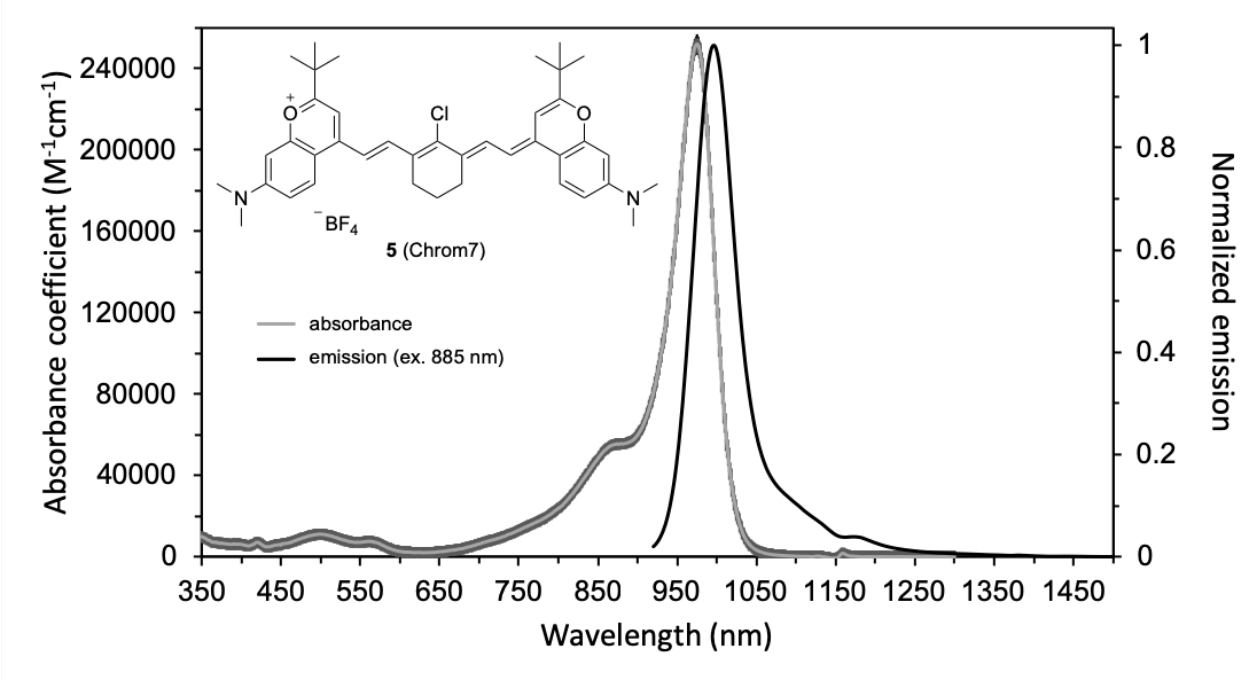
Absorbance coefficient (M-1cm-1)
Normalized emission
Wavelength (nm)
Cl
BF4
5 (Chrom7)
absorbance
emission (ex. 885 nm)

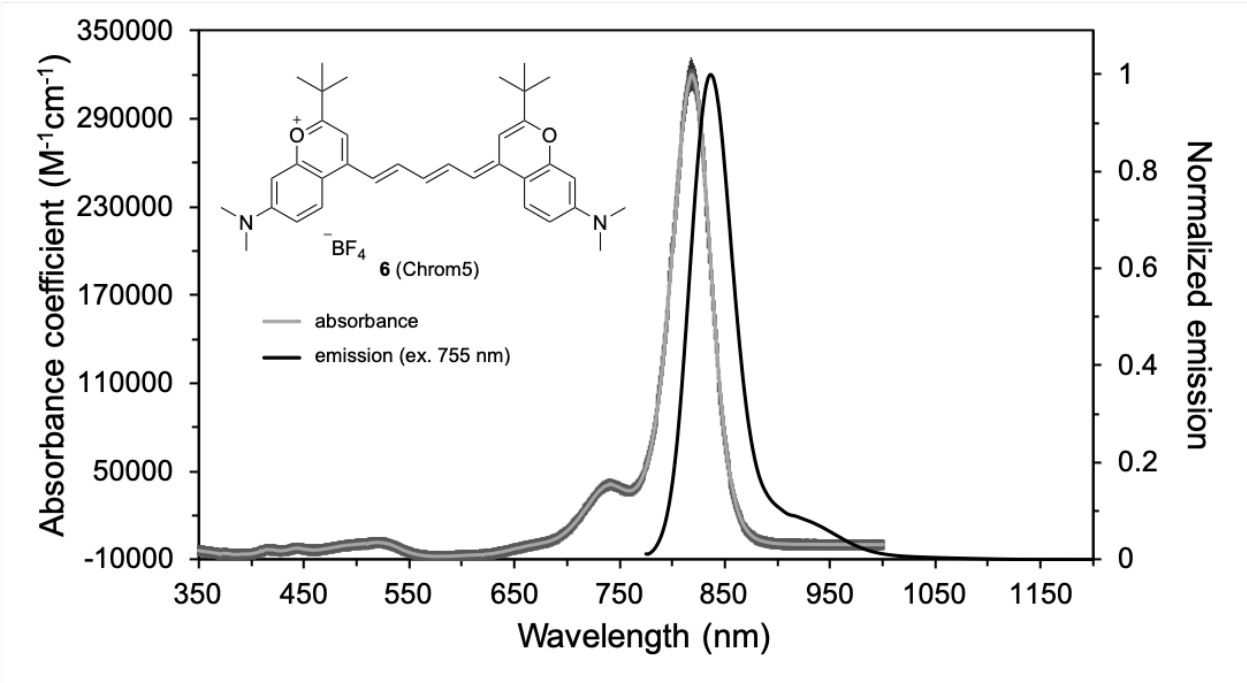
Absorbance coefficient (M-1cm-1)
Normalized emission
Wavelength (nm)
BF4
6 (Chrom5)
absorbance
emission (ex. 755 nm)

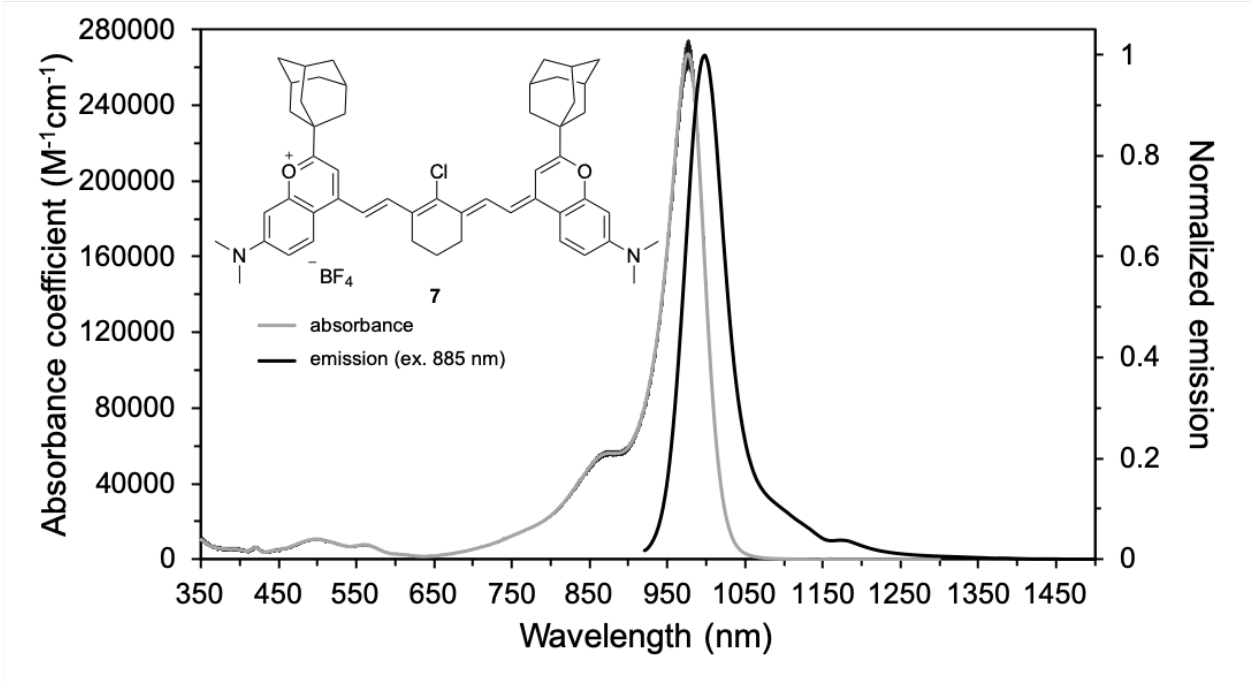
Absorbance coefficient (M-1cm-1)
Normalized emission
Wavelength (nm)
absorbance
emission (ex. 885 nm)
7
Cl
BF4

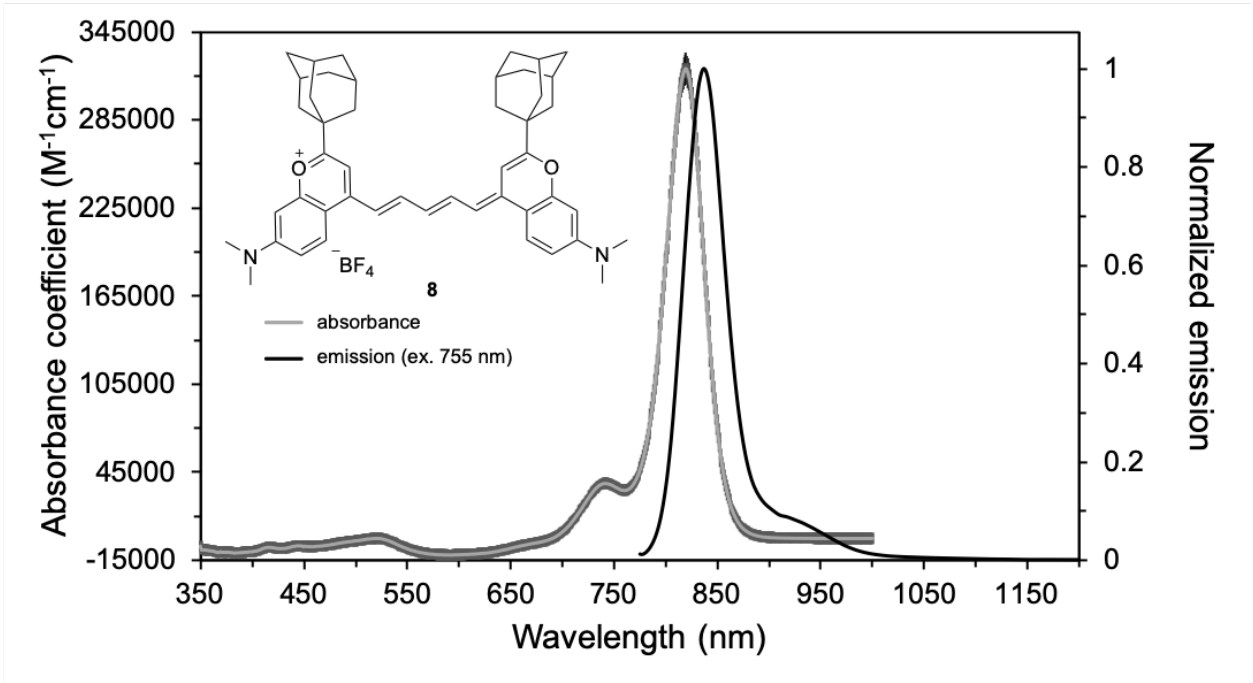
Absorbance coefficient (M-1cm-1)
Normalized emission
Wavelength (nm)
absorbance
emission (ex. 755 nm)
8
BF4

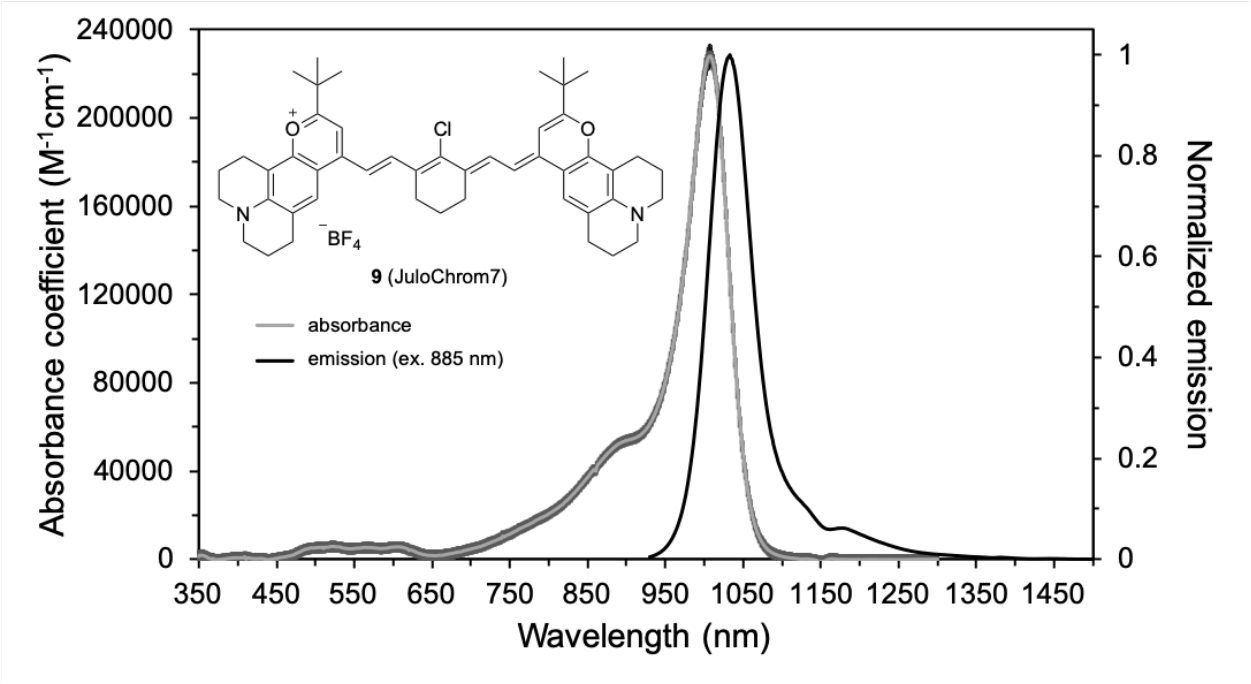
Absorbance coefficient (M-1cm-1)
Normalized emission
Wavelength (nm)
9 (JuloChrom7)
absorbance
emission (ex. 885 nm)
Cl
BF4

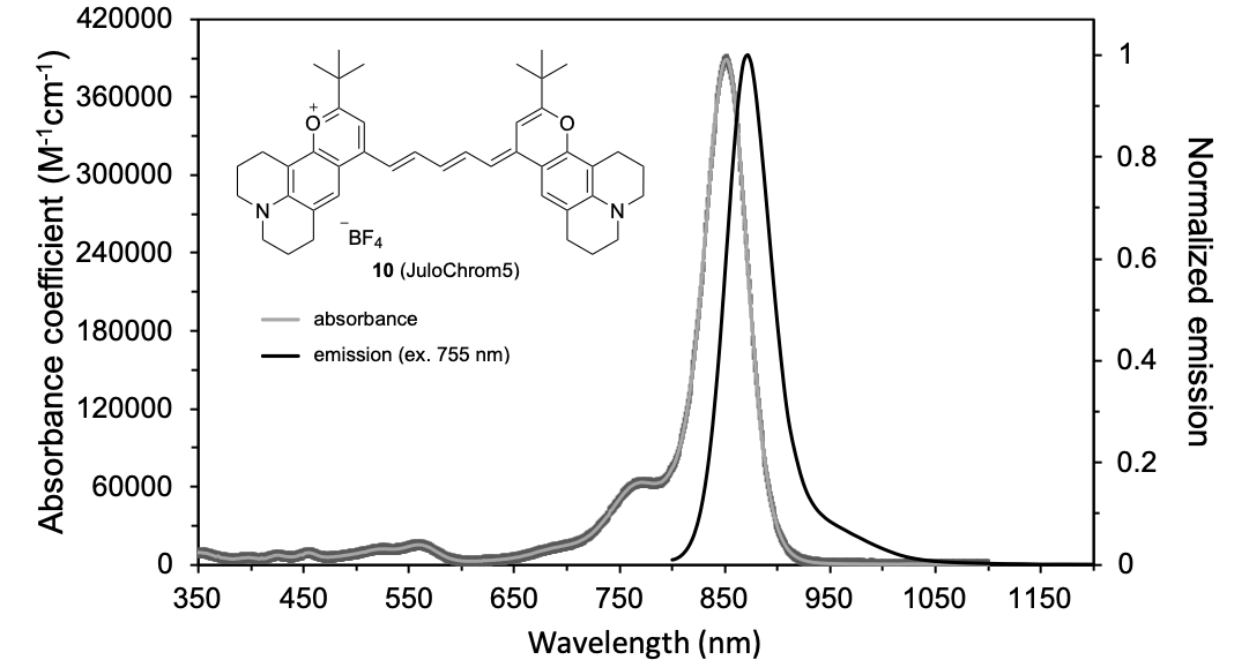
Absorbance coefficient (M-1cm-1)
Normalized emission
Wavelength (nm)
10 (JuloChrom5)
absorbance
emission (ex. 755 nm)
BF4

XI. Crystallographic information

Table S5. Crystal data and structure refinement for **4** (JuloFlav5)

Empirical formula	C53 H61 B F4 N2 O5 S3	
Formula weight	989.02	
Temperature	100(2) K	
Wavelength	1.54178 Å	
Crystal system	Triclinic	
Space group	P -1	
Unit cell dimensions	a = 12.9984(5) Å	a= 101.472(2)°.
	b = 13.0604(5) Å	b= 90.570(2)°.
	c = 15.5647(6) Å	g = 111.570(2)°.
Volume	2398.17(16) $Å^3$	
Z	2	
Density (calculated)	1.370 Mg/m^3	
Absorption coefficient	1.969 mm^{-1}	
F(000)	1044	
Crystal size	.2 x .2 x .18 mm^3	
Theta range for data collection	2.909 to 69.453°.	
Index ranges	-15<=h<=15, -15<=k<=15, -18<=l<=18	
Reflections collected	45262	
Independent reflections	8621 [R(int) = 0.0437]	
Completeness to theta = 67.679°	96.6 %	
Absorption correction	Semi-empirical from equivalents	
Max. and min. transmission	0.75 and 0.67	
Refinement method	Full-matrix least-squares on F^2	
Data / restraints / parameters	8621 / 0 / 619	
Goodness-of-fit on F^2	1.066	
Final R indices [I>2sigma(I)]	R1 = 0.0453, wR2 = 0.1234	
R indices (all data)	R1 = 0.0522, wR2 = 0.1287	
Extinction coefficient	n/a	
Largest diff. peak and hole	0.643 and -0.600 $e.Å^{-3}$	

Table S6. Crystal data and structure refinement for **5** (Chrom7)

Empirical formula	C43 H54 B Cl7 F4 N2 O2	
Formula weight	965.84	
Temperature	100(2) K	
Wavelength	1.54178 Å	
Crystal system	Triclinic	
Space group	P-1	
Unit cell dimensions	a = 14.0234(3) Å	a= 88.1450(10)°.
	b = 18.9593(5) Å	b= 79.6560(10)°.
	c = 19.1502(4) Å	g = 70.0770(10)°.
Volume	4706.73(19) $Å^3$	
Z	4	
Density (calculated)	1.363 Mg/m^3	
Absorption coefficient	4.298 mm^{-1}	
F(000)	2008	
Crystal size	0.200 x 0.200 x 0.100 mm^3	
Theta range for data collection	2.346 to 69.503°.	
Index ranges	-16<=h<=17, -21<=k<=22, -22<=l<=23	

Reflections collected	96540
Independent reflections	16916 [R(int) = 0.0414]
Completeness to theta = 67.679°	96.5 %
Absorption correction	Semi-empirical from equivalents
Max. and min. transmission	0.75 and 0.58
Refinement method	Full-matrix least-squares on F^2
Data / restraints / parameters	16916 / 0 / 1101
Goodness-of-fit on F^2	1.038
Final R indices [I>2sigma(I)]	R1 = 0.0486, wR2 = 0.1211
R indices (all data)	R1 = 0.0585, wR2 = 0.1269
Extinction coefficient	n/a
Largest diff. peak and hole	0.826 and -0.894 e.$Å^{-3}$

XII. References:

1. Schindelin, J. *et al.* Fiji: an open-source platform for biological-image analysis. *Nat. Methods* **2012**, *9*, 676–82.
2. Rueden, C. T. *et al.* ImageJ2: ImageJ for the next generation of scientific image data. *BMC Bioinformatics* **2017**, *18*, 1–26.
3. Cosco, E. D.; Spearman, A. L.; Ramakrishnan, S.; Lingg, J. G. P.; Saccomano, M.; Pengshung, M.; Arus, B. A.; Wong, K. C. Y.; Glasl, S.; Ntziachristos, V.; Warmer, M.; McLaughlin, R. R.; Bruns, O. T.; Sletten, E. M. Shortwave infrared polymethine fluorophores matched to excitation lasers enable noninvasive, multicolor in vivo imaging in real time. *Nat. Chem.* **2020**, in revision.
4. Peter Kovesi. Good Colour Maps: How to Design Them. arXiv:1509.03700 [cs.GR] 2015.
5. Cosco, E. D.; Caram, J. R.; Bruns, O. T.; Franke, D.; Day, R. A.; Farr, E. P.; Bawendi, M. G.; Sletten, E. M. Flavylium Polymethine Fluorophores for Near- and Shortwave Infrared Imaging. *Angew. Chemie Int. Ed.* **2017**, *56*, 13126–13129.
6. Semonin, O. E. *et al.* Absolute photoluminescence quantum yields of IR-26 Dye, PbS, and PbSe quantum dots. *J. Phys. Chem. Lett.* **2010**, *1*, 2445–2450.
7. Hatami, S. *et al.* Absolute photoluminescence quantum yields of IR26 and IR-emissive Cd1−xHgxTe and PbS quantum dots – method- and material-inherent challenges. *Nanoscale* **2015**, *7*, 133–143.